GRAZING IN TIMES OF FADING LIGHT

How zooplankton shapes the ecosystem at the Western Antarctic Peninsula during autumnal shifts of growth limiting factors

Sebastian Böckmann

Bremen, August 2024

Kolloquium: ~~Oktober 2024~~ 21.11.2024

Universität Bremen

EXAMINATION COMMITTEE

1. Examiner Dr. Scarlett Trimborn
Alfred-Wegener-Institute for Polar and Marine Research
Bremerhaven, Germany

2. Examiner Prof. Dr. Tilmann Harder
University of Bremen
Bremen, Germany

3. Examiner Prof. Dr. Martin Diekmann
University of Bremen
Bremen, Germany

1. Reviewer Prof. Dr. Morten H. Iversen
Alfred-Wegener-Institute for Polar and Marine Research
Bremerhaven, Germany

~~2. Reviewer Prof. Dr. Walker O. Smith Jr.~~
~~Virginia Institute of Marine Science, William & Mary~~
~~Gloucester Point, Virginia, USA~~

2. Reviewer Prof. Dr. Rob Middag
Royal Netherlands Institute for Sea Research
Texel, Netherlands

3. Reviewer Dr. Lavenia Ratnarajah
University of Tasmania
Hobart, Tasmania, Australia

ACKNOWLEDGMENTS

First, I would like to thank my immediate colleagues. In particular, my supervisors Scarlett Trimborn and Florian Koch for providing a pleasant and appreciative work environment. I am especially thankful for the space you gave me to develop my own ideas, for your patience, when I was too confident about those ideas and for your constructive criticism in numerous discussions and written exchanges. I'd also like to express my appreciation for the other members of my working group, who significantly contributed to the trusting and friendly atmosphere at AWI and aboard Polarstern: Franziska, Jenna, Marianne, Jasmin, Anna, Silke, Jeff and Giulia. Beyond being friendly and supportive colleagues, I'd like to stress the roles of Christian, Tina and Doro for taking and measuring countless samples and for teaching me laboratory techniques and protocols.

Rob Middag

Further, I'd like to thank my examiners: Morten Iversen, ~~Walker Smith~~ and Lavenia Ratnarajah for their willingness to review this thesis, as well as Scarlett Trimborn, Tilmann Harder and Martin Diekmann for acting as examiners in the colloquium. Furthermore, I want to thank my supporters in academia, who are not part of the above mentioned groups. Thank you Bettina Meyer for being an essential member of the POSER project and for guiding the Polarstern campaign that this dissertation is based on. Thank you Kai Bischof, for welcoming me in your working group at the University of Bremen. Thank you Luis Laglera, for being a patient and supportive supervisor, with whom I was able to discuss methodological details, whenever I doubted my work. Thank you Ryan Driscoll for providing zooplankton data for PS112. Finally, and in particular thank you Hendrik for mentoring me over the last 10+ years, for your always prompt and constructive feedbacks and for continuously providing perspectives and suggesting fruitful directions. I'd like to add appreciation for Florian's, Hendrik's and my wife Anne's general criticism of this theses' first draft, which greatly improved the final version. The graduate school POLMAR also falls into the group of supporters in academia. Thank you to both Claudias for encouragement and backup, whenever I felt a little lost in the bureaucratic maze of our institute.

Thanks to all the PS112 field campaign scientists and crew. It was an unforgettable experience and thanks again Scarlett, for providing me with the opportunity to join. Being part of a Polarstern expedition to Antarctica used to be one of my goals in life, and is now one giant tick on my bucket list.

Finally, I'd like to thank my family, foremost my parents and grandparents for their limitless support over decades. You managed to support me with the self-confidence and the necessary resources to pursue an uncertain but highly fulfilling career path. The last words shall be reserved for my wonderful wife and daughter. Thank you Anne for your willingness to understand my work and improving it with countless hours of discussions, for your role as the provider in our little family that gave me the necessary space to take my time during the dissertation process, and for simply accepting me the way I am. And eventually, thank you Ronja for forcing my mind off work. Your contribution made me realize how I work best.

ABSTRACT

The efficiency of the biological carbon pump at the Western Antarctic Peninsula (WAP) is determined by autotrophic carbon fixation in phytoplankton on the one hand, and heterotrophic carbon recycling by consumption and respiration on the other. Although phytoplankton primary production (PP) forms the basis of the WAP's trophic food web, and influences the world's climate directly by significant carbon sequestration, key aspects directly influencing phytoplankton biomass production and heterotrophic respiration are poorly constrained.

Since the WAP is a highly seasonal ecosystem, a balanced investigation covering all seasons is necessary, in order to better understand annual succession dynamics of plankton communities. To date, empirical data of various biogeochemical parameters has been collected mostly in spring and summer. Besides plankton biomass and production, empirical data on small zooplankton (SZP, <200 µm) grazing for the WAP region is largely lacking. It is paramount to constrain the role of SZP at the WAP, since SZP constitutes the dominant sink of phytoplankton biomass in the Southern Ocean (SO), and is therefore capable of regionally shaping plankton communities. The latter is a major factor in determining the quality and quantity of carbon transport up the trophic ladder, as well as down into the deep ocean. Finally, impacted by climate change, the WAP is one of the fastest warming regions in Antarctica resulting in a withdrawal of the SO key species krill to colder habitats further south. In the vacated, often iron (Fe) limited regions, the range of salps has expanded dramatically. Although it is known that planktonic grazers influence Fe recycling in the water column, the biogeochemical implications of a population shift from krill to salps for recycling of bioavailable Fe, and therefore the potential for PP so far widely remained unexplored. In order to close these ecological knowledge gaps, this dissertation presents result from experiments and data collections focusing on the following 3 hypotheses. First, in austral autumn, plankton biomass distribution, production and micronutrient utilization follow spatial patterns, rooted in the influence zones of different SO surface currents. Second, SZP grazing dominates carbon cycling at the WAP in austral autumn and third, a shift from krill to salps results in reduced recycling of bioavailable Fe at the WAP. Finally, the hypotheses that SZP shapes the patchy distribution of biomass parameters in the sampling area and that an increase of salps increases carbon sequestration via the biological carbon pump, are discussed.

All presented studies were performed in the framework of the POSER project (Population shift and ecosystem response—krill vs. salps), aboard RV Polarstern (PS112) between March and May 2018. The surface water (25 m) of 10 stations around the WAP was sampled for 41 parameters, representing physico-chemical conditions, biomass, biological production and trace element utilization. Three dilution experiments were performed to investigate the gross growth and SZP grazing induced mortality of different functional groups in the planktonic community. One experiment in the offshore Drake Passage investigated the recycling and the bioavailability of iron to phytoplankton in the presence of krill and salp fecal pellets.

The encountered conditions resulted in a categorization of different regions, mainly the northern, offshore zone under the influence of the Antarctic Circumpolar Current and a southern inshore zone in the Bransfield Strait, although this partitioning was markedly weaker than in summer. Parameters representing biomass were heterogeneously distributed and lower than in summer, but fitted the few published values on the region in austral autumn well. The analysis of trace element uptake suggested no immediate limitation by iron, zinc or vitamin B_{12}. SZP grazing pressure was heterogeneously distributed, but represented the dominant sink of particulate organic carbon at all sampled stations. This parameter, not the classically investigated chlorophyll a, proved to be the parameter yielding most reliable interpretable results in the dilution experiments. Salp fecal pellets were found to release more Fe than krill fecal pellets, which was additionally shown to be more bioavailable to phytoplankton. Given the substantial influence, zooplankton organisms unfold bottom-up and top-down on the primary production, the observed patchy distribution of biomass parameters was attributed to the evidently patchy distribution of zooplankton grazers and predators and their complex interactions. Multiple observations, reaching from dietary preferences, over more efficient iron recycling, to an expected weakening of the SZP community by salps, suggested that the observed shift from krill to salps in the study area, might improve conditions for large diatoms and reduce respiration in the upper water column, thusly increasing carbon sequestration by the biological carbon pump.

ZUSAMMENFASSUNG

Die Effizienz der biologischen Kohlenstoffpumpe an der Westantarktischen Halbinsel (WAP) wird einerseits durch die Kohlenstofffixierung des Phytoplanktons und andererseits durch das Kohlenstoffrecycling durch heterotrophe Konsumption und Atmung bestimmt. Obwohl die planktonische Primärproduktion (PP) die trophische und energetische Grundlage des WAP-Ökosystems bildet und das Weltklima durch erhebliche Kohlenstoffbindung direkt beeinflusst, wurden Schlüsselaspekte, die die Phytoplankton-Biomasseproduktion und die heterotrophe Atmung direkt beeinflussen, nur unzureichend beschrieben.

Um das stark saisonale WAP-Ökosystem zu verstehen, ist eine ausgewogene Untersuchung über alle Jahreszeiten hinweg erforderlich, wobei die ganzjährige Abfolge der Planktongemeinschaften überwacht werden muss. Empirische Daten zu den unterschiedlichsten biogeochemischen Parametern liegen jedoch meist nur für Frühjahr und Sommer vor. Neben Herbst- und Winterdaten über Planktonbiomasse und -produktion fehlen für die WAP-Region weitgehend empirische Daten zur Beweidung durch kleines Zooplankton (SZP, <200 μm). Die Eingrenzung der Rolle von SZP an der WAP ist von größter Bedeutung, da SZP die dominierende Senke der Phytoplankton-Biomasse im Südpolarmeer (SO) darstellt und daher in der Lage ist, Planktongemeinschaften regional zu formen und letztendlich sowohl den Kohlenstofftransport die trophische Leiter hinauf, als auch hinab in die Tiefen des Ozeans zu beeinflussen. Schließlich ist die WAP eine der sich im Zuge des Klimawandels am schnellsten erwärmenden Regionen in der Antarktis, was zu einem Rückzug der Schlüsselart Krill in kältere Lebensräume weiter südlich führt. In den frei gewordenen, oft eisen (Fe) armen Regionen breiten sich zunehmend Salpen aus. Obwohl bekannt ist, dass planktonische Konsumenten das Fe-Recycling in der Wassersäule stark beeinflussen, blieben die biogeochemischen Auswirkungen dieser Populationsverschiebung auf das Recycling von bioverfügbarem Fe und damit das Potenzial für die PP unerforscht. Um diese wichtigen ökologischen Wissenslücken zu schließen, präsentiert die vorliegende Dissertation Ergebnisse aus Experimenten und Datensammlungen, die sich auf die folgenden drei Hypothesen konzentrieren. Erstens folgt im Südherbst die Verteilung, Produktion und Mikronährstoffnutzung von Planktonbiomasse räumlichen Mustern, die in den Einflusszonen verschiedener Oberflächenströmungen verwurzelt sind. Zweitens dominiert die SZP-Beweidung den Kohlenstoffkreislauf an der WAP im Südherbst und drittens führt eine Verlagerung von Krill zu Salpen zu einem verringerten Recycling von bioverfügbarem Fe an der WAP. Aufbauend auf diesen Studienergebnissen werden die Hypothesen diskutiert, dass SZP die lückenhafte Verteilung von Biomasseparametern im Probennahmegebiet prägt und dass eine Zunahme der Salpen die Kohlenstoffsequestrierung über die biologische Kohlenstoffpumpe erhöht.

Alle vorgestellten Studien wurden im Rahmen des POSER-Projekts (Population Shift and Ecosystem Response – Krill vs. Salps) an Bord der *FS Polarstern* (PS112) zwischen März und Mai 2018 durchgeführt. Im Oberflächenwasser (25 m) von 10 Stationen rund um die WAP wurden 41 Parameter

untersucht, die physikalisch-chemische Bedingungen, Biomasse, biologische Produktion und Spurenelementnutzung repräsentieren. Drei Verdünnungsexperimente wurden durchgeführt, um das Bruttowachstum und die, durch die Beweidung mit kleinem Zooplankton verursachte Mortalität verschiedener funktioneller Gruppen in der Planktongemeinschaft zu untersuchen. Ein Experiment in der vorgelagerten Drake-Passage untersuchte das Recycling und die Bioverfügbarkeit von Eisen für Phytoplankton in Gegenwart von Krill- und Salp-Kotpellets.

Die vorgefundenen Bedingungen deuteten auf eine Differenzierung des Probennahmegebiets in eine nördliche Zone im offenen Ozean unter dem Einfluss des antarktischen Zirkumpolarstroms und eine südliche Küstenzone in der Bransfieldstraße hin, allerdings war diese Differenzierung deutlich schwächer ausgeprägt als im Sommer. Die Biomasseparameter waren heterogen verteilt und niedriger als im Sommer, passten aber gut zu den wenigen veröffentlichten Werten für die Region im Herbst. Die Analyse der Spurenelementaufnahme ergab keine unmittelbare Limitation durch Eisen, Zink oder Vitamin B_{12}. Der Weidedruck von kleinem Zooplankton war heterogen verteilt, stellte jedoch an allen beprobten Stationen die dominierende Senke für partikulären organischen Kohlenstoff dar. Dieser Parameter, nicht das klassisch untersuchte Chlorophyll a, erwies sich als der Parameter, der in den Verdünnungsexperimenten am zuverlässigsten interpretierbare Ergebnisse lieferte. Es wurde festgestellt, dass Salp-Kotpellets mehr Eisen freisetzen als Krill-Kotpellets, was sich außerdem als besser bioverfügbar für Phytoplankton erwies. Angesichts des erheblichen Einflusses, den Zooplanktonorganismen bottom-up und top-down auf die Primärproduktion entfalten, wurde die beobachtete lückenhafte Verteilung der Biomasseparameter auf die offensichtlich lückenhafte Verteilung von planktonischen Weidegängern und Räubern sowie deren komplexe Wechselwirkungen zurückgeführt. Mehrere Beobachtungen, die von den Ernährungspräferenzen der Salpen über ein effizienteres Eisenrecycling, bis hin zu einer erwarteten Schwächung der SZP-Gemeinschaft durch Salpen reichten, deuteten darauf hin, dass die beobachtete Verlagerung von Krill zu Salpen im Untersuchungsgebiet die Bedingungen für große Kieselalgen verbessern und die heterotrophe Atmung in der oberen Wassersäule verringern könnte, wodurch der Kohlenstoffexport der biologischen Kohlenstoffpumpe gestärkt werden könnte.

TABLE OF CONTENTS

Iron, zinc and vitamin B_{12} uptake characteristics of autumn phytoplankton at the northern tip of the Western Antarctic Peninsula

ABBREVIATIONS & ACRONYMS

ACC	Antarctic Circumpolar Current
ANOVA	One-way analysis of variance
AS	Antarctic Sound
BC	Bransfield Current
Bq	Becquerel
BP	Bacterial Production
BS	Bransfield Strait
C	Carbon
Cd	Cadmium
Chl a	Chlorophyll a
Cl	Chlorine
CO_2	Carbon dioxide
Co	Cobalt
Cu	Copper
d	Dissolved … (for trace metals, e.g. dFe = dissolve iron)
DIC	Dissolved inorganic carbon
DIN or NO_x	Dissolved inorganic nitrogen
DNA	Deoxyribonucleic acid
DOC	Dissolved organic carbon
DP	Drake Passage
Fe	Iron
FP	Fecal pellet
FRRf	Fast repetition rate fluorometer
FSW	Filtered seawater
F_v/F_m	Photophysiological efficiency (apparent maximum quantum yield of photosynthesis of PSII)
g	Grazer induced mortality
H	Hydrogen
HCl	Hydrochloric acid
HDNA	High DNA (heterotrophic bacteria)
HF	Hydrofluoric acid
HNO_3	Nitric acid
HNLC areas	High nutrient (alternatively nitrogen) low chlorophyll areas
k	Gross growth rate
LDNA	Low DNA (heterotrophic bacteria)
LSF	Large size fraction

M	molar
Mn	Manganese
Mn*	Manganese deficiency coefficient
N	Nitrogen
n	Number of replicates
Na	Sodium
NaOH	Sodium hydroxide
NE	Autotrophic nanoeukaryotes
P	Phosphorous
PE	Autotrophic picoeukaryotes
PO_4	Phosphate
PP	Primary production
PSI & PSII	Photosystem I and Photosystem II
POC	Particulate organic carbon
PON	Particulate organic nitrogen
r	Apparent growth rate
R^2	Coefficient of determination
SD	Standard deviation
Si	Silicate
SO	Southern Ocean
SSF	Small size fraction
SWP	Seawater with phytoplankton
SZP	Small zooplankton
TCA	Trichloroacetic acid
TEP	Transparent exopolymer particles
TM	Trace metal(s)
vol	volume
WAP	Western Antarctic Peninsula
Zn	Zinc
μ	Net growth rate
σ_{PSII}	Functional absorption cross section of PSII

LIST OF FIGURES

LIST OF TABLES

1

GENERAL INTRODUCTION

1.1 Significance of the Southern Ocean and the planktonic realm

The Southern Ocean (SO) is a unique system of global significance, providing ecosystem services of inestimable value. In order for these services to remain available, the SO needs to be protected in its functionality. The precondition for protection however, is awareness derived from research on the SO, today dating back well over 100 years to the nineteenth century [1].

The term SO has been used ambiguously in the literature, bearing on different latitudes as the northern boundary. For the purpose of this dissertation SO refers to the sea south of the subantarctic front. Following this definition, the SO's uniqueness originates from first, its constraint by the Antarctic Circumpolar Current (ACC) instead of continents [1,2], second, its magnitude of annual fluctuation in sea-ice extent [1,3,4] and third, its endemic species [1,5]. The SO's global significance is rooted in its connection to all major world's oceans, facilitating significant export of macronutrients into these waters[2,6,7] and its driving force in the global ocean circulation [1,8,9]. From a human perspective, the SO offers many ecosystem services. Historically, whalers, sealers and fishermen have fished down the SO food web [10–13]. Collapsing stocks and the resulting negative ecosystem feedback loops, such as reduced iron (Fe) input and recycling [14–18], have been addressed in more recent times by strict local catch quotas, which have been shown to help increasing depleted stocks [11,19]. In contrast, the SO's inestimable global significance for the regulation of the world's climate cannot be tackled locally, due to the SO's sensitivity to climate change itself, which is a global phenomenon [20,21]. The SO acts as the primary conduit by which >40% of the anthropogenic CO_2 currently residing in the world ocean entered the waterbody[22], thanks to its cold surface in which carbon dioxide (CO_2) readily dissolves. Subsequently the CO_2 is transported inside the water column to the subtropical convergence, the primary locus of anthropogenic CO_2 storage in the southern hemisphere [23,24]. Furthermore, the albedo of Antarctica contributes to the heat balance of the planet. This reflection of sunlight is critically dependent on the extent of sea ice, which is retrogressive due to the warming of the ocean's surface [25]. Currently, the SO still contributes to mitigating the effects of climate change [26] that currently produce a damage of 143 billion dollars per year worldwide, by extreme weather events alone [27].

The plankton communities in the trophogenic epipelagial (open water column from the surface down to ~ 200 m) facilitate the majority of SO carbon fixation, as well as carbon recycling. Worldwide, the epipelagial is by far the largest habitat with light exposure and the most important source of energy fixation by planktonic production for everything that comes below [28]. The word plankton does not constitute a taxonomic group. Plankton is defined as all organisms that drift in the water, because their powers of locomotion are insufficient to make significant way against the current [29]. Depending on the taxonomic domain and kingdom, plankton is subdivided into phytoplankton (plants, mostly unicellular algae), zooplankton (animals), bacterioplankton (bacteria), virioplankton (viruses) and mycoplankton (fungi). Furthermore, a subdivision can be made by size in femto-, pico-, nano-, micro-, meso-, macro-

and megaplankton, covering the ranges of 0.02-0.2 µm, 0.2-2 µm, 2-20 µm, 20-200 µm, 0.2-20 mm, 2-20 cm and 20-200 cm respectively [29]. Despite the phytoplankton's comparably small standing stock of biomass worldwide (0.5-2.4 Gt of carbon [30] compared to 450 Gt of carbon in land plants [31]), it shows a remarkably high production. Marine and terrestrial primary producers account for roughly equal shares of the 104.9 Gt of carbon fixed per year [32]. Phytoplankton cells are rapidly consumed [31], making them an efficient vector of energy and biomass to higher trophic levels. Consequently, marine production supports a standing stock biomass of marine consumers that is between 2-5 times larger than the producers' standing stock, while on land, consumers account for only 4.4% of land plant's biomass [30,31]. Simultaneously, a share of the carbon fixed by phytoplankton evades recycling by consumption and respiration and sinks to the deep sea, constituting the biological carbon pump [33].

1.2 The Western Antarctic Peninsula habitat

The waters around the Western Antarctic Peninsula (WAP) represent a partition of the SO and are the sampling area for all studies that contributed to the presented dissertation. The WAP waters have been studied intensively due to their biological productivity [34] on the one hand, which supports grazers in great diversity and abundance [35] like krill, salps, seabirds and marine mammals [34,36] and on the other hand, because the WAP is one of the fastest warming regions in Antarctica [37]. However, little data on biological parameters exists on the WAP in austral autumn [38,39]. To the author's knowledge, only 8 studies based on field samplings have been published that focus on WAP autumn phytoplankton dynamics [39–46]. However, to understand the strongly seasonal WAP ecosystem, biogeochemical data from all seasons is needed. Before these knowledge gaps are addressed in chapter 2, in the following paragraphs the study area is presented with respect to the dominating surface currents, the growth limiting factors and the annual phytoplankton distributions and successions.

1.2.1 Oceanographic characteristics

Two different major surface currents dominate north of the Antarctic Peninsula (Figure 1). The Drake Passage (DP) is a constituent of the ACC. In the vicinity of the WAP, the offshore region is characterized by great depth (>5000 m) [47] and low biomass in comparison to the inshore regions further south [26,48–50]. Furthermore, the waters of the DP and beyond show a decrease in temperature with increasing latitude [51], resulting in comparably warm waters in the northern section of the map in figure 1 [52]. Additionally, the open DP (with exceptions) generally shows lower salinity values than waters further south [51,52] and lower dissolved trace metal concentrations than on-shelf areas [50,53].
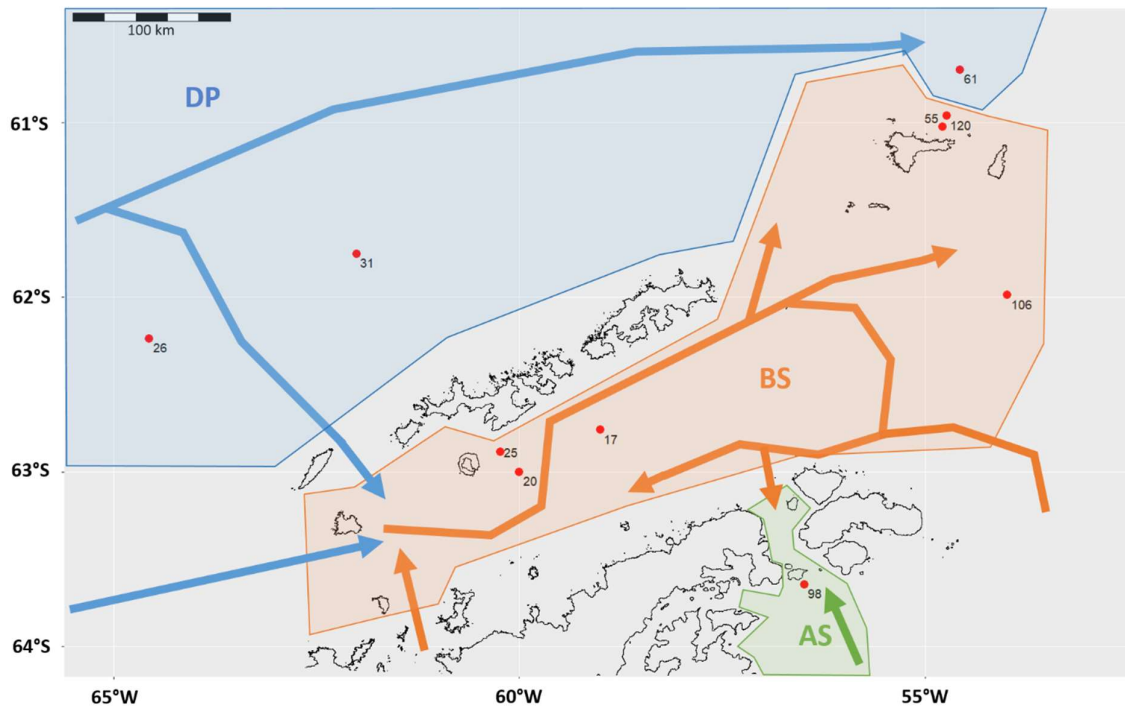
Figure 1 Map of the sampling area, indicating oceanic regions, differentiable by oceanographic characteristics (see chapter 2). Drake Passage (DP) under the influence of the Antarctic Circumpolar Current, Bransfield Strait (BS) under the influence of the Bransfield current, Antarctic sound (AS) under the influence of the Weddell Sea. Red, numbered dots represent sampling locations. Arrows represent dominant surface currents: from the open ocean (blue), under the influence of WAP on-shelf waters (orange) and Weddell Sea influence (green). For details, see chapter 2.

The Brasfield Strait (BS), between the South Shetland Islands and the Antarctic continent, comprises shallow shelf waters and a deep trench immediately south of the islands [47]. The southwest to northeast bound Bransfield Current (BC) [35,54] originates in shelf waters from the southern WAP as well as warm waters with low concentrations of dissolved trace metals from the ACC to the north. Close to the WAP's shores an inverted current transports water masses from the BC and the Weddell Sea from north east to south west [55,56]. Inshore waters are characterized by higher biomass [26,48–50] and higher dissolved trace metal concentrations [50]. Disregarding the depth of the water column, or the proximity to shore, concentrations of macronutrients (nitrogen, phosphorous and silica) are generally high around the WAP [34]. Other factors, such as the presence and availability of Fe, light and manganese (Mn) limit biological production bottom-up, as discussed in the following subchapter, emphasizing on Fe as the limiting factor targeted by one of the presented studies.

1.2.2 Bottom-up growth limitation: Iron, light and manganese

Iron - Fe limitation is considered a strong factor [53,57–61], in the explanation of the low productivity of the SO. *De novo* sources of Fe in the SO are upwelling [48], dust deposition, sea ice [62], resuspension of coastal sediments and erosion from land in form of, for example, glacial run-off [63–66]. Consequently, in vast

areas of the open SO, the potential sources of allochthone Fe (as opposed to Fe recycled inside the water column) are reduced to aeolian dust input, since all other sources are confined to the continent. Disregarding the degree of Fe bioavailability, which is not binary concept [67,68], Fe needs to be truly dissolved beyond the operational definition of solutes (particles <0.2 μm;[69]), to be picked up by cells [70]. The dissolution of Fe however, proves chemically challenging in oxygenated seawater, since Fe is poorly soluble therein. Therefore, although Fe is the fourth most abundant element in the earth's crust (5.63%) [71] dissolved Fe (dFe) concentrations in seawater can be as low as 0.05 nM [72]. In the presence of oxygen, Fe is rapidly oxidized from its soluble and bioavailable form Fe(II) to the poorly soluble Fe(III) [73]. The chief factor increasing Fe(III) solubility is the complexation with ligands to which 99% of Fe in the SO is bound [74,75]. Ligands are organic compounds that facilitate the solution of otherwise poorly soluble substances [74,76]. In doing so, the species of ligands is decisive for the bioavailability of the bound Fe to plankton organisms [77].

Once picked up into an organism, Fe is ideally suited to catalyze essential electron transfer reactions [78], because of its oxidation-reduction properties. Since additionally, the development of live took place in an anoxic, highly reduced ocean with abundant Fe supply [79,80] , Fe has always occupied a pivotal role in living organisms, even after oxygenic photosynthesis oxidized the ocean and made Fe poorly available. In all plant cells, Fe is used in a number of electron transfer chains and enzymes, including photosynthesis and nitrogen fixation [79,81–84]. Fe is the central atom of hemoglobin and myoglobin and therefore of high importance in the transport and storage of oxygen [85] in animals. In microorganisms it is used in processes such as amino acid synthesis, respiration, methanogenesis, the citric acid cycle and DNA biosynthesis [86]. The competition of organisms for the sparse Fe in the epipelagial of many oceans entails a depletion of the surface waters, resulting in concentrations that are only a fraction of those found in the deep [84], consequently leading to a nutrient like depth profile [87]. To cope with limiting conditions, phytoplankton species have evolved different strategies. First, the uptake of Fe mediated by siderophores (strong Fe ligands produced by microorganisms;[88]) or reductive Fe uptake [89] can be maximized [72,78]. Second, Fe requirements can be minimized by stoichiometry changes between Fe intensive compounds and Fe independent compounds, or the replacement of Fe atoms by other trace metals [78,82,90–93]. Third, the cell size can be reduced [78].

Light and Iron - All photoautotrophic life, which includes all phytoplankton, closely depends on light availability [94]. In the extensive periods of polar darkness in the SO, all other factors influencing phytoplankton growth are irrelevant, since the energy source for growth is unavailable. The latitude largely dictates the light regime, both in day length, as well as light intensity determined by the angle of the sun [46,94]. Lower angles lead to a stronger reflection of irradiance [42] making light, even in the long days of polar summer, limiting at times [94]. The light intensity has a strong influence on air and ocean temperature and hence the stratification of the water column, as well as sea-ice melting [95]. Reflexively,

the sea-ice cover [96] and the stratification of the waterbody intensely influence the light availability to phytoplankton cells [97,98] leading to strong interrelations between primary light supply and the effective light availability to phytoplankton, which strongly determines phytoplankton growth. Low surface temperatures, weak density stratification, little summertime surface solar irradiance, and strong wind stress act together in light-limiting growth rates of SO phytoplankton communities [99,100]. If light is available, interrelations between the light and Fe supply unfold. In extension of Liebig's classical description of resource limitation by the law of the minimum [101], Saito et al. (2008) postulated three types of co-limitation [102]. Type III co-limitation is particularly relevant for the SO. It exists, if the presence of one nutrient is necessary to acquire the other. In the SO, Fe and light are type III co-limited at times[59,103–107], since a lack of Fe can alter the efficiency of the photosynthetic apparatus. Fe availability furthermore influences metabolic pathways and thereby impacts the capabilities to make use of other possibly limiting resources [78,81,91,108].

Manganese and Iron - Beyond Fe, Mn is the second most important trace metal in marine phytoplankton as apparent from the extended Redfield Ratio $((C_{106}N_{16}P_1)_{*1000}Fe_8Mn_4Zn_{0.8}Cu_{0.4}Co_{0.2}Cd_{0.2})$[83] and has recently shifted into attention as a potentially limiting trace metal in the SO [109,110]. With increasing light during spring and early summer, Mn-limiting conditions can occur, provided a sufficient Fe input takes place [111]. Factors aggravating Mn limitation are an increase in the ratio of the Mn rich photosystem II to the Fe rich photosystem I [111], or an abundant supply of Zn (common in the SO [112]) Cu and Cd [111,113,114], since all four elements compete for the same transporter as an uptake mechanism. Mn/Fe co-limitations of phytoplankton production can occur [115,116], as reported from the Drake Passage [110], the Weddell Sea [109] and the Ross Sea [117,118] as a result of an increase in the production of reactive oxygen species in photosynthesis under Fe stress, followed by an increased demand of Mn due to its utilization in superoxide dismutase [117]. Excluding the Mn/Fe co-limitation effect, Mn deficiency is confined to near Antarctica, southeast of New Zealand and the Indian Ocean, due to low Mn quotas, caused by high surface dZn concentrations and high growth rates [117]. However, including the Fe-Mn link by reactive oxygen species resulting from photosynthesis, Mn deficiency plays a larger role in the SO [117].

From the bottom-up perspective, the presence and bioavailability of these three limiting factors constitute the frame within which phytoplankton production can take place in the WAP ecosystem.

1.2.3 Phytoplankton production and succession

The phytoplankton (~350 descried species in 2017) forms the biological base of the SO food web [26]. Phytoplankton production close to the WAP exhibits large annual variations [42,119], resulting in an ecosystem of seasonal extremes, in which bloom formations can yield cell concentrations of 10^8 cells L^- ^{1} and chlorophyll a (Chl a) concentrations as high as 50 μg L^{-1} [26], while in winter, primary production (PP) collapses. Bloom formations are strongly correlated to sea-ice retreat. Phytoplankton production in

the WAP area begins with an early peak in the northern offshore regions of the DP, while blooms in the BS begin later, but reach higher biomass and persist over a longer period of time[96]. The phytoplankton community around the WAP is dominated by diatoms and cryptomonads in terms of biomass, but small unidentified flagellates (usually <5 µm) are always dominant in cell numbers [36,120]. While the haptophyte *Phaeocystis antarctica* is found in the ocean around the WAP, blooms of this species are mainly recorded from other regions in Antarctica, such as the Ross Sea or Prydz Bay [121,122]. *P. antarctica* blooms precede diatom bloom formations [121]. Conversely, cryptomonad blooms often succeed diatom blooms [36,123]. The transition between both has been attributed to sedimentation [124], advection [123] and grazing [120]. At the WAP a strong inshore/offshore gradient, both in phytoplankton community composition and biomass has been observed. Exemplarily, a study reported that the dominant genera of diatoms changed from *Odontella*, *Eucampia* and *Thalassiosira* to *Corethron*, *Fragilariopsis* and *Nitzschia* [120] along the gradient, determined by the water masses and their characteristics, the occurrence of fronts and the ice edge [36].

So far, it remains unknown, if the described gradients in biogeochemical characteristics observed in summer, also prevail in austral autumn. The presented dissertation contributes to closing these knowledge gaps by presenting a large set of purposefully collected biogeochemical data from the season of autumn and comparing it to the already existing summer values.

1.3 Planktonic grazers at the Western Antarctic Peninsula

Little information exists on small zooplankton (SZP, merges zooplankton groups <200 µm [29,125]) grazing at the WAP based on dilution experiments and none of the published research broaches the issue of SZP grazing in austral autumn [126–129]. This knowledge gap needs to be closed, since SZP grazing is the dominant sink of biomass in all oceans[130], and could therefore significantly shape the distribution of biomass during the decline of summer phytoplankton blooms, induced by decreasing light and a deepening of the mixed layer in autumn[119]. In addition, grazing measured in dilution experiments so far almost exclusively focused on Chl a as a measured parameter, omitting all grazing on Chl a free organisms and particles. Finally, while the release of Fe by the dominant SO grazers krill and salps has been investigated, no empirical data so far exists that compares the Fe bioavailability between the fecal pellets (FP) of both species, which act as a source of Fe and ligands. Before these knowledge gaps are addressed in chapters 3 (results of 3 dilution experiments from the autumnal WAP, based on a wide array of parameters) and chapter 4 (investigation of the Fe-bioavailability in the presence of krill and salp FP), here the target groups of zooplankton relevant in this dissertation are presented. The focus lies on grazing/predation pressure on the one hand, and Fe recycling on the other.

1.3.1 Grazing and predation

Small zooplankton – Multiple transfer steps of particulate organic carbon (POC) up the trophic chain, as well as significant shares of POC respiration are largely determined by organisms undeterminable by the naked eye, at the base of the planktonic food web [131]. SZP consumes on average between 49-77% of PP worldwide, with numbers in polar waters being slightly lower (53–57%) [130]. In extreme cases, SZP grazing has been shown to account for a phytoplankton mortality between 100% [132,133] and up to 762% [134] of PP in the SO. To describe the community of microorganisms <200 µm, which exists in relationships of commensalism, resource competition and predation, the term 'microbial loop' was coined by Azam et al. in 1983 [135]. The microbial loop hypothesis assumes that bacteria and phytoplankton compete for mineral nutrients [136], while simultaneously bacteria benefit from dissolved organic matter excretion by phytoplankton. Flagellates and other SZP groups influence the outcome of this bottom-up competition by top-down predation pressure [135]. Heterotrophic nanoflagellates (collective term often used to describe the nanozooplankton community) in the size range of 3-10 µm are considered predators of bacteria in the size range of 0.3-1 µm [135]. Thusly, carbon, originating from particles too small for many grazers to ingest effectively, is transported through the food chain via SZP, starting with nanoflagellates feeding on bacteria [135], continuing with microzooplankton and macrozooplankton feeding on nanoplankton [131], to copepods and krill feeding on microzooplankton [137–139] (Figure 2). It is thus evident, that SZP plays a substantial role in the carbon cycle. The microzooplankton members of the SZP community (20-200 µm) in the study area were determined, and comprised mainly tintinnids, aloricate ciliates, heterotrophic dinoflagellates and micrometazoans [140].
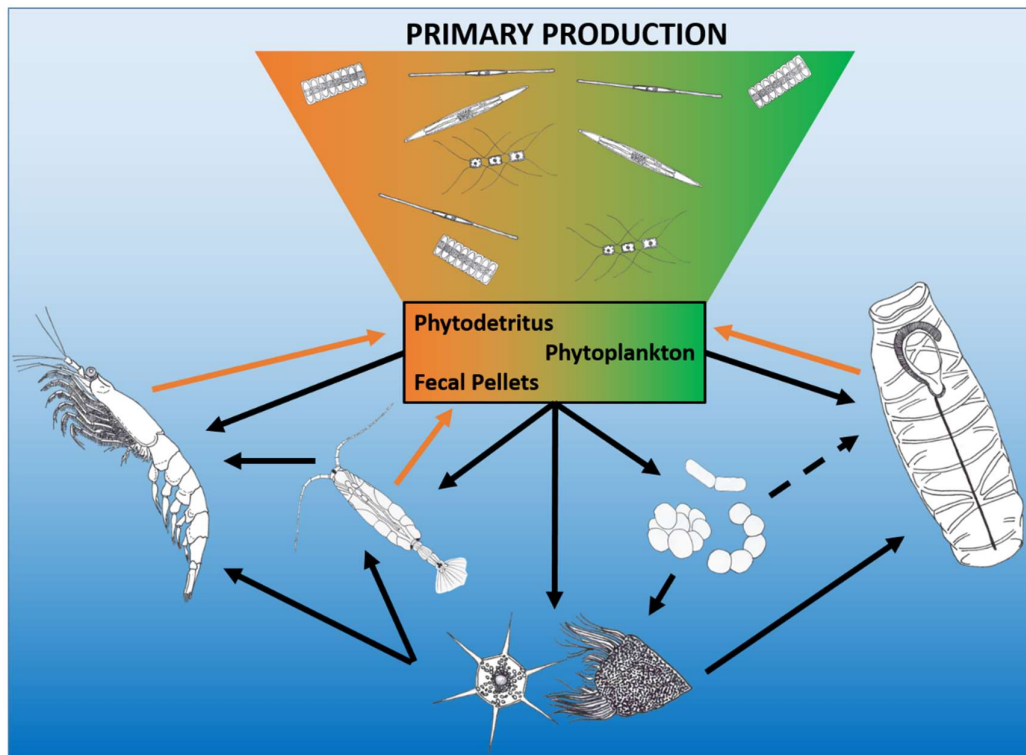
Figure 2 Trophic network in the epipelagial of the Western Antarctic Peninsula. Grazing and predation (black arrows), fecal pellet (FP) production (brown arrows), possible grazing (broken arrow). All depicted heterotrophic groups (bottom left to right: krill, copepods, small zooplankton (SZP), heterotrophic bacteria and salps) are known to feed on (or colonize) FP, thereby hampering the efficiency of the biological carbon pump. Krill, copepods and salps are known to repackage fresh primary production and already egested FP in form of their own FP. SZP grazing of bacteria makes bacterial carbon available to higher grazers like krill and copepods.

Krill - Krill (mostly *Euphausia superba,* hereafter used synonymously) is a planktonic crustacean endemic to the SO, and believed to be one of the most successful animal species living on the planet, reaching $8*10^{14}$ post-larvae individuals with a weight of 379 10^6 t in summer. The post larvae production is estimated conservatively to reach 342-536 10^6 t yr^{-1} [141]. Due to its population size, krill forms a cornerstone of the Antarctic food web, both, as grazer and prey. Between 90 10^6 t and 387 10^6 t of krill are annually consumed by whales, fish, birds and seals [142]. Krill itself, is capable of feeding on a large range of food items [142], like phytoplankton (down to a size of 2-3 μm [142]), resuspended detritus [143], mesozooplankton [142], possibly salps [144] and engages in cannibalism when the food environment becomes severe [145,146] (Figure 2). Predation pressure inflicted by swarms of krill can erase 50.8 – 59 % of PP [147,148] and alter the structure of zooplankton communities by reducing copepod abundance [149]. The central position in the food web in combination with its population size put krill in a pivotal trophic role, funneling primary and secondary production from the nano- and microplankton to higher consumers of the SO ecosystem. Notwithstanding the krill's evidently important role as grazer, prey, nutrient recycler and carbon exporter in the contemporary SO, estimations suggest that the current size of the krill population is only 63% of its pre-whaling size [18,141]. Especially in the region of the Antarctic Peninsula plume the decline in krill stocks is pronounced [150]. Climate change and its subsequent effects lead to a

migration to higher latitudes [151]. Around the WAP as in other regions of the SO krill stocks have experienced a ≥ twofold decrease per decade in the years between 1976-2003 [150]. In formerly krill dominated areas, another filter feeder spreads: Salps.

Salps - While two recognized salp species are found in the SO (*Salpa thompsoni* and *Ihlea racovitzai,* Tunicates) [152], *Salpa thompsoni* (from here on referred to as "salps") is by far the most abundant. Salp abundances have increased in the past decades and are expected to keep growing [141]. In so called 'salp years local swarms of salps (up to 4000 individuals per 1000 m^3 [152]) dominate the planktonic biomass, which is facilitated by a combination of rapid asexual procreation and high consumption rates. This often results in an exclusion of other zooplankton organisms, by depriving them of their food source [152–154], since salps can account for a daily consumption of 0.3-108 % of the daily PP [152]. Although salps utilize a mucus net for feeding, suggesting that they feed on particles indiscriminately [155], a recent discovery has shown that salps are able to feed selectively [156]. While particles between a size of 4 µm up to 1000 µm can be filtered from the water with an efficiency of up to 100 %, [155,157] particles as small as ~1 µm can be retained in the mucus net with a lower efficiency, making salps potentially direct grazers of bacteria (Figure 2). Ingestion rates of salps are among the highest recorded for grazers and the highest ever observed for herbivorous zooplankton in the SO. Clearance rates reached 430 ml h^{-1} for individuals in a size spectrum of 1-5 cm and 5400 ml h^{-1} for the largest individuals in a size spectrum of 5-12 cm [152]. It is however worth noting that salps aren't able to successfully graze in high phytoplankton concentrations (>1 mg Chl m^{-3}) presumably due to a clogging of their filtering apparatus [158]. While many grazers in the SO ecosystem are, to a wide extent, geared towards krill consumption [142], it is incorrect to consider salps a trophic dead end, since they are preyed upon by at least 202 species including fish, turtles, and crustaceans [159]. Despite their translucent body, salps have a high tissue density and nitrogen content. Paired with a soft body and an inability to escape, salps are an easily accessible food source for other organisms [160]. Pakhomov et al. 2002 list species that consume salps in energetically meaningful amounts [161] and even krill has been observed to feed on salps [144].

Summarized, each of the presented zooplankton groups can consume large shares of PP, up to a decrease of standing stock biomass, leading to an exclusion of competitors by food deprivation and direct top-down grazing, if each of the species encounters their respective favorable conditions. Hence, a shaping influence on the primary producers and the ecosystem as a whole in from of top-down pressure can be safely assumed.

1.3.2 Iron recycling by planktonic grazers

It was found that Fe recycled by grazers can be 4-7 fold easier accessible for organisms than inorganic Fe [162]. The supply of Fe to the SO ecosystem by grazer induced recycling has been researched for a few decades [163–165]. Recycling in the photic zone is probably the main source of dFe and ligands [166] and is

greatly facilitated by grazers [162,163,167] and predators [168–171]. Krill stores and recycles macro- and micronutrients in the surface waters of the SO [164,172–175], which can be released by defecation of, and predation on krill [176–178]. Since adult krill does not require all Fe accumulated in its prey >90% of the Fe ingested are excreted. By mechanical and enzymatic destruction of particles, significantly increased Fe dissolution in the acidic, low-oxygen guts of animals [75,173,179], and the production of ligands in the course of digestion, krill directly contributes of 0.2-4.3 nmol Fe L^{-1} d^{-1} [168] to the dFe pool. Furthermore, krill is suspected to actively transport nutrient from large depths (3500 m) to the surface by vertical migration [143,180,181]. While the krill's contribution to Fe recycling has been shown to be substantial, the current results on Fe recycling and release by salps are still ambiguous. While calculations suggests that salps could be responsible for a significant release of Fe [182,183], empirical measurements point the other way [184]. A common point of all studies on the topic with chapter 4 is that in comparison to the total Fe that the excreted FP contain, little (<7%) is released into the water [184–186]. The presented dissertation aims to constraining the actual contributions of krill and salps to the bioavailable pool of dFe (chapter 4), because in Fe limited regions, the bioavailability of Fe directly influences the biological carbon pump.

1.4 The biological carbon pump

The process of atmospheric CO_2 being assimilated into POC and dissolved organic carbon (DOC), which is subsequently transported to the deep sea by sinking particles, advection or vertical mixing, as well as transport by animals is called the biological carbon pump [33,187]. In the previous subchapter processes have been presented, by which planktonic grazers at the WAP stimulate PP (by Fe-fertilization) and simultaneously reduce the amount of PP available for export to depth (by consumption and subsequent POC respiration). How the dynamic equilibrium, determining the mean annual carbon export at the WAP will change precisely, when krill is replaced by salps [150,151] is difficult to predict with certainty, since many interrelations between numerous planktonic groups need to be accounted for. Rough estimations on changes in carbon export, due to a population shift from krill to salps exist, based on the carbon export efficiency of their FP [188]. However, the indirect influences of krill and salps on primary producers and the microbial loop, and the resulting repercussions on the carbon export, remain nebulous. It is paramount to constrain these processes, since carbon sequestration to the deep ocean represents a direct contribution to the reduction of atmospheric CO_2, particular pronounced in the SO, since this region is a major conduit for the transport of anthropogenic CO_2 into the ocean's interior[22]. After the mechanisms of the biological carbon pump have been introduced in the following paragraphs, chapter 5 postulates a hypothesis on how the biological carbon pump will react to a shift from a krill dominance to a salp dominance in the SO, based on all results presented in this dissertation.

It has been assumed that >20% of epipelagic PP exits the proximate surface waters [189]. <10% of PP leaves the euphotic zone in the central gyres [190], while this number can grow up to 30-100% in polar regions [191], stressing the importance of the high latitudes for CO_2 export not only by the solubility pump

(uptake of CO_2 into the waterbody in regions of low temperatures [192]), but also by the biological carbon pump. However, this significant export flux needs to be differentiated from the sequestration flux below 1000 m [193], which amounts to only 3-10% of the fixed carbon [33] due to consumption and respiration. Carbon reaching the deep ocean is considered to be sequestered for 1000 years or more and has even been investigated and controversially discussed as a commercial way for CO_2 sequestration [194–198]. Conversely, carbon remineralized at the bottom of the mesopelagic zone (~1000 m) will only remain 100 years in the ocean [193]. Above that, the storage time is even significantly shorter [193]. Of the >97% of carbon that does not reach the deep sea [33], 15% is processed by bacteria [33], 30-70% by microzooplankton [33,199], and 20-35% by mesozooplankton [200]. Consequently, in order for the biological carbon pump to work, POC must be produced in large quantities[201] and the sinking POC must evade complete zooplankton respiration and remineralization, either by a great sinking velocity, or by mass occurrences, over-saturating grazing capacities.

1.4.1 Zooplankton FP

Aggregated organic material [202] in form of FP appears predestined to fuel the biological carbon pump, due to high sinking velocities (up to 220 m d^{-1} for copepod and appendicularian FP, 504 m d^{-1} for doliolid FP, 646 and 1800 m d^{-1} for heteropod and pteropod FP respectively, and 1313 m d^{-1} for chaetognath FP; [33]). The presence and activity of the different groups of possible grazers, thusly strongly influences the POC sequestration potential and thereby the sequestration potential for the greenhouse gas CO_2 [203]. Krill and salp FP are considered significant drivers of the FP carbon pump [204,205]. At 300 m, a study performed parallel to the here presented works found that salp and krill FP contribute 75% of carbon to the total flux [188]. Both groups combined are believed to repackage and remove 12-37% of phytoplankton production per day into FPs [205]. The sinking rates of krill FPs vary significantly even under laboratory conditions depending on packaging density, pellet volume and mineral ballast between 27-1218 m d^{-1} (median= 304 m d^{-1}) [206]. Sinking rates of salp FP are even larger ranging from 200 to 2700 m d^{-1} across different salp species and depending on the salp's size [207–209], as well as on the structural integrity of the FPs [210]. Besides the sinking velocity, the efficiency of carbon export is logically tied to the carbon content of FP, which falls between 2.25% and 39.2% in salp FP dry weight [209,211–213] and between 0.8 and 29% (median 9.8%) of krill FP dry weight.

In sharp contrast to these considerations, stressing the importance of FP for carbon export, empirical studies proved that only ~13% of the carbon egested into the upper water column reached a depth of 300 m [210]. It has been reported from the WAP that 80% of produced salp FP were retained in the mixed layer due to fragmentation[188]. Coprophagy (ingestion of fecal material) and coprohexi (destruction of fecal material) by copepods and microzooplankton are known processes that reduce the sinking speed of FP material and retaining it in the upper water column [210,214–218] (Figure 2). It has even been suggested that coprohexi increases microbial growth, benefitting zooplankton due to a trophic upgrading of

refractory substances by microorganisms, if the latter are eventually consumed by the zooplankton (microbial gardening) [219,220]. These interactions between different trophic levels in the SO plankton may provide one explanation, why the contribution of FP to carbon export flux in the SO has been reported to be highly variable depending on season and depth (<1-67% in depths between 100-200 m [33,221]). As opposed to the 'passive' flux by FP material, the 'active' downward flux of carbon by zooplankton vertical migration may be as high as 10-50% of total vertical carbon flux [222]. Salps for example, are able to perform daily migrations in the upper 500 m [223] and krill has been encountered down to 3500 m [143], which may have important implications for the flux of carbon into deeper waters.

1.4.2 Phytodetritus

Sedimentation pulses of phytodetritus and marine snow (collective term for aggregated macroscopic particles >500 μm originating from phytodetritus, appendicularian houses, fecal matter, and other miscellaneous detrital particles [33]) from the euphotic zone are an important component of the biological carbon pump. At many investigated sites, these pulses represented the majority of the annual input of organic matter from the epipelagic to the benthos [33]. These pulses of export to significant depths were observed to be often associated with diatoms [33,191,224], which occur in large abundances in the SO. Pulses were observed to occur periodically, due to seasonal plankton blooms, such as the austral summer bloom in the SO. In addition to diatoms, observations suggested a large contribution of picoplankton to the biological carbon pump (87% of POC export via detritus and 76% of carbon exported through the mesozooplankton[225]). Although these high percentages of picoplankton contribution to carbon export were doubted and alternative estimates only reach as high as 23% [226], the contribution of picoplankton to carbon export remains significant. In comparison to FP, the sinking velocities of individual diatom cells (typically <1–10 m d^{-1}) or marine snow particles (10-150 m d^{-1}) are low. If aggregation in itself increases sedimentation velocity has been controversially discussed [33,227–229], but in larger, heterogeneous aggregates, a ballasting of high density particles increase the sedimentation speed of the aggregate as a whole [230,231]. Aggregation can happen by either ingestion and repackaging [202], or by mere collision of particles which are subsequently clustered due to adhesive substances such as transparent exopolymer particles (TEP) [232,233]. While an increased sedimentation velocity generally increases export rates, aggregation can also make small particles available to larger grazers, which in turn can either lead to respiration (counteracting the biological carbon pump) or repackaging in larger FP, further increasing the sedimentation velocity (enhancing the carbon pump).

Summarized, a great variety of players (i.e. phytoplankton, zooplankton, bacteria, TEP) and processes (i.e. production, respiration, repackaging, aggregation) reciprocally influence each other, forming local conditions that result in individual carbon fluxes to depth that vary substantially by season and oceanic area, but in total remove significant shares of CO_2 from the atmosphere.

1.5 Aims and scope

The presented dissertation aims at closing gaps in our understanding of the interplay between grazers and primary producers in the epipelagial of the Southern Ocean (SO), exemplarily assessed at 10 stations around the WAP in austral autumn (Figure 1).

Purposefully collected data from field samples and onboard experiments are presented to investigate the following hypotheses:

1) In austral autumn, plankton biomass distribution, production and micronutrient utilization follows spatial patterns rooted in the influence zones of different SO surface currents.

Chapter 2 investigates regional differences in plankton biomass and production, as well as macronutrient and trace element (trace metals and vitamin B_{12}) concentrations and utilization across the entire sampling area in austral autumn, reaching from the open DP in the north, to the BS in the south.

2) SZP grazing dominates carbon cycling at the WAP in austral autumn.

Chapter 3 describes the importance of SZP grazing in the carbon cycling of the upper water column at three locations around the WAP. Furthermore, the usefulness of other parameters than Chl a, most prominently POC, as a biomass proxy are discussed .

3) A shift from krill to salps results in reduced recycling of bioavailable Fe at the WAP.

Chapter 4 highlights the differences between the two species in respect to total Fe excretion and the bioavailability of the excreted Fe to plankton organisms .

The synopsis of all three publications and the datasets they are based on, allows for the formulation of two concluding hypotheses, which are discussed in chapter 5.

4) The patchy distribution of plankton biomass and production is rooted in the interplay between regional, physicochemical characteristics and local grazing pressure.

Merging the results of chapter 2 and 3, which individually address bottom-up and top-down factors, shaping the WAP ecosystem in austral fall, a unified hypothesis emerges, explaining the distributional patterns of planktonic biomass, which is addressed in chapter 5.2.

5) The shift from krill to salps increases the carbon sequestration potential of the WAP ecosystem.

Evaluating the role of salps on recycling of bioavailable Fe (chapter 4), the microbial loop community and large diatoms, in chapter 5.3 I propose the hypothesis that salps indirectly increase the carbon sequestration potential of the SO.

1.6 List of publications and declaration of own contribution

Publication I

Böckmann, S., Koch, F., Meyer, B. & Trimborn, S. Iron, zinc and vitamin B12 uptake characteristics of fall phytoplankton at the northern Western Antarctic Peninsula. (2024). – In preparation

Content – During Polarstern expedition PS112, the WAP region was sampled at 10 stations for 41 parameters. The results hint towards a differentiation of the sampling area in a northern offshore region in the DP influenced by the ACC and a southern inshore region in the BS, although this differentiation was less decisive than in summer.

Contribution - The sampling was carried out by Florian Koch, Franziska Pausch, Anna Pagnone, Dorothee Wilhelms-Dick and myself. The data was analyzed by myself and with the help of the co-authors. The manuscript was written by myself and revised with the help of the co-authors.

Publication II

Böckmann, S., Trimborn, S., Schubert, H. & Koch, F. Grazing by nano- and microzooplankton on heterotrophic picoplankton dominates the biological carbon cycling around the Western Antarctic Peninsula. Polar Biol. March, (2024).

Content - During Polarstern expedition PS112, dilution experiments were performed to investigate the grazing pressure of SZP on different functional groups inside the plankton community. The results showed that SZP grazing pressure is the dominant POC sink and that POC, rather than the classically investigated Chl a was the parameter, which more reliably yielded interpretable results.

Contribution - The experiment was designed and performed by Florian Koch. The data analysis was done by myself. The data was interpreted by Florian Koch and myself. The manuscript was written by myself and revised with the help of the co-authors.

Publication III

Böckmann, S. et al. Salp fecal pellets release more bioavailable iron to Southern Ocean phytoplankton than krill fecal pellets. Curr. Biol. 31, 1–10 (2021).

Content – During Polarstern expedition PS112, SO seawater was incubated with krill and salp FP. Afterwards, the ambient phytoplankton community was incubated in the preconditioned water. The findings demonstrate that salp FP release more Fe per added FP carbon and that Fe from water incubated with salp FP is more bioavailable than Fe from water incubated with krill FP.

Contribution - The experiment was designed by Scarlett Trimborn, Christel Hassler and Florian Koch and performed by Florian Koch and myself. The data was analyzed by myself and with the help of the co-authors. The manuscript was written by myself and revised with the help of the co-authors.

The declaration of own contribution to multi-author articles and manuscripts can be found at the end of the thesis.

1.7 References cited in chapter 1

1. Griffiths, H. J. Antarctic Marine Biodiversity – What Do We Know About the Distribution of Life in the Southern Ocean? *PLoS One* **5**, e11683 (2010).

2. Orsi, A. H., Whitworth, T. & Nowlin, W. D. On the meridional extent and fronts of the Antarctic Circumpolar Current. *Deep-Sea Research Part I* **42**, 641–673 (1995).

3. Gloersen, P., Campbel, W. J., Cavalieri, D. J., Comiso, J. G. & Parkinson, C. L. *Arctic and Antarctic Sea Ice, 1978 - 1987 Satellite Passive-Microwave Observation and Analysis*. *NASA SP-511* (1992).

4. Grosfeld, K. & Treffeisen, R. Meereisportal. *Alfred-Wegener-Institute for Polar and Marine Research* https://www.meereisportal.de/en/ (2024).

5. Gutt, J., Sirenko, B. I., Smirnov, I. S. & Arntz, W. E. How many macrozoobenthic species might inhabit the Antarctic shelf? *Antarct Sci* **16**, 11–16 (2004).

6. Rintoul, S. R. The global influence of localized dynamics in the Southern Ocean. *Nature* **558**, 209–218 (2018).

7. Hauck, J., Lenton, A., Langlais, C. & Matear, R. The fate of carbon and nutrients exported out of the Southern Ocean. *Global Biogeochem Cycles* **32**, 1–27 (2018).

8. Hempel, G. & Hempel, I. *Faszination Meeresforschung - Ein Ökologisches Lesebuch*. (H. M. Hauschild GmbH, Bremen, 2006).

9. Kalvelage, T. *POLARSTERN - Forschen Im Eis*. (Tessloff Verlag, Nürnberg, 2022).

10. Ainley, D. G. & Pauly, D. Fishing down the food web of the Antarctic continental shelf and slope. *Polar Record* **50**, 92–107 (2014).

11. Rocha, R. C., Clapham, P. J. & Ivashchenko, Y. V. Emptying the oceans: A summary of industrial Whaling catches in the 20th century. *Marine Fisheries Review* **76**, 37–48 (2015).

12. Testa, G., Neira, S., Giesecke, R. & Piñones, A. Projecting environmental and krill fishery impacts on the Antarctic Peninsula food web in 2100. *Prog Oceanogr* **206**, (2022).

13. Grant, S. M., Hill, S. L., Trathan, P. N. & Murphy, E. J. Ecosystem services of the Southern Ocean: Trade-offs in decision-making. *Antarct Sci* **25**, 603–617 (2013).

14. Pershing, A. J., Christensen, L. B., Record, N. R., Sherwood, G. D. & Stetson, P. B. The impact of whaling on the ocean carbon cycle: Why bigger was better. *PLoS One* **5**, 1–9 (2010).

15. Willis, J. Could whales have maintained a high abundance of krill ? *Evol Ecol Res* **9**, 651–662 (2007).

16. Lavery, T. J. *et al.* Whales sustain fisheries: Blue whales stimulate primary production in the Southern Ocean. *Mar Mamm Sci* **30**, 888–904 (2014).

17. Lavery, T. J. *et al.* Iron defecation by sperm whales stimulates carbon export in the Southern Ocean. *Proceedings of the Royal Society B: Biological Sciences* **277**, 3527–3531 (2010).

18. Smetacek, V. *Are Declining Antarctic Krill Stocks a Result of Global Warming or of the Decimation of Whales? Impacts of Global Warming on Polar Ecosystems* (2008).

19. Herr, H. *et al.* Return of large fin whale feeding aggregations to historical whaling grounds in the Southern Ocean. *Sci Rep* **12**, 1–15 (2022).

20. Sarmiento, J. L., Hughes, T. M. C., Stouffer, R. J. & Manabe, S. Simulated response of the ocean carbon cycle to anthropogenic climate warming. *Nature* **393**, 245–249 (1998).

21. Marinov, I., Gnanadesikan, A., Toggweiler, J. R. & Sarmiento, J. L. The Southern Ocean biogeochemical divide. *Nature* **441**, 964–967 (2006).

22. Khatiwala, S., Primeau, F. & Hall, T. Reconstruction of the history of anthropogenic CO2 concentrations in the ocean. *Nature* **462**, 346–349 (2009).

23. Sabine, C. L. *et al.* The Oceanic Sink for Anthropogenic CO2. *Science (1979)* **305**, 367–371 (2004).

24. Caldeira, K. & Duffy, P. B. The Role of the Southern Ocean in Uptake and Storage of Anthropogenic Carbon Dioxide. *Science (1979)* **287**, 620–622 (2000).

25. Riihelä, A., Bright, R. M. & Anttila, K. Recent strengthening of snow and ice albedo feedback driven by Antarctic sea-ice loss. *Nat Geosci* **14**, 832–836 (2021).

26. Deppeler, S. L. & Davidson, A. T. Southern Ocean Phytoplankton in a Changing Climate. *Front Mar Sci* **4**, (2017).

27. Newman, R. & Noy, I. The global costs of extreme weather that are attributable to climate change. *Nat Commun* **14**, (2023).

28. Nielsen, E. S. The use of radio-active carbon (C14) for measuring organic production in the sea. *ICES Journal of Marine Science* **18**, 117–140 (1952).

29. Lalli, C. M. & Parsons, T. R. *Biological Oceanography - An Introduction*. (Elsevier Butterworth-Heinemann, Burlington, 1993). doi:10.1016/0022-0981(96)02604-4.

30. Buitenhuis, E. T. *et al.* MAREDAT: Towards a world atlas of MARine Ecosystem DATa. *Earth Syst Sci Data* **5**, 227–239 (2013).

31. Bar-On, Y. M., Phillips, R. & Milo, R. The biomass distribution on Earth. *Proc Natl Acad Sci U S A* **115**, 6506–6511 (2018).

32. Field, C. B., Behrenfeld, M. J., Randerson, J. T. & Falkowski, P. Primary Production of the Biosphere: Integrating Terrestrial and Oceanic Components. *Science (1979)* **281**, 237–240 (1998).

33. Turner, J. T. Zooplankton fecal pellets, marine snow, phytodetritus and the ocean's biological pump. *Prog Oceanogr* **130**, 205–248 (2015).

34. Steinberg, D., Martinson, D. & Costa, D. Two Decades of Pelagic Ecology of the Western Antarctic Peninsula. *Oceanography* **25**, 56–67 (2012).

35. Meredith, M. P., Stefels, J. & van Leeuwe, M. Marine studies at the western Antarctic Peninsula: Priorities, progress and prognosis. *Deep Sea Research Part II: Topical Studies in Oceanography* **139**, 1–8 (2017).

36. Ducklow, H. W. *et al.* Marine pelagic ecosystems: The West Antarctic Peninsula. *Philosophical Transactions of the Royal Society B: Biological Sciences* **362**, 67–94 (2007).

37. Vaughan, D. G. *et al.* Recent rapid regional warming on the Antarctic Peninsula. *Climate Change* **60**, 243–274 (2003).

38. Lange, P. K., Ligowski, R. & Tenenbaum, D. R. Phytoplankton in the embayments of King George Island (Antarctic Peninsula): A review with emphasis on diatoms. *Polar Record* **54**, 158–175 (2018).

39. Trefault, N. *et al.* Annual phytoplankton dynamics in coastal waters from Fildes Bay, Western Antarctic Peninsula. *Sci Rep* **11**, 1–16 (2021).

40. Selph, K. E. *et al.* Phytoplankton distributions in the Shackleton Fracture Zone/Elephant Island region of the Drake Passage in February-March 2004. *Deep Sea Res 2 Top Stud Oceanogr* **90**, 55–67 (2013).

41. Pan, B. J. *et al.* Environmental drivers of phytoplankton taxonomic composition in an Antarctic fjord. *Prog Oceanogr* **183**, 102295 (2020).

42. Lipski, M. Variations of physical conditions, nutrients and chlorophyll a contents in Admiralty Bay (King George Island, South Shetland islands, 1979). *Pol Polar Res* **8**, 307–332 (1987).

43. Kopczynska, E. E. Annual study of phytoplankton in Admiralty Bay, King George Island, Antarctica. *Pol Polar Res* **17**, 151–164 (1996).

44. Vernet, M. *et al.* Primary production within the sea-ice zone west of the Antarctic Peninsula: I-Sea ice, summer mixed layer, and irradiance. *Deep Sea Res 2 Top Stud Oceanogr* **55**, 2068–2085 (2008).

45. Yilmaz, I. N. *et al.* Effects of Different Commercial Feeds and Enrichments on Biochemical Composition and Fatty Acid Profile of Rotifer (Brachionus Plicatilis, Müller 1786) and Artemia Franciscana. *Turk J Fish Aquat Sci* **18**, 81–90 (2018).

46. van Leeuwe, M. A. *et al.* Annual patterns in phytoplankton phenology in Antarctic coastal waters explained by environmental drivers. *Limnol Oceanogr* **65**, 1651–1668 (2020).

47. Dotto, T. S., Mata, M. M., Kerr, R. & Garcia, C. A. E. A novel hydrographic gridded data set for the northern Antarctic Peninsula. *Earth Syst Sci Data* **13**, 671–696 (2021).

48. de Jong, J. *et al.* Natural iron fertilization of the Atlantic sector of the Southern Ocean by continental shelf sources of the Antarctic Peninsula. *J Geophys Res Biogeosci* **117**, 1–25 (2012).

49. Schulz, I. *et al.* Remarkable structural resistance of a nanoflagellate-dominated plankton community to iron fertilization during the Southern Ocean experiment LOHAFEX. *Mar Ecol Prog Ser* **601**, 77–95 (2018).

50. Trimborn, S., Hoppe, C. J. M., Taylor, B. B., Bracher, A. & Hassler, C. Physiological characteristics of open ocean and coastal phytoplankton communities of Western Antarctic Peninsula and Drake Passage waters. *Deep Sea Res 1 Oceanogr Res Pap* **98**, 115–124 (2015).

51. Gutt, J. *The Expedition on the Research Vessel 'Polarstern' to the Antarctic in 2013 (ANT-XXIX/3). Reports on Polar and Marine Research* vol. 665 (2013).

52. Plum, C. *et al.* Mesozooplankton trait distribution in relation to environmental conditions and the presence of krill and salps along the northern Antarctic Peninsula. *J Plankton Res* **43**, 927–944 (2021).

53. Martin, J. H., Fitzwater, S. E. & Gordon, R. M. Iron deficiency limits phytoplankton growth in Antarctic waters. *Global Biogeochem Cycles* **4**, 5–12 (1990).

54. Zhou, M., Niiler, P. P., Zhu, Y. & Dorland, R. D. The western boundary current in the Bransfield Strait, Antarctica. *Deep Sea Res 1 Oceanogr Res Pap* **53**, 1244–1252 (2006).

55. Sangrà, P. *et al.* The Bransfield current system. *Deep Sea Res 1 Oceanogr Res Pap* **58**, 390–402 (2011).

56. Zhou, X., Zhu, G. & Hu, S. Influence of tides on mass transport in the Bransfield Strait and the adjacent areas, Antarctic. *Polar Sci* **23**, 100506 (2020).

57. Behrenfeld, M. J. & Kolber, Z. Widespread Iron Limitation of Phytoplankton in the South Pacific Ocean. *Science (1979)* **283**, 840–843 (1999).

58. Tagliabue, A. *et al.* The integral role of iron in ocean biogeochemistry. *Nature* **543**, 51–59 (2017).

59. Boyd, P. W. Environmental factors controlling phytoplankton processes in the Southern Ocean. *J Phycol* **38**, 844–861 (2002).

60. Blain, S. & Tagliabue, A. *Iron Cycle in Oceans*. *Iron Cycle in Oceans* (2016). doi:10.1002/9781119136859.

61. Gran, H. H. On the conditions for the production of plankton in the sea. *Rapports et Proces-verbaux des Réunions. Conseil International pour l'Éxploration de la Mer* **75**, 37–46 (1931).

62. Salmon, E., Hofmann, E. E., Dinniman, M. S. & Smith, W. O. Evaluation of iron sources in the Ross Sea. *Journal of Marine Systems* **212**, 103429 (2020).

63. Duce, R. A. & Tindale, N. W. Atmospheric transport of iron and its deposition in the ocean. *Limnol Oceanogr* **36**, 1715–1726 (1991).

64. Lannuzel, D., Schoemann, V., de Jong, J., Tison, J.-L. & Chou, L. Distribution and biogeochemical behaviour of iron in the East Antarctic sea ice. *Mar Chem* **106**, 18–32 (2007).

65. Moore, J. K. & Braucher, O. Sedimentary and mineral dust sources of dissolved iron to the world ocean. *Biogeosciences* **5**, 631–656 (2008).

66. Gerringa, L. J. A. *et al.* Iron from melting glaciers fuels the phytoplankton blooms in Amundsen Sea (Southern Ocean): Iron biogeochemistry. *Deep Sea Research Part II: Topical Studies in Oceanography* **71–76**, 16–31 (2012).

67. Shaked, Y. & Lis, H. Disassembling iron availability to phytoplankton. *Front Microbiol* **3**, (2012).

68. Fourquez, M. *et al.* Chasing iron bioavailability in the Southern Ocean: Insights from Phaeocystis antarctica and iron speciation. *Sci Adv* **9**, (2023).

69. Tagliabue, A. *et al.* Surface-water iron supplies in the Southern Ocean sustained by deep winter mixing. *Nat Geosci* **7**, 314–320 (2014).

70. Rich, H. W. & Morel, F. M. M. Availability of Well-Defined Iron Colloids to the Marine Diatom Thalassiosira weissflogii. *Limnol. Oceanogr.* **35**, 652–662 (1990).

71. Taylor, S. R. Abundance of elements in the crust: A new table. *Geochimica and Cosmochimica Acta* **28**, 1273–1285 (1964).

72. Hudson, R. J. M. & Morel, F. M. M. Iron transport in marine phytoplankton: Kinetics of cellular and medium coordination reactions. *Limnol Oceanogr* **35**, 1002–1020 (1990).

73. Sung, W. & Morgan, J. J. Kinetics and Product of Ferrous Iron Oxygenation in Aqueous Systems. *Environ Sci Technol* **14**, 561–568 (1980).

74. Hassler, C. *et al.* Iron bioavailability in the Southern Ocean. in *Oceanography and Marine Biology: An Annual Review* vol. 50 1–64 (2012).

75. Liu, X. & Millero, F. J. The solubility of iron in seawater. *Mar Chem* **77**, 43–54 (2002).

76. Kuma, K., Nishioka, J. & Matsunaga, K. Controls on iron(III) hydroxide solubility in seawater: The influence of pH and natural organic chelators. *Limnol. Oceanogr.* **41**, 396–407 (1996).

77. Lis, H., Shaked, Y., Kranzler, C., Keren, N. & Morel, F. M. M. Iron bioavailability to phytoplankton: an empirical approach. *ISME J* **9**, 1003–1013 (2015).

78. Morel, F. M. M., Rueter, J. G. & Price, N. M. Iron nutrition of phytoplankton and its possible importance in the ecology of ocean regions with high nutrient and low biomass. *Oceanography* **4**, 56–61 (1991).

79. Behrenfeld, M. J. & Milligan, A. J. Photophysiological Expressions of Iron Stress in Phytoplankton. *Ann Rev Mar Sci* **5**, 217–246 (2013).

80. Rouxel, O. J., Bekker, A. & Edwards, K. J. Iron Isotope Constraints on the Archean and Paleoproterozoic Ocean Redox State. *Science (1979)* **307**, 1088–1091 (2005).

81. Twining, B. S. & Baines, S. B. The Trace Metal Composition of Marine Phytoplankton. *Ann Rev Mar Sci* **5**, 191–215 (2013).

82. Sandmann, G. Consequences of iron deficiency on photosynthetic and respiratory electron transport in blue-green algae. *Photosynth Res* **6**, 261–271 (1985).

83. Morel, F. M. M., Milligan, A. J. & Saito, M. A. Marine Bioinorganic Chemistry: The Role of Trace Metals in the Oceanic Cycles of Major Nutrients. in *Treatise on Geochemistry* (eds. Elderfield, H., Holland, H. D. & Turekian, K. K.) 113–143 (Elsevier, 2003).

84. Morel, F. M. M. The Biogeochemical Cycles of Trace Metals in the Oceans. *Science (1979)* **300**, 944–947 (2003).

85. Moyes, Christopher, D. & Schulte, Patricia, M. *Tierphysiologie*. (Pearson Education Deutschland GmbH, München, 2006).

86. Sandy, M. & Butler, A. Microbial Iron Acquisition: Marine and Terrestrial Siderophores. *Chem Rev* **109**, 4580–4595 (2009).

87. Martin, J. H. Glacial-interglacial CO2 change: The Iron Hypothesis. *Paleoceanography* **5**, 1–13 (1990).

88. Goldman, S. J., Lammers, P. J., Berman, M. S. & Sanders Loehr, J. Siderophore-mediated in iron uptake in different strains of Anabaena sp. *J Bacteriol* **156**, 1144–1150 (1983).

89. Shaked, Y., Kustka, A. B. & Morel, F. M. M. A general kinetic model for iron acquisition by eukaryotic phytoplankton. *Limnol Oceanogr* **50**, 872–882 (2005).

90. Sunda, W. G., Swift, D. G. & Huntsman, S. A. Low iron requirement for growth in oceanic phytoplankton. *Nature* **351**, 55–57 (1991).

91. Strzepek, R. F., Hunter, K. A., Frew, R. D., Harrison, P. J. & Boyd, P. W. Iron-light interactions differ in Southern Ocean phytoplankton. *Limnol Oceanogr* **57**, 1182–1200 (2012).

92. Sandmann, G. & Böger, P. COPPER-INDUCED EXCHANGE OF PLASTOCYANIN AND CYTOCHROME c-533 IN CULTURES OF ANABAENA VARIABILIS AND PLECTONEMA BORYANUM. *Plant Sci Lett* **17**, 417–424 (1980).

93. Sandmann, G. & Malkin, R. Iron-Sulfur Centers and Activities of the Photosynthetic Electron Transport Chain in Iron-Deficient Cultures of the Blue-Green Alga Aphanocapsa. *Plant Physiol* **73**, 724–728 (1983).

94. Bazzani, E., Lauritano, C. & Saggiomo, M. Southern Ocean Iron Limitation of Primary Production between Past Knowledge and Future Projections. *J Mar Sci Eng* **11**, (2023).

95. Clarke, A., Meredith, M. P., Wallace, M. I., Brandon, M. A. & Thomas, D. N. Seasonal and interannual variability in temperature, chlorophyll and macronutrients in northern Marguerite Bay, Antarctica. *Deep Sea Res 2 Top Stud Oceanogr* **55**, 1988–2006 (2008).

96. Ferreira, A. *et al.* Climate change is associated with higher phytoplankton biomass and longer blooms in the West Antarctic Peninsula. *Nat Commun* **15**, (2024).

97. Smith, W. O. & Jones, R. M. Vertical mixing, critical depths, and phytoplankton growth in the Ross Sea. *ICES Journal of Marine Science* **72**, 1952–1960 (2015).

98. Sverdrup, H. U. On conditions for the vernal blooming of phytoplankton. *Journal du Conseil International pour l'Exploraton de la Mer* **18**, 287–295 (1953).

99. Mitchell, B. G., Brody, E. A., Holm-Hansen, O., McClain, C. & Bishop, J. Light limitation of phytoplankton biomass and macronutrient utilization in the Southern Ocean. *Limnol Oceanogr* **36**, 1662–1677 (1991).

100. Nelson, D. M. & Smith, W. Sverdrup revisited: Critical depths, maximum chlorophyll and the control of Southern Ocean productivity by the irradiance-mixing regime. *Limnol Oceanogr* **36**, 1650–1661 (1991).

101. Liebig, J. *Chemistry in Its Application to Agriculture and Physiology*. (London, 1847).

102. Saito, M. A., Goepfert, T. J. & Ritt, J. T. Some thoughts on the concept of colimitation: Three definitions and the importance of bioavailability. *Limnol Oceanogr* **53**, 276–290 (2008).

103. Boyd, P. W. *et al.* Control of phytoplankton growth by iron supply and irradiance in the subantarctic Southern Ocean: Experimental results from the SAZ Project. *J Geophys Res Oceans* **106**, 31573–31583 (2001).

104. Sunda, W. G. & Huntsman, S. A. Interrelated influence of iron, light and cell sizeonmarine phytoplanktongrowth. *Nature* **2051**, 389–392 (1997).

105. Boyd, P. *et al.* Role of iron, light, and silicate in controlling algal biomass in subantarctic waters SE of New Zealand. *Geo* **104**, 395–408 (1999).

106. Moore, C. M. *et al.* Iron-light interactions during the CROZet natural iron bloom and EXport experiment (CROZEX) I: Phytoplankton growth and photophysiology. *Deep Sea Res 2 Top Stud Oceanogr* **54**, 2045–2065 (2007).

107. Moore, C. M., Hickman, A. E., Poulton, A. J., Seeyave, S. & Lucas, M. I. Iron-light interactions during the CROZet natural iron bloom and EXport experiment (CROZEX): II-Taxonomic responses and elemental stoichiometry. *Deep Sea Res 2 Top Stud Oceanogr* **54**, 2066–2084 (2007).

108. Price, N. M., Ahner, B. A. & Morel, F. M. M. The equatorial Pacific Ocean: Grazer-controlled phytoplankton populations in an iron-limited ecosystem. *Limnol Oceanogr* **39**, 520–534 (1994).

109. Balaguer, J. *et al.* Iron and manganese availability drives primary production and carbon export in the Weddell Sea. *Current Biology* **33**, 4405-4414.e4 (2023).

110. Balaguer, J., Koch, F., Hassler, C. & Trimborn, S. Iron and manganese co-limit the growth of two phytoplankton groups dominant at two locations of the Drake Passage. *Commun Biol* **5**, 1–12 (2022).

111. Hawco, N. J., Tagliabue, A. & Twining, B. S. Manganese Limitation of Phytoplankton Physiology and Productivity in the Southern Ocean. *Global Biogeochem Cycles* **36**, (2022).

112. Ye, N. *et al.* The role of zinc in the adaptive evolution of polar phytoplankton. *Nat Ecol Evol* **6**, 965–978 (2022).

113. Sunda, W. G. Feedback interactions between trace metal nutrients and phytoplankton in the ocean. *Front Microbiol* **3**, 1–22 (2012).

114. Sunda, W. G. & Huntsman, S. A. Antagonisms between cadmium and zinc toxicity and manganese limitation in a coastal diatom. *Limnol Oceanogr* **41**, (1996).

115. Lohan, M. C. & Tagliabue, A. Oceanic micronutrients: Trace metals that are essential for marine life. *Elements* **14**, 385–390 (2018).

116. Browning, T. J. & Moore, C. M. Global analysis of ocean phytoplankton nutrient limitation reveals high prevalence of co-limitation. *Nat Commun* **14**, 1–12 (2023).

117. Anugerahanti, P. & Tagliabue, A. Process controlling iron-manganese regulation of the Southern Ocean biological carbon pump. *Philosophical Transactions of the Royal Society A: Mathematical, Physical and Engineering Sciences* **381**, (2023).

118. Wu, M. *et al.* Manganese and iron deficiency in Southern Ocean Phaeocystis antarctica populations revealed through taxon-specific. *Nat Commun* 1–10 (2019) doi:10.1038/s41467-019-11426-z.

119. Vernet, M. *et al.* Primary production throughout austral fall, during a time of decreasing daylength in the western Antarctic Peninsula. *Mar Ecol Prog Ser* **452**, 45–61 (2012).

120. Garibotti, I. A. *et al.* Phytoplankton spatial distribution patterns along the western Antarctic Peninsula (Southern Ocean). *Mar Ecol Prog Ser* **261**, 21–39 (2003).

121. Smith, W. O. & Trimborn, S. Annual Review of Marine Science Phaeocystis: A Global Enigma. *Annual Review of Marine Science* 417–441 (2024).

122. Smith, W. O. Primary productivity measurements in the Ross Sea, Antarctica: A regional synthesis. *Earth Syst Sci Data* **14**, 2737–2747 (2022).

123. Moline, M. A. & Prézelin, B. B. Long-term monitoring and analyses of physical factors regulating variability in coastal Antarctic phytoplankton biomass, in situ productivity and taxonomic composition over subseasonal, seasonal and interannual time scales. *Mar Ecol Prog Ser* **145**, 143–160 (1996).

124. Castro, C. G., Ríos, A. F., Doval, M. D. & Pérez, F. F. Nutrient utilisation and chlorophyll distribution in the Atlantic sector of the Southern Ocean during Austral summer 1995-96. *Deep Sea Res 2 Top Stud Oceanogr* **49**, 623–641 (2002).

125. Dussart, B. H. Les différentes catégories de plancton. *Hydrobiologia* **26**, 72–74 (1965).

126. Burkill, P. H., Edwards, E. S. & Sleight, M. A. Microzooplankton and their role in controlling phytoplankton growth in the marginal ice zone of the Bellingshausen Sea. *Deep Sea Research Part II: Topical Studies in Oceanography* **42**, 1277–1290 (1995).

127. Tsuda, A. & Kawaguchi, S. Microzooplankton grazing in the surface water of the Southern Ocean during an austral summer. *Polar Biol* **18**, 240–245 (1997).

128. Garzio, L., Steinberg, D., Erickson, M. & Ducklow, H. Microzooplankton grazing along the Western Antarctic Peninsula. *Aquatic Microbial Ecology* **70**, 215–232 (2013).

129. Price, L. M. Microzooplankton Community Structure and Grazing Impact Along the Western Antarctic Peninsula. (College of William and Mary, 2012). doi:10.25773/v5-8b8j-1h33.

130. Schmoker, C., Hernández-León, S. & Calbet, A. Microzooplankton grazing in the oceans: impacts, data variability, knowledge gaps and future directions. *J Plankton Res* **35**, 691–706 (2013).

131. Laval-Peuto, M., Heinbokel, J. F., Anderson, O. R., Rassoulzadegan, F. & Sherr, B. F. Role of micro- and nanozooplankton in marine food webs. *Int J Trop Insect Sci* **7**, 387–395 (1986).

132. Li, C., Sun, S., Zhang, G. & Ji, P. Summer feeding activities of zooplankton in Prydz Bay, Antarctica. *Polar Biol* **24**, 892–900 (2001).

133. Pearce, I., Davidson, A. T., Thomson, P. G., Wright, S. & van den Enden, R. Marine microbial ecology off East Antarctica (30 - 80°E): Rates of bacterial and phytoplankton growth and grazing by heterotrophic protists. *Deep Sea Res 2 Top Stud Oceanogr* **57**, 849–862 (2010).

134. Pearce, I., Davidson, A. T., Wright, S. & Van Den Enden, R. Seasonal changes in phytoplankton growth and microzooplankton grazing at an Antarctic coastal site. *Aquatic Microbial Ecology* **50**, 157–167 (2008).

135. Azam, F. *et al.* The Ecological Role of Water-Column Microbes in the Sea. *Mar Ecol Prog Ser* **10**, 257–263 (1983).

136. Ratnarajah, L. *et al.* Resource Colimitation Drives Competition Between Phytoplankton and Bacteria in the Southern Ocean. *Geophys Res Lett* **48**, 1–11 (2021).

137. Berk, S. G., Brownlee, D. C., Heinle, D. R., Kling, H. J. & Colwell, R. R. Ciliates as a food source for marine planktonic copepods. *Microb Ecol* **4**, 27–40 (1977).

138. Calbet, A. & Saiz, E. The ciliate-copepod link in marine ecosystems. *Aquatic Microbial Ecology* **38**, 157–167 (2005).

139. Schmidt, K., Atkinson, A., Petzke, K.-J., Voss, M. & Pond, D. W. Protozoans as a food source for Antarctic krill, Euphausia superba: Complementary insights from stomach content, fatty acids, and stable isotopes. *Limnol Oceanogr* **51**, 2409–2427 (2006).

140. Monti-Birkenmeier, M. *et al.* Spatial distribution of microzooplankton in different areas of the northern Antarctic Peninsula region, with an emphasis on tintinnids. *Polar Biol* **44**, 1749–1764 (2021).

141. Atkinson, A., Siegel, V., Pakhomov, E. A., Jessopp, M. J. & Loeb, V. A re-appraisal of the total biomass and annual production of Antarctic krill. *Deep Sea Res 1 Oceanogr Res Pap* **56**, 727–740 (2009).

142. Siegel, V. *Biology and Ecology of Antarctic Krill*. (Springer International Publishing, 2016). doi:10.1007/978-3-319-29279-3.

143. Clarke, A. & Tyler, P. A. Adult Antarctic Krill Feeding at Abyssal Depths. *Current Biology* **18**, 282–285 (2008).

144. Kawaguchi, S. & Takahashi, Y. Antarctic krill (Euphausia superba Dana) eat salps. *Polar Biol* **16**, 479–481 (1996).

145. Price, H. J., Boyd, K. R. & Boyd, C. M. Omnivorous feeding behavior of the Antarctic krill Euphausia superba. *Mar Biol* **97**, 67–77 (1988).

146. Hamner, W. M. & Hamner, P. P. Behavior of Antarctic krill (*Euphausia superba*): schooling, foraging, and antipredatory behavior. *Canadian Journal of Fisheries and Aquatic Sciences* **57**, 192–202 (2000).

147. Perissinotto, R., Pakhomov, E. A., McQuaid, C. D. & Froneman, P. W. In situ grazing rates and daily ration of Antarctic krill Euphausia superba feeding on phytoplankton at the Antarctic Polar Front and the Marginal Ice Zone. *Mar Ecol Prog Ser* **160**, 77–91 (1997).

148. Pakhomov, E. A., Perissinotto, R., Froneman, P. W. & Miller, D. G. M. Energetics and feeding dynamics of euphausia superba in the South Georgia region during the summer of 1994. *J Plankton Res* **19**, 399–423 (1997).

149. Atkinson, A., Ward, P., Hill, A., Brierley, A. S. & Cripps, G. C. Krill-copepod interactions at South Georgia, Antarctica, II. Euphausia superba as a major control on copepod abundance. *Mar Ecol Prog Ser* **176**, 63–79 (1999).

150. Atkinson, A., Siegel, V., Pakhomov, E. & Rothery, P. Long-term decline in krill stock and increase in salps within the Southern Ocean. *Nature* **432**, 100–103 (2004).

151. Atkinson, A. *et al.* Krill (Euphausia superba) distribution contracts southward during rapid regional warming. *Nat Clim Chang* **9**, 142–147 (2019).

152. Perissinotto, R. & A. Pakhomov, E. The trophic role of the tunicate Salpa thompsoni in the Antarctic marine ecosystem. *Journal of Marine Systems* **17**, 361–374 (1998).

153. Park, C. & Wormuth, J. H. Distribution of antarctic zooplankton around Elephant Island during the austral summers of 1988, 1989, and 1990. *Polar Biol* **13**, 215–225 (1993).

154. Heron, A. C. Population ecology of a colonizing species: The pelagic tunicate Thalia democratica - I. Individual growth rate and generation time. *Oecologia* **10**, 269–293 (1972).

155. Madin, L. P. Field observations on the feeding behavior of salps (Tunicata: Thaliacea). *Mar Biol* **25**, 143–147 (1974).

156. Pauli, N.-C. *et al.* Selective feeding in Southern Ocean key grazers—diet composition of krill and salps. *Commun Biol* **4**, 1061 (2021).

157. Harbison, G. R. & McAlister, V. L. The filter-feeding rates and particle retention efficiencies of three species of Cyclosalpa (Tunicata, Thaliacea). *Limnol Oceanogr* **24**, 875–892 (1979).

158. Perissinotto, R. & Pakhomov, E. A. Feeding association of the copepod Rhicalanus gigas with the tunicate salp Salpa thompsoni in the southern ocean. *Mar Biol* **127**, 479–483 (1997).

159. Henschke, N., Everett, J. D., Richardson, A. J. & Suthers, I. M. Rethinking the Role of Salps in the Ocean. *Trends Ecol Evol* **31**, 720–733 (2016).

160. Heron, A., McWilliam, P. & Dal Pont, G. Length-weight relation in the salp Thalia democratica and potential of salps as a source of food. *Mar Ecol Prog Ser* **42**, 125–132 (1988).

161. Pakhomov, E. A., Froneman, P. W. & Perissinotto, R. Salp/krill interactions in the Southern Ocean: spatial segregation and implications for the carbon flux. *Deep Sea Research Part II: Topical Studies in Oceanography* **49**, 1881–1907 (2002).

162. Nuester, J., Shema, S., Vermont, A., Fields, D. M. & Twining, B. S. The regeneration of highly bioavailable iron by meso- and microzooplankton. *Limnol Oceanogr* **59**, 1399–1409 (2014).

163. Hutchins, D. A. & Bruland, K. W. Grazer-mediated regeneration and assimilation of Fe, Zn and Mn from planktonic prey. *Mar Ecol Prog Ser* **110**, 259–270 (1994).

164. Ratnarajah, L., Nicol, S. & Bowie, A. R. Pelagic Iron Recycling in the Southern Ocean: Exploring the Contribution of Marine Animals. *Front Mar Sci* **5**, 1–9 (2018).

165. Ratnarajah, L. Regenerated iron : How important are different zooplankton groups to oceanic productivity ? *Current Biology* **31**, R848–R850 (2021).

166. Boyd, P. W., Ibisanmi, E., Sander, S. G., Hunter, K. A. & Jackson, G. A. Remineralization of upper ocean particles: Implications for iron biogeochemistry. *Limnol Oceanogr* **55**, 1271–1288 (2010).

167. Sarthou, G. *et al.* The fate of biogenic iron during a phytoplankton bloom induced by natural fertilisation: Impact of copepod grazing. *Deep Sea Res 2 Top Stud Oceanogr* **55**, 734–751 (2008).

168. Tovar-Sanchez, A., Duarte, C. M., Hernández-León, S. & Sañudo-Wilhelmy, S. A. Krill as a central node for iron cycling in the Southern Ocean. *Geophys Res Lett* **32**, 1–4 (2007).

169. Nicol, S. *et al.* Southern Ocean iron fertilization by baleen whales and Antarctic krill. *Fish and Fisheries* **11**, 203–209 (2010).

170. Wing, S. *et al.* Seabirds and marine mammals redistribute bioavailable iron in the Southern Ocean. *Mar Ecol Prog Ser* **510**, 1–13 (2014).

171. Ratnarajah, L. *et al.* Physical speciation and solubility of iron from baleen whale faecal material. *Mar Chem* **194**, 79–88 (2017).

172. Atkinson, A. *et al.* South Georgia, Antarctica: A productive, cold water, pelagic ecosystem. *Mar Ecol Prog Ser* **216**, 279–308 (2001).

173. Schmidt, K. *et al.* Zooplankton Gut Passage Mobilizes Lithogenic Iron for Ocean Productivity. *Current Biology* **26**, 2667–2673 (2016).

174. Lehette, P., Tovar-Sánchez, A., Duarte, C. M. & Hernández-León, S. Krill excretion and its effect on primary production. *Mar Ecol Prog Ser* **459**, 29–38 (2012).

175. Ratnarajah, L. & Bowie, A. R. Nutrient Cycling: Are Antarctic Krill a Previously Overlooked Source in the Marine Iron Cycle? *Current Biology* **26**, R884–R887 (2016).

176. Ratnarajah, L., Bowie, A. R., Lannuzel, D. & Klaus, M. The Biogeochemical Role of Baleen Whales and Krill in Southern Ocean Nutrient Cycling. *PLoS One* 1–18 (2014) doi:10.1371/journal.pone.0114067.

177. Ratnarajah, L. *et al.* Understanding the variability in the iron concentration of Antarctic krill. *Limnol Oceanogr* **61**, 1651–1660 (2016).

178. Ratnarajah, L. *et al.* A preliminary model of iron fertilisation by baleen whales and Antarctic krill in the Southern Ocean : Sensitivity of primary productivity estimates to parameter uncertainty. *Ecol Modell* **320**, 203–212 (2016).

179. Tang, K. W., Glud, R. N., Glud, A., Rysgaard, S. & Nielsen, T. G. Copepod guts as biogeochemical hotspots in the sea: Evidence from microelectrode profiling of Calanus spp. *Limnol Oceanogr* **56**, 666–672 (2011).

180. Marin, V. H., Brinton, E. & Huntley, M. Depth relationships of Euphausia superba eggs, larvae and adults near the Antarctic Peninsula, 1986-87. *Deep Sea Research Part A, Oceanographic Research Papers* **38**, 1241–1249 (1991).

181. Kunze, E., Dower, J. F., Beveridge, I., Dewey, R. & Bartlett, K. P. Observations of biologically generated turbulence in a coastal inlet. *Science (1979)* **249**, 484–493 (2006).

182. Strohal, P., Tuta, J. & Kolar, Z. INVESTIGATIONS OF CERTAIN MICROCONSTITUENTS IN TWO TUNICATES1. *Limnol Oceanogr* **14**, 265–268 (1969).

183. Maldonado, M. T., Surma, S. & Pakhomov, E. A. Southern Ocean biological iron cycling in the pre-whaling and present ecosystems. *Philosophical Transactions of the Royal Society A: Mathematical, Physical and Engineering Sciences* **374**, 20150292 (2016).

184. Cabanes, D. J. E. *et al.* First Evaluation of the Role of Salp Fecal Pellets on Iron Biogeochemistry. *Front Mar Sci* **3**, 1–10 (2017).

185. Schlosser, C. *et al.* Mechanisms of dissolved and labile particulate iron supply to shelf waters and phytoplankton blooms off South Georgia, Southern Ocean. *Biogeosciences* **15**, 4973–4993 (2018).

186. Schmidt, K. *et al.* Seabed foraging by Antarctic krill: Implications for stock assessment, bentho-pelagic coupling, and the vertical transfer of iron. *Limnol Oceanogr* **56**, 1411–1428 (2011).

187. Ducklow, H. H. W., Steinberg, D. D. K., Buessler, K. & Buesseler, K. O. Upper ocean carbon export and the biological pump. *Oceanography- ...* **14**, 50–58 (2001).

188. Pauli, N.-C. *et al.* Krill and salp faecal pellets contribute equally to the carbon flux at the Antarctic Peninsula. *Nat Commun* **12**, 7168 (2021).

189. Buesseler, K. O. & Boyd, P. W. Shedding light on processes that control particle export and flux attenuation in the twilight zone of the open ocean. *Limnol Oceanogr* **54**, 1210–1232 (2009).

190. Neuer, S. *et al.* Differences in the biological carbon pump at three subtropical ocean sites. *Geophys Res Lett* **29**, 3–6 (2002).

191. Buesseler, K. O. The decoupling of production and particulate export in the surface ocean. *Global Biogeochem Cycles* **12**, 297–310 (1998).

192. Raven, J. A. & Falkowski, P. G. Oceanic sinks for atmospheric CO2. *Plant Cell Environ* **22**, 741–755 (1999).

193. Passow, U. & Carlson, C. A. The biological pump in a high CO2 world. *Mar Ecol Prog Ser* **470**, 249–271 (2012).

194. Boyd, P. W. *et al.* A mesoscale phytoplankton bloom in the polar Southern Ocean stimulated by iron fertilization. *Nature* **407**, 695–702 (2000).

195. Coale, K. H. *et al.* Southern ocean iron enrichment experiment: Carbon cycling in high and low Si waters. *Science (1979)* **304**, 408–14 (2004).

196. Buesseler, K. O. & Boyd, P. W. CLIMATE CHANGE: Will Ocean Fertilization Work? *Science (1979)* **300**, 67–68 (2003).

197. Smetacek, V. *et al.* Deep carbon export from a Southern Ocean iron-fertilized diatom bloom. *Nature* **487**, 313–319 (2012).

198. de Baar, H. J. W. Synthesis of iron fertilization experiments: From the Iron Age in the Age of Enlightenment. *J Geophys Res* **110**, C09S16 (2005).

199. Calbet, A. & Landry, M. R. Phytoplankton growth, microzooplankton grazing, and carbon cycling in marine systems. *Limnol Oceanogr* **49**, 51–57 (2004).

200. Hernández-León, S. & Ikeda, T. A global assessment of mesozooplankton respiration in the ocean. *J Plankton Res* **27**, 153–158 (2005).

201. Ratnarajah, L. *et al.* Distribution and export of particulate organic carbon in East Antarctic coastal polynyas. *Deep Sea Res 1 Oceanogr Res Pap* **190**, (2022).

202. Burd, A. B. & Jackson, G. A. Particle aggregation. *Ann Rev Mar Sci* **1**, 65–90 (2009).

203. McNair, H. M., Morison, F., Graff, J. R., Rynearson, T. A. & Menden-Deuer, S. Microzooplankton grazing constrains pathways of carbon export in the subarctic North Pacific. *Limnol Oceanogr* **66**, 2697–2711 (2021).

204. Clarke, A., Quetin, L. B. & Ross, R. M. Laboratory and field estimates of the rate of faecal pellet production by Antarctic krill, Euphausia superba. *Mar Biol* **98**, 557–563 (1988).

205. Pakhomov, E. A. Salp/krill interactions in the eastern Atlantic sector of the Southern Ocean. *Deep Sea Res 2 Top Stud Oceanogr* **51**, 2645–2660 (2004).

206. Atkinson, A., Schmidt, K., Fielding, S., Kawaguchi, S. & Geissler, P. A. Variable food absorption by Antarctic krill: Relationships between diet, egestion rate and the composition and sinking rates of their fecal pellets. *Deep Sea Research Part II: Topical Studies in Oceanography* **59–60**, 147–158 (2012).

207. Phillips, B., Kremer, P. & Madin, L. P. Defecation by Salpa thompsoni and its contribution to vertical flux in the Southern Ocean. *Mar Biol* **156**, 455–467 (2009).

208. Pakhomov, E. A., Dubischar, C. D., Strass, V., Brichta, M. & Bathmann, U. V. The tunicate Salpa thompsoni ecology in the Southern Ocean. I. Distribution, biomass, demography and feeding ecophysiology. *Mar Biol* **149**, 609–623 (2006).

209. Bruland, K. W. & Silver, M. W. Sinking rates of fecal pellets from gelatinous zooplankton (Salps, Pteropods, Doliolids). *Mar Biol* **63**, 295–300 (1981).

210. Iversen, M. H. *et al.* Sinkers or floaters? Contribution from salp pellets to the export flux during a large bloom event in the Southern Ocean. *Deep Sea Research Part II: Topical Studies in Oceanography* **138**, 116–125 (2017).

211. Small, L. F., Fowler, S. W., Moore, S. A. & LaRosa, J. Dissolved and fecal pellet carbon and nitrogen release by zooplankton in tropical waters. *Deep Sea Research Part A, Oceanographic Research Papers* **30**, 1199–1220 (1983).

212. Bathmann, U. V. Mass occurrence of Salpa fusiformis in the spring of 1984 off Ireland: implications for sedimentation processes. *Mar Biol* **97**, 127–135 (1988).

213. Caron, D. A., Madin, L. P. & Cole, J. J. Composition and degradation of salp fecal pellets: Implications for vertical flux in oceanic environments. *J Mar Res* **47**, 829–850 (1989).

214. Gonzalez, H. E. & Smetacek, V. The possible role of the cyclopoid copepod Oithona in retarding vertical flux. *PoLAR* **113**, 233–246 (1994).

215. Poulsen, L. K. & Kiørboe, T. Coprophagy and coprorhexy in the copepods Acartia tonsa and Temora longicornis: Clearance rates and feeding behaviour. *Mar Ecol Prog Ser* **299**, 217–227 (2005).

216. Poulsen, L. K. & Iversen, M. H. Degradation of copepod fecal pellets: Key role of protozooplankton. *Mar Ecol Prog Ser* **367**, 1–13 (2008).

217. Svensen, C., Riser, C. W., Reigstad, M. & Seuthe, L. Degradation of copepod faecal pellets in the upper layer: Role of microbial community and Calanus finmarchicus. *Mar Ecol Prog Ser* **462**, 39–49 (2012).

218. Iversen, M. H. & Poulsen, L. K. Coprorhexy, coprophagy, and coprochaly in the copepods Calanus helgolandicus, Pseudocalanus elongatus, and Oithona similis. *Mar Ecol Prog Ser* **350**, 79–89 (2007).

219. Iversen, M. H. Is microbial gardening a food gamble or a safe bet? (Comment on DOI 10.1002/bies.201400100). *BioEssays* **36**, 1126 (2014).

220. Mayor, D. J., Sanders, R., Giering, S. L. C. & Anderson, T. R. Microbial gardening in the ocean's twilight zone: Detritivorous metazoans benefit from fragmenting, rather than ingesting, sinking detritus: Fragmentation of refractory detritus by zooplankton beneath the euphotic zone stimulates the harvestable productio. *BioEssays* **36**, 1132–1137 (2014).

221. Smith, W. O., Shields, A. R., Dreyer, J. C., Peloquin, J. A. & Asper, V. Interannual variability in vertical export in the Ross Sea: Magnitude, composition, and environmental correlates. *Deep Sea Res 1 Oceanogr Res Pap* **58**, 147–159 (2011).

222. Bollens, S., Quenette, J. & Rollwagen-Bollens, G. Predator-enhanced diel vertical migration in a planktonic dinoflagellate. *Mar Ecol Prog Ser* **447**, 49–54 (2012).

223. Nishikawa, J. & Tsuda, A. Diel vertical migration of the tunicate Salpa thompsoni in the Southern Ocean during summer. *Polar Biol* **24**, 299–302 (2001).

224. Buesseler, K. O. *et al.* Revisiting Carbon Flux Through the Ocean's Twilight Zone. *Science (1979)* **316**, 567–570 (2007).

225. Richardson, T. L. & Jackson, G. A. Small Phytoplankton and Carbon Export from the Surface Ocean. *Science (1979)* **315**, 838–840 (2007).

226. Stukel, M. R. & Landry, M. R. Contribution of picophytoplankton to carbon export in the equatorial Pacific: A reassessment of food web flux inferences from inverse models. *Limnol Oceanogr* **55**, 2669–2685 (2010).

227. Shanks, A. L. The abundance, vertical flux, and still-water and apparent sinking rates of marine snow in a shallow coastal water column. *Cont Shelf Res* **22**, 2045–2064 (2002).

228. Iversen, M. H. & Ploug, H. Ballast minerals and the sinking carbon flux in the ocean: Carbon-specific respiration rates and sinking velocity of marine snow aggregates. *Biogeosciences* **7**, 2613–2624 (2010).

229. Iversen, M. H. & Lampitt, R. S. Size does not matter after all: No evidence for a size-sinking relationship for marine snow. *Prog Oceanogr* **189**, 102445 (2020).

230. Iversen, M. H., Nowald, N., Ploug, H., Jackson, G. A. & Fischer, G. High resolution profiles of vertical particulate organic matter export off Cape Blanc, Mauritania: Degradation processes and ballasting effects. *Deep Sea Res 1 Oceanogr Res Pap* **57**, 771–784 (2010).

231. Iversen, M. H. & Robert, M. L. Ballasting effects of smectite on aggregate formation and export from a natural plankton community. *Mar Chem* **175**, 18–27 (2015).

232. Passow, U. Production of transparent exopolymer particles (TEP) by phyto- and bacterioplankton. *Mar Ecol Prog Ser* **236**, 1–12 (2002).

233. Passow, U. Transparent exopolymer particles (TEP) in aquatic environments. *Prog Oceanogr* **55**, 287–333 (2002).

2

PUBLICATION 1

IRON, ZINC AND VITAMIN B$_{12}$ UPTAKE
CHARACTERISTICS OF AUTUMN PHYTOPLANKTON
AT THE NORTHERN TIP OF THE WESTERN
ANTARCTIC PENINSULA

In preparation

Iron, zinc and vitamin B_{12} uptake characteristics of autumn phytoplankton at the northern tip of the Western Antarctic Peninsula

Sebastian Böckmann[1,2], Florian Koch[2], Bettina Meyer[3,4,5], Scarlett Trimborn[2,*]

[1] Department of Marine Botany, University of Bremen, Bremen, Germany

[2] Department of Ecological Chemistry, Alfred Wegener Institute, Helmholtz Center for Polar and Marine Research, Bremerhaven, Germany

[3] Department Polar Biological Oceanography, Alfred Wegener Institute Helmholtz Centre for Polar and Marine Research, Bremerhaven, Germany

[4] Institute for Chemistry and Biology of the Marine Environment, University of Oldenburg, 26129, Oldenburg, Germany

[5] Helmholtz Institute for Functional Marine Biodiversity (HIFMB), Oldenburg, Germany

*Corresponding author and lead contact: scarlett.trimborn@awi.de

---

Author contribution

F.K. conceived and designed research. F.K. and S.B. conducted the field work. S.B. analyzed the data and wrote the first draft. All authors contributed to writing, review and editing. Funding was acquired by S.T. and B.M. This study was supervised by F.K. and S.T.

Acknowledgements

Abstract

Very little information on trace metal (TM) availability, phytoplankton TM uptake rates and their implications for biomass buildup and primary production (PP) in the Western Antarctic Peninsula (WAP) region exist for autumn. Here, we present an extensive dataset (41 measured and calculated biogeochemical parameters from 10 stations) covering the months of March and April 2018. We compiled a picture of biomass distribution and trace element utilization (Fe, Zn and vitamin B_{12}) in relation to environmental physico-chemical conditions. The distribution of hydrographic parameter values and trace element concentrations suggested a differentiation of the sampling area in a northern offshore zone under the influence of the Antarctic Circumpolar Current and a southern inshore zone in the Bransfield Strait. Overall, parameter values representing biomass and PP were higher inshore than offshore. Still, this gradient, characteristic for summer, was less pronounced during autumn. Generally, biomass and production values were lower than in summer during this study but aligned well with the few results published on the season and region. No clear trace metal limitation was deducible from the data, drawing the picture of a system in which biological production collapsed due to light shortage at the end of its annual growth season.

Introduction

The Western Antarctic Peninsula (WAP) is one of the most biologically diverse and productive parts of Antarctica [1]. It yields seasonally high primary production (PP) rates [2] amounting to an annual production of ~182 g C m^{-2} y^{-1} [3], which supports large numbers of grazers like krill and salps, which in turn serve as food to top predators like seabirds and marine mammals [2,4]. Simultaneously, the WAP is one of the fastest-warming regions in Antarctica. Its heating rate (3.7 ± 1.6 °C century^{-1}) significantly exceeds the planetary rate of global warming (0.6 ± 0.2 °C in the 20th century) by several times [5]. Additionally, the WAP, as a high-latitude ecosystem, exhibits a strong seasonality. The onset of plankton growth in spring builds up on a replenishment of nutrients in the surface waters by wind driven deep winter mixing and is initiated by the increasing availability of light linked to an increasing day length and increasing light intensity due to a higher solar angle [6]. Subsequently, rising temperatures induce a melting of sea ice, which, on the one hand, forms a thin surface layer of low-density seawater, supporting rapid phytoplankton growth [6] and, on the other, releases dissolved iron (dFe) [7] and phytoplankton cells [6]. Thus, the melting ice seeds the open water with primary producers and potentially limiting nutrients. All effects combined result in an onset of phytoplankton growth at the transition from the sea-ice zone to the open water, progressing inshore, following the retreating ice [8]. Stronger water stratification, supported by increasing water temperatures in the surface ocean [9], positively influences the light availability [10] during summer. Satellite data showed that the peak of chlorophyll a (Chl a) in the Drake Passage (DP) is reached on average already between November and December, while in the Bransfield Strait (BS) Chl a concentrations reach their maximum values between December and February and exhibit a noticeable decline between March and April [11]. Long term satellite observations supported the influence of sea-ice, identifying its extend as the main driver controlling the length of phytoplankton blooms in early autumn [11]. The studies also highlight that Chl a concentrations in autumn have increased during the last decades [12], from which they draw the conclusion that climate change may increase PP in the WAP region, particularly in autumn [11]. While these general trends are well constrained, the mechanisms controlling the dynamics of the rich, but highly variable coastal plankton communities are not well described in detail [6].

Oceanographically, at the northern tip of the WAP, two distinct regions can be defined: The off-shelf area in the DP under the influence of the Antarctic Circumpolar Current (ACC) and the on-shelf areas, south of the ACC's boundary [1,13]. The off-shelf SO is characterized by low dissolved iron (dFe)

concentrations [14]. The deficiency of Fe is considered to be growth limiting for phytoplankton [15], leaving vast amounts of nitrogen and phosphorous unused and resulting in so called high nitrogen, low chlorophyll (HNLC) areas. This general observation was confirmed for the DP [14,16]. In contrast, regarding phytoplankton and krill production, the shelf waters around the South-Shetland Islands, to which the BS belongs, are among the most productive waters in the Antarctic [17]. High dFe values on the shelf occur due to benthic Fe diffusion and sediment resuspension supported by high turbulence in areas of rugged bottom topography [14].

The WAP's biological oceanographic features stimulated many field studies in the past. However, most studies focused on the WAP's plankton community dynamics from spring to summer, with an overall shortage of studies in autumn or year-round measuring series, including autumn and winter as a result of the logistical challenges to work under high latitude winter conditions [18,19]. To the author's knowledge, only 8 field studies exist that report autumn phytoplankton dynamics at the WAP [6,19–24]. The currently published body of literature suggests that the autumn community at the WAP is characterized by, in comparison to summer [9,25] low surface Chl a values [19,20,23,26], low primary production (PP) [23] and low biomass [22,23] due to shortening day length and a deepening of the mixed layer [23]. Since macronutrients are rarely growth-limiting in the SO, except for transient nitrogen limitation in the uppermost surface ocean [27], macronutrients are still abundant in autumn [19]. In contrast, in autumn dFe was significantly lower than 1 nM at various stations around the northern tip of the WAP [21]. In general, compared to biomass parameters trace metal (TM) and vitamin B_{12} uptake rates are rarely measured and reported [28] and exist only for spring and summer, although low cobalt and vitamin B_{12} concentrations have been reported as potentially limiting [29,30]. Likewise, for the WAP, Fe uptake of offshore and onshore phytoplankton communities was only quantified during summer (Trimborn et al. 2015), and information on zinc (Zn) and vitamin B_{12} uptake by phytoplankton at the WAP is to our knowledge non-existent. Also, information on bacterial production (BP), as well as direct measurements of particulate organic carbon and nitrogen (POC and PON) so far, is lacking for phytoplankton at the WAP during autumn. However, a proper representation of all seasons is the basis for understanding the WAP ecosystem in its year-round succession, because the seasonality is particularly pronounced in high latitude regions and, therefore, decisive for the dynamics of the system [19,22–24].

To fill this knowledge gap, this study aimed to describe plankton biomass distribution in relation to macronutrient and trace element (Fe, Zn and vitamin B_{12}) concentrations and utilization around the WAP in autumn. It highlights the regional differences between stations in the DP north of the Southern Shetland Islands under the influence of the Antarctic Circumpolar Current (ACC), the inner BS, and the Antarctic Sound (AS) being under the influence of the Weddell Sea.

Material & Methods

This study was performed in the framework of the POSER project (**Po**pulation **s**hift and **e**cosystem **r**esponse - krill vs. salps), aboard RV Polarstern (PS112) between March and May 2018. Figure 1 shows the sampling area in the DP (stations 26, 31, 55, 61 and 120), BS (stations 17, 20, 25 and 106), and the AS (station 98). At stations 26, 61 and 106, using a polyethylene line connected to an ALMATEC membrane pump, after 1 h of flushing, Antarctic seawater was sampled carefully (laminar flow, 3-6 L min^{-1}, bubble-free bottle filling) using trace metal clean techniques, successfully used since 2014 [16,31,32]. At all other stations, water was sampled using an acid-cleaned 30 L go-flow bottle. All samples were taken from a depth of 25 m.
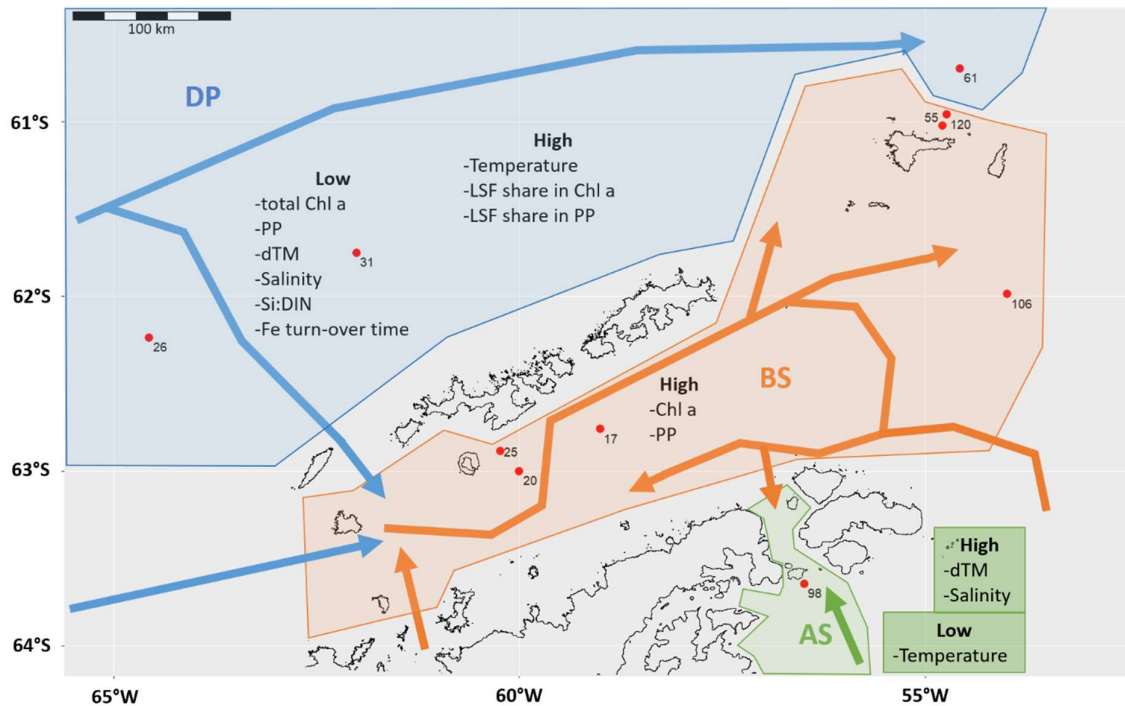
Figure 1 Overview of sampling area. Arrows show main surface current patters in the Drake Passage (DP, blue), Bransfield Strait (BS, brown) and Antarctic Sound (AS, green), which were taken from Zhou et al., 2006, 2020; Sangrà et al., 2011; Meredith et al., 2017. *At 10 stations (red dots) biogeochemical parameters were measured. Parameters, which were particularly high or low in the respective regions are listed in the figure: Dissolved trace metal concentrations (dTM), chlorophyll a (Chl a), primary production (PP), dissolved silicate to dissolved inorganic nitrogen ratio (Si:DIN), iron (Fe). LSF represents the large size fraction of particulate matter >2 µm.*

Hydrographic parameters

Geocoordinates, depth, temperature and salinity were measured using the ship's sensors. Seawater pH was measured on the NBS scale with a pH-meter (827 pH mobile with Aquatrode plus Pt1000 electrode, Metrohm, Herisau, Switzerland) calibrated with a three-point calibration (buffers certified by National Institute of Standards and Technology) [36]. Throughout the manuscript, concentrations are given in square brackets (e.g. "…the concentration(s) of Chl a…" reads: "…the [Chl a]…".

dTM

The procedure of dTM measurements was identical to dFe analysis in Böckmann et al., 2021: Samples for the determination of total [dTM] were taken in a clean room container. 100 mL from each treatment bottle were filtered on two trace metal clean filtration racks over a 0.2 µm filter with a negative pressure of 200 mbar applied. The filtrate was used to sample for dTM. In between samplings all equipment involved was rinsed 30 min in 1 M HCl and MilliQ (18.2 MΩ.cm). Back at AWI Bremerhaven prior to analysis, all seawater samples were acidified to pH 1.7 with sub-boiled HNO_3 (distilled 65% HNO_3, pro analysis, Merck). [dTM] in seawater samples were analyzed via standard addition using a SeaFAST system (Elemental Scientific) coupled to an Element2 (Thermo Scientific) mass spectrometer. Therefore, each seawater samples was separated into 4 aliquots and spiked with commercially available ICP-MS single element standards (SCP Science 1000 mg L^{-1}). Standards for external calibration were prepared from seawater spiked with commercially available ICP-MS single element standards (SCP Science; 1000 mg L^{-1}). The SeaFAST system eliminates matrix components, such as the major ions in seawater (Na, Mg, and Cl) and preconcentrates the samples by a factor of 40. This procedure reduces possible interferences by the matrix and enables to analyze expected low concentrations of elements of interest. The Nass-7 reference material was used to validate the quality of the analysis of trace elements

in seawater at the beginning and end of a batch run. Because the element concentrations of the reference material were much higher than the concentrations expected in the seawater samples, the reference material was analyzed in a 1:10 dilution. The analysis of the Nass-7 reference material (n = 6) showed good results.

To identify contaminations or measurement errors, the consistency of the 5 [dTM] values were tested among each other. For each station ranks were assigned to each [dTM], with 1 representing the lowest [dTM] and 10 representing the highest [dTM] within the dataset. If a [dTM] showed a strong deviation from the remaining 4, this was considered indicative of a contamination, or wrong measurement. The rank table is not shown in the manuscript.

Macronutrients

Samples for inorganic macronutrients were taken by filtering 10 mL samples from all treatments through a 0.2 μm syringe filter (ThermoFisher Scientific) into a 15 mL polyethylene sample vial (Falcon). Samples were stored at -2m0 °C until analysis. The inorganic nutrients were measured on an Evolution III autoanalyser (Alliance Instruments GmbH, Salzburg, Austria). Methods were modified after Grasshoff et al. (1999) and manufacturer's instructions (Seal Analytical, https://seal-analytical.com, accessed June 27, 2019) [37]. Ammonium was determined with a slightly modified method after Holmes et al., 1999.

Chl a

Total Chl a samples were collected by filtering samples onto glass fiber filters (GF/F, pore size ∼0.6 μm, Whatman). In addition, size fractionated samples were taken, where the small size fraction (SSF) included particles <2 μm, while the large size fraction (LSF) consisted of particles >2 μm. Chl a samples in the LSF were collected by filtration of the LSF on a 2 μm polycarbonate filter. Chl a in the SSF was collected by subtracting the Chl a in the LSF from the total Chl a. All filters were stored frozen until subsequent analysis via standard fluorometric methods [39] on a Trilogy Fluorometer (Turner Designs) using the non-acidification module.

POC & PON

POC and PON were sampled, by filtering water (total POC and total PON) and 2 μm filtrate (SSF POC and SSF PON) onto precombusted (15 h, 500 °C) glass fiber filters (GF/F, pore size ∼0.6 μm, Whatman). The filters were stored at −20 °C and dried for >12 h at 60 °C prior to sample preparation. The analysis was performed using a Euro Vector CHNS-O elemental analyzer (Euro Elemental Analyzer 3000, HEKAtech GmbH, Wegberg, Germany) and by utilization of the Callidus 5.1 software. Contents of POC and PON were corrected for blank measurements and normalized to filtered volume.

BP and PP

PP measurements were carried out according to Koch et al., 2011. Briefly: 0.37 MBq of ^{14}C-bicarbonate (Perkin Elmer) was added to triplicate bottles and incubated in an on-deck incubator, allowing for ambient temperature and light conditions. Incubations were terminated after 24 h by filtering up to 100 mL from each bottle onto 0.2 μm pore size polycarbonate filters. At the beginning and end of the incubation, a 250 μL aliquot of each bottle was removed to quantify total activity. After degassing the filters to remove any leftover ^{14}C-bicarbonate and adding scintillation cocktail, samples were measured with a scintillation counter (PackardCarb2100TR) and rates calculated according to JGOFS [41]. BP was estimated using the Kirchman et al., 1985 ^{3}H-Leucine incorporation technique, further adapted for microcentrifuges by Smith and Azam, 1992. Samples were collected from the CTD and five 1.5 mL aliquots were incubated at in situ temperatures conditions in the dark, after adding radioactive ^{3}H-Leucine (Perkin Elmer, specific activity 123.8 Ci mmol^{-1}) and non-radioactive leucine for a total leucine concentration of 20 nM. To two of the five replicates, 200 μL of 50% trichloroacetic acid (TCA) was

added (final concentration 5% vol:vol) at the beginning of the incubation (dead controls). After a two hour incubation, TCA was also added to the remaining three samples in order to terminate leucine incorporation and all samples were centrifuged for 10 min at 16000 g. After carefully removing the supernatant, 1.5 mL of cold 5% TCA was added, the sample was vortexed and again spun down as described above. Finally, the supernatant was removed, 1.5 mL of UltimateGold uLLt (Perkin Elmer) liquid scintillation cocktail was added and the samples were analyzed on a Tri-Carb 2900 TR (Perkin Elmer) liquid scintillation counter. Rates of leucine incorporation was then calculated according to Fourquez et al., 2020.

Fe, Zn and vitamin B_{12} uptake

Assuming low ambient Fe, Zn and vitamin B_{12} concentrations [40] and to avoid any possible concentration effects on uptake rates [45], a trace amount of 950 Bq of $^{55}FeCl_3$ and $^{65}ZnCl_3$ (specific activity 117.07 Ci/g and 329 Ci/g, respectively, Perkin Elmer, MA, USA) and 950 Bq of $^{57}Co\text{-}B_{12}$ (specific activity 7.84 MBq μg^{-1}, MP-Biomedical) was added to triplicate, 200 ml water samples in polycarbonate bottles. After an incubation period of 24 h in on deck incubators at ambient light and temperature conditions the cells were size fractionated by filtering them onto 0.2 and 2 mm filters, allowing for the determination of size class specific uptake of the tracer [40]. For the ^{55}Fe samples, each filter was rinsed 3 times with oxalate solution that was gravity-filtered for approx. 2 min between each rinsing step, followed by 3 rinses with natural 0.2 mm filtered seawater [46]. Finally, each filter was collected in a scintillation vial, amended with 10 mL scintillation cocktail (Ultima Gold, Perkin Elmer) and mixed thoroughly (Vortex). Counts per min were estimated for each sample on the shipboard scintillation counter (Tri-Carb2900TR). Counts per min were then converted into disintegrations per min taking into account the radioactive decay and custom quench curves. Uptake of ^{55}Fe, ^{65}Zn and $^{57}Co\text{-}B_{12}$ uptake was calculated by using the equation:

$$((\frac{A_f}{A_{tot}}) * [TE]) / t$$

where A_f is the activity on the filters, A_{tot} is the total activity added, [TE] is the ambient concentration of the trace metal/B_{12} + the concentration added with the tracer and t equals the length of the incubation in hours.

Photophysiology

In order to assess the photophysiological efficiency (F_v/F_m) of the in situ phytoplankton community, a fast repetition rate fluorometer (FRRf) in combination with a FastAct Laboratory system (FastOcean PTX), both from Chelsea Technologies Group ltd. was used (same method as described in Böckmann et al., 2021). All measurements were taken at 2°C following a 60 min dark acclimation period, assuring that all photosystem II (PSII) reaction centers were fully oxidized and non-photochemical quenching was relaxed. Iterative algorithms for the induction and relaxation phases were applied to estimate minimum Chl a fluorescence (F_0) and maximum Chl a fluorescence (F_m). The apparent maximum quantum yield of photosynthesis of PSII (F_v/F_m) could then be calculated according to the equation

$$\frac{F_v}{F_m} = \frac{F_m - F_0}{F_m}$$

Furthermore, the functional absorption cross section of PSII (σ_{PSII}) was assessed.

Statistical analyses

Multiple correlation analyses were performed for the entire dataset at the $p = 0.05$ significance thresholds using the Spearman algorithm. Large sets of parameters that show a high variance of values are likely to return numerous significant correlations of parameter pairs, which are not significantly correlated, if tested alone. Therefore, the p-values of each parameter pair were tested by individual correlation

analysis of two parameters at a time. The rank-based Spearman correlation was used to minimize the influence of stations with exceptionally high values on the correlation analysis, such as station 17 (Table 1). Turnover times were calculated for dFe and dZn by dividing the respective dTM pool by the uptake rate [47] (Table 3). Statistical significance of differences in individual parameter values between regions were tested using the t-test.

Results

Hydrographic and nutrient setting

All 10 stations were sampled in austral autumn, from the end of March to the end of April (Table 1, Figure 1). The water temperature ranged from 1.6°C to -1.8°C, with warmest water temperatures measured north of the South Shetland Islands (DP, stations 26, 31 and 61) and coldest water found in the AS (station 98). Salinity ranged from 33.7 to 34.3 (Table 1). The surface water's pH ranged between 7.71 and 8.01 and showed no discernable correlation to the stations' geographic locations. Macronutrients (P, N and Si) concentrations were not depleted at any of the sampled stations (Table 1). The lowest [Si] were measured at the off-shelf DP stations 26, 31 and 61, while all other stations had [Si] > 60 µM. Also, lowest [dTM] were recorded for the offshore DP stations (Table 1). The [dFe] was lowest at offshore DP station 61 (0.29 nmol L^{-1}), while values for all other stations were higher, ranging from 1.31 ± 0.03 to 3.76 ± 0.13 nmol L^{-1}. At station 26, the [dCu] was very low, while at station 55, the [dCo] was very high in comparison to all other stations, but consistent with other high [dTM] at this station and therefore considered valid.

Table 1 Hydrographic conditions and nutrient concentrations ([nutrient]) at each station sampled at 25 m depth. Stations were clustered according to the sampling region: Drake Passage (DP) under the influence of the ACC, Bransfield Strait (BS) under the influence of the BC, Antarctic Sound (AS). Station number (#), latitude (Lat), longitude (Long), surface water temperature (Temp [°C]), surface water salinity (Sal), phosphate (PO$_4$, [μmol L^{-1}]), silicate (Si, [μmol L^{-1}]), dissolved inorganic nitrogen (DIN, [μmol L^{-1}]), dissolved iron (dFe), dissolved manganese (dMn), dissolved cobalt (dCo), dissolved copper (dCu) and dissolved zinc (dZn). Dissolved trace metal concentrations given in nmol L^{-1}, except for dCo, which is given in pmol L^{-1} at all stations. Missing values are marked n.d. [Macronutrients] measurements are shown as mean ± standard deviation of 2 replicates, [TM] are shown as mean ± standard deviation of 3 replicates.

Region	#	Date	Lat	Long	Temp	Sal	pH	[PO$_4$]	[Si]	[DIN]	[dFe]	[dMn]	[dCo]	[dCu]	[dZn]
DP	26	04/02	-62.24	-64.56	1.2	33.7	7.92	1.69 ± 0.02	23.5 ± 0.2	26.9 ± 0.2	n.d.	0.09 ± 0.01	28 ± 0	1.01 ± 0.01	2.23 ± 0.14
DP	31	04/03	-61.75	-62.01	1.6	33.8	7.85	1.72 ± 0.00	44.8 ± 0.2	27.3 ± 0.2	1.31 ± 0.31	0.42 ± 0.03	38 ± 1	1.33 ± 0.02	5.05 ± 0.47
DP	61	04/11	-60.7	-54.57	1.4	33.8	7.96	1.86 ± 0.00	58.5 ± 1.1	29.2 ± 0.1	0.29 ± 0.01	0.98 ± 0.01	51 ± 0	1.30 ± 0.02	3.33 ± 0.08
BS	17	03/25	-62.76	-59.01	0.7	34.2	7.99	1.07 ± 0.01	63.7 ± 0.1	22.5 ± 0.1	1.85 ± 0.03	2.51 ± 0.03	82 ± 0	1.53 ± 0.03	3.90 ± 0.08
BS	20	03/26	-63.00	-60.00	-0.2	34.3	7.75	1.74 ± 0.10	66.4 ± 4.0	26.8 ± 2.1	3.76 ± 0.13	2.62 ± 0.01	76 ± 1	1.77 ± 0.00	6.28 ± 0.12
BS	25	04/01	-62.89	-60.24	1.1	34.1	7.71	1.59 ± 0.01	72.9 ± 0.4	27.2 ± 0.1	1.88 ± 0.15	3.05 ± 0.03	73 ± 1	1.71 ± 0.03	4.84 ± 0.52
BS	55	04/08	-61.02	-54.79	1.1	34.1	8.01	1.87 ± 0.01	73.1 ± 0.7	29.4 ± 0.2	3.09 ± 0.03	3.21 ± 0.03	163 ± 2	1.69 ± 0.01	5.72 ± 0.10
BS	106	04/20	-61.99	-53.99	0.9	34.2	7.74	1.92 ± 0.00	77.5 ± 0.3	29.7 ± 0.1	1.65 ± 0.05	1.85 ± 0.05	63 ± 5	1.52 ± 0.02	5.40 ± 0.15
BS	120	04/27	-60.96	-54.74	0.9	33.7	7.95	1.90 ± 0.01	75.5 ± 0.6	29.6 ± 0.1	1.31 ± 0.03	2.18 ± 0.04	73 ± 2	1.59 ± 0.05	n.d.
AS	98	04/17	-63.65	-56.49	-1.8	34.3	7.88	1.99 ± 0.01	70.1 ± 0.2	29.7 ± 0.2	3.13 ± 0.03	3.60 ± 0.06	116 ± 3	1.50 ± 0.03	6.20 ± 0.10

Biomass parameters

In comparison to all other stations, at station 17 markedly elevated values of [Chl a], [POC] and PP were observed (Figure 2). At the other stations, [Chl a] and [POC] were lower. Even though biomass was low, this did not preclude elevated PP rates for some stations (31, 61, 25 and 120). Overall PP ranged between 2 and 27 µg C L^{-1} d^{-1}. Generally, the PP was low, and showed a patchy distribution in space and time (Figure 2C). Only for stations 17, 25 and 120 PP exceeded 20 µg C L^{-1} d^{-1}. Similar to PP, Supplementary Table 1 shows that BP was highest at station 25 (0.90 ± 0.19 µg C L^{-1} d^{-1}) and second highest at station 17 (0.59 ± 0.02 µg C L^{-1} d^{-1}), but in contrast to PP, station 120 showed low values of BP (0.07 ± 0.00 µg C L^{-1} d^{-1}).

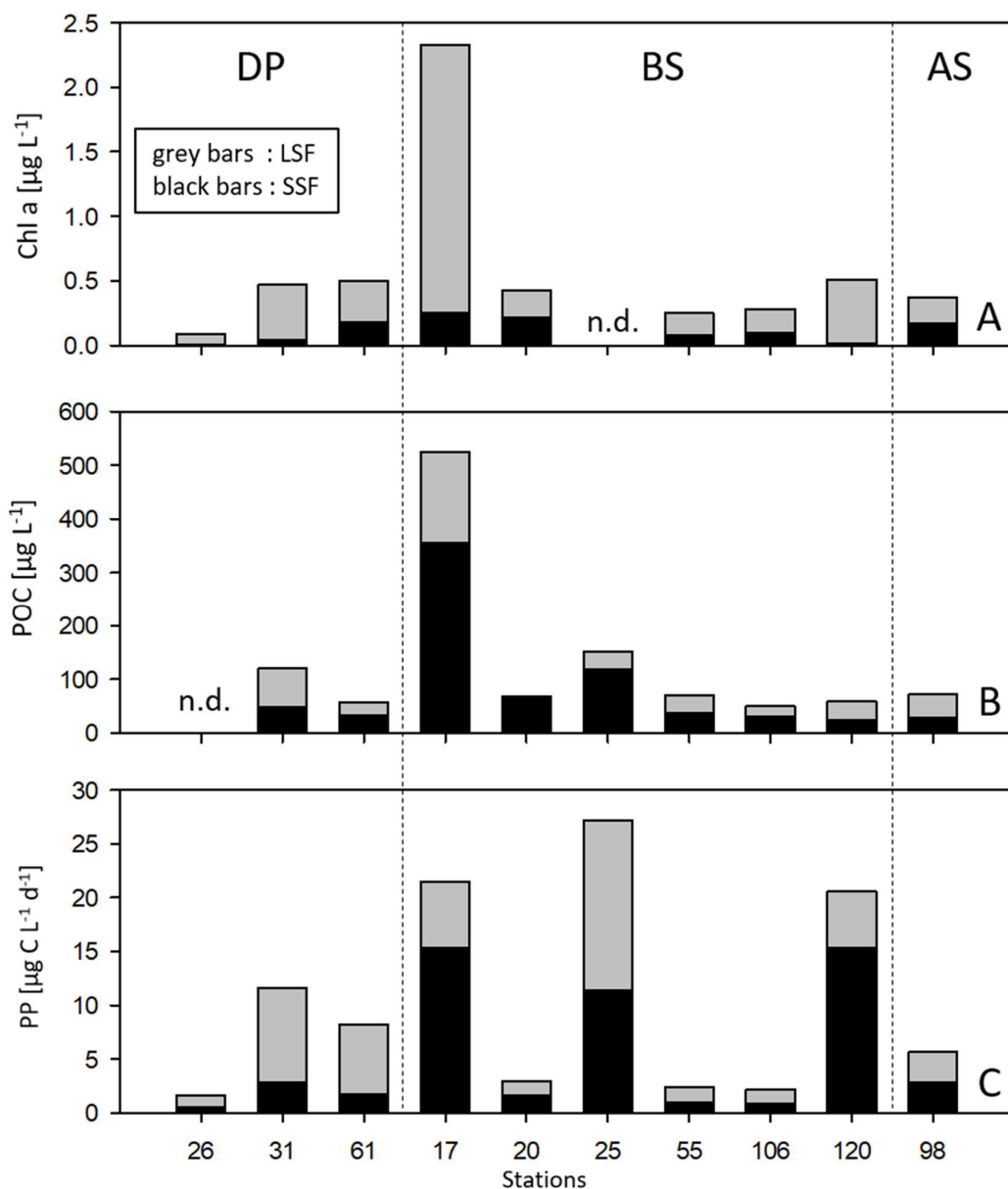*Figure 1 Biomass parameters differentiated by size fraction in Drake Passage (DP), Bransfield Strait (BS) and Antarctic Sound (AS). Small size fraction <2 µm (SSF, black bars), large size fraction >2 µm (LSF, grey bars) of chlorophyll a (Chl a, panel A), particulate organic carbon (POC, panel B) and primary production (PP, panel C) at the respective stations. Values are given as means of 3 measurements. n.d. = no data*

To separate pico- (<2 μm: SSF) from micro- and nanoplankton (>2 μm: LSF), [Chl a], [POC], [PON] and PP were size-fractionated (Figure 2). It is apparent that at almost all stations, the LSF contained the bulk of the Chl a (range of $49 \pm 4\%$ to 109 ± 11 %, with a median of 68%). Interestingly, although accounting for most of the Chl a, the LSF contributed only about half of the PP (range of $25 \pm 3\%$ to $79 \pm 5\%$, with a median of 59%) and the SSF even contributed the majority of POC (range of $39 \pm 3.2\%$ to $90 \pm 17.6\%$, with a median of 60%).

Trace element uptake

The uptake rates of dFe varied between 37 ± 5 and 160 ± 14 pmol L^{-1} d^{-1} (Figure 3A). The last 4 sampled stations (61, 98, 106, 120) showed the lowest values. At all stations, the LSF accounted for the bulk of dFe uptake (Figure 3A, range of $54 \pm 11.5\%$ to $100 \pm 68.4\%$ with a median of 70%). Generally, dFe uptake rates were 1.5-5.3 times higher than the dZn uptake rates (Figure 4A). At most stations (7 of 9), LSF also picked up most of the dZn (range of $40 \pm 24.4\%$ to $100 \pm 28\%$ with a median of 65%). Since the total [dTM] are a factor in the calculation of the dTM uptake rates, and since the [dFe] at station 26 and the [dZn] at station 120 were considered invalid (Table 1) the respective uptake rates of dFe and dZn were likewise considered unreliable (marked n.d. in Figures 3 and 4). The uptake of vitamin B_{12} lay between 0.01 ± 0.00 and 0.12 ± 0.01 pmol L^{-1} d^{-1} (Supplementary Figure 2) was mostly accounted for by the SSF (range of $59.7 \pm 14.2\%$ to $88 \pm 2.9\%$ with a median of 73.1%).

Figure 3 Fe-uptake rates in Drake Passage (DP), Bransfield Strait (BS) and Antarctic Sound (AS): Size fractionated (A) small size fraction <2 µm (SSF, black bars) and a large size fraction >2 µm (LSF, grey bars), normalized to POC (B) and normalized to PP (C). Values in panel A are shown as means of 3 replicates. Values in panels B and C are shown as means of 3 replicates ± standard deviation. n.d. = no data.

The POC normalized dFe uptake rates were similar, being between 3.5 ± 2 and 17.6 ± 1.6 µmol mol^{-1} d^{-1} (Figure 3B). Normalized to PP however, the range of dFe uptake values (27.6 ± 6.5 to 495.8 ± 25.3 µmol mol^{-1}, Figure 3C) increased to more than one order of magnitude. Similar to Fe, POC normalized dZn uptake rates ranged between 1.7 ± 0.5 and 5.7 ± 1.1 µmol mol^{-1} d^{-1} (Figure 4B) but in contrast to Fe, the PP normalized values only differed by a factor of 4 (range of 27.6 ± 5.6 and 119 ± 7.3 µmol mol^{-1} d^{-1}, Figure 4C). Stations of low PP showed a high PP specific dFe and dZn uptake and vice versa.
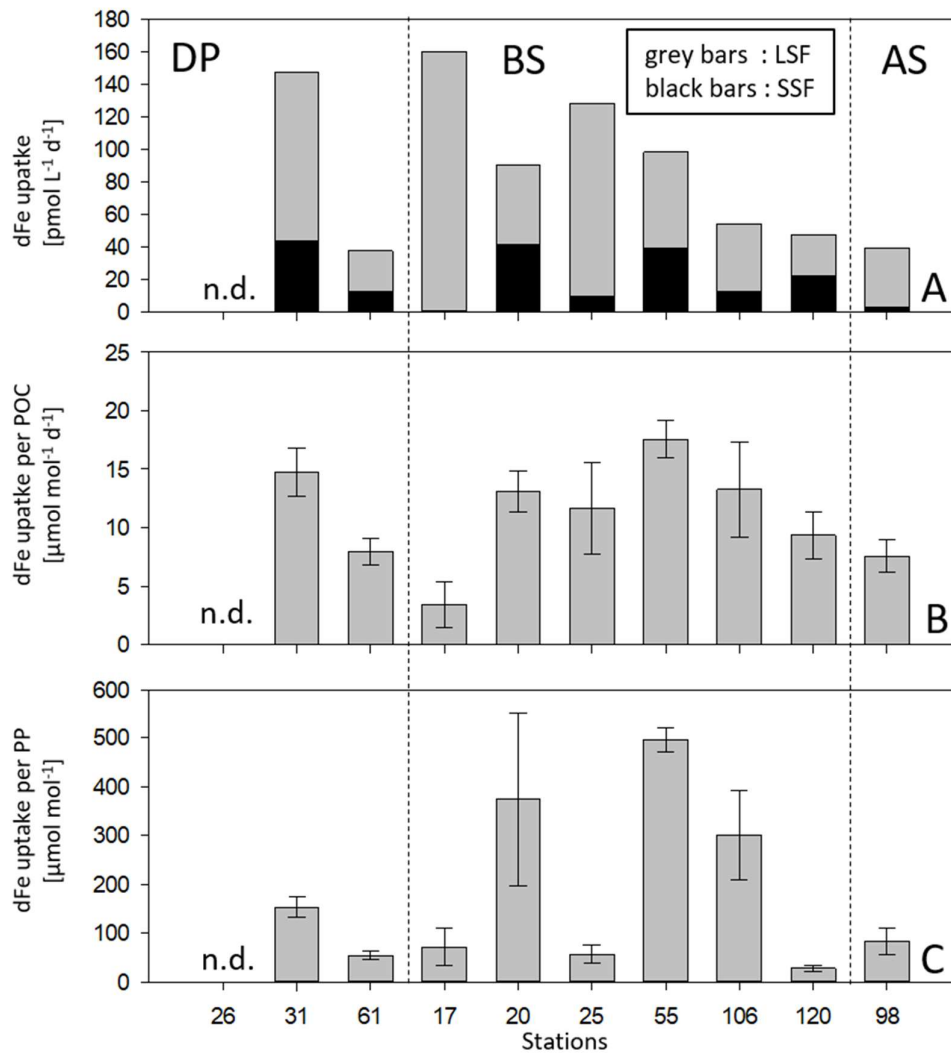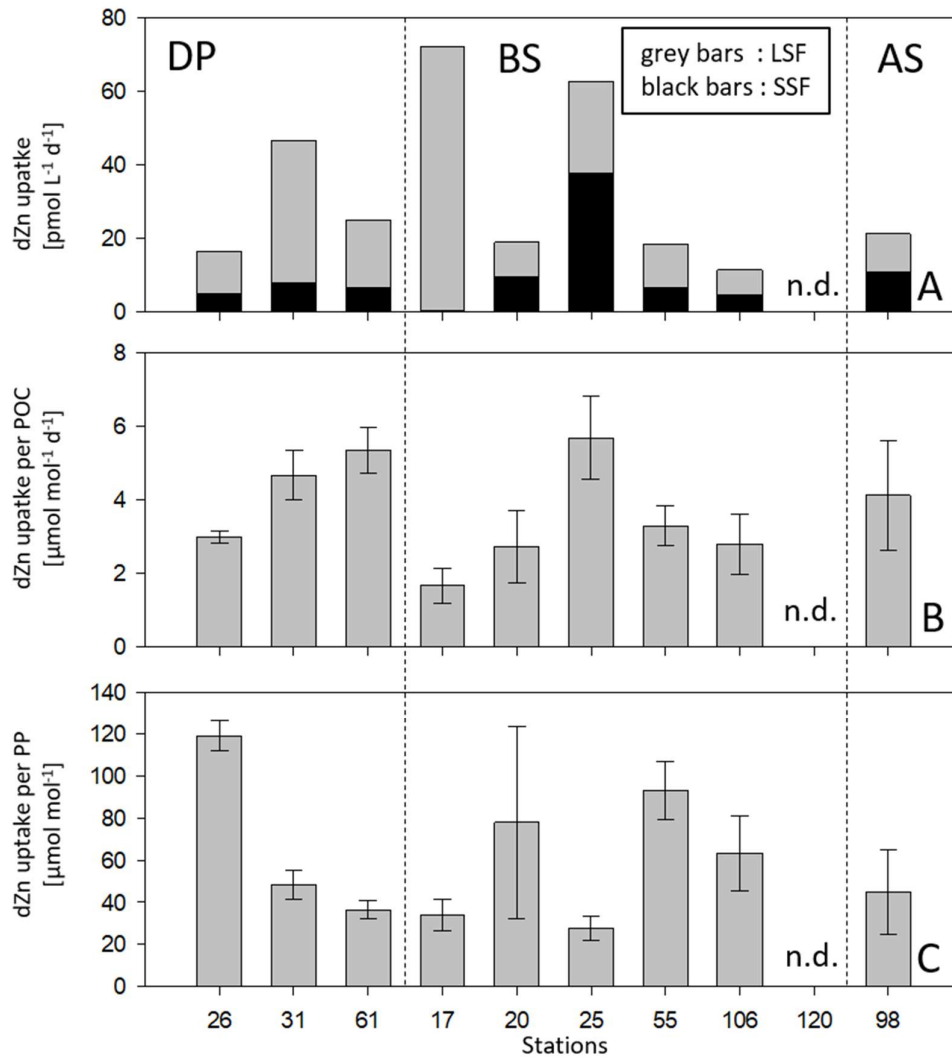
Figure 4 Zn-uptake rates in Drake Passage (DP), Bransfield Strait (BS) and Antarctic Sound (AS): Size fractionated (A) small size fraction <2 µm (SSF, black bars) and a large size fraction >2 µm (LSF, grey bars), normalized to POC (B) and normalized to PP (C). Values in panel A are shown as means of 3 replicates. Values in panels B and C are shown as means of 3 replicates ± standard deviation. n.d. = no data.

Photophysiology

The F_v/F_m value of the DP stations was on average lower than values of the BS stations (averages of 0.28 ± 0.07 and 0.42 ± 0.10 respectively, Supplementary Table 1). However, this difference was not statistically significant ($p = 0.095$). As opposed to the F_v/F_m value, the σ_{PSII} was significantly higher at the DP stations than at the BS stations (averages of 5.7 ± 1.4 and 3.4 ± 0.8 respectively, $p = 0.045$).

Discussion

This study supports and extends the limited data published so far on phytoplankton trace metal availability and uptake in austral autumn at the WAP. It highlights that oceanographic characteristics such as the ACC influence on the offshore DP stations (26, 31 and 61) in contrast to the nearshore regime under the influence of the BC (17, 20, 25, 55, 106 and 120) persist from summer into autumn, but much less pronounced (Figure 1). In contrast to summer conditions, irrespective of the sampling region, dTM availability was high and did not exert control on biomass and PP in autumn, pinpointing other environmental factors, like lower light availability responsible for phytoplankton growth in autumn.

Weak differentiation between regions in autumn in comparison to summer

The synoptic view on all biogeochemical parameters suggests a partitioning of the sampling area in 2 distinct regions, even though only few measured parameters (σ_{PSII}, [dMn] and [dCu]) showed significant differences between these zones: The offshore DP stations in the north influenced by the ACC and the inshore BS stations further south, influenced by the Bransfield Current [11]. The influence of the different currents strongly determined the temperature, salinity and [dTM], evident from the high degree of significant correlations between these parameters (Supplementary Figure 1, bottom-right cluster). Based on oceanographic settings laid out by Plum et al., 2021 stations 26 and 31 lay very close to the southern front of the ACC which, judging by the parameter values, extended its influence to station 61 (Figure 1). As common for the HNLC waters of the DP, the surface water at these stations, coming from the north, was characterized by comparatively warm temperatures with a low salinity and low [dTM] (Table 1, significantly different between DP and BS for [dMn] and [dCu] with $p < 0.001$ and $p = 0.002$ respectively) [25,48]. The on-shelf stations in the BS and in close proximity to Elephant Island (17, 20, 25, 55, 106 and 120) were influenced by the Bransfield Current [1,33,35] originating in shelf waters from the WAP further south, and warm, low-dTM waters from the ACC to the north (Figure 1). Additionally the BS is also commonly influenced by Weddell Sea shelf waters, which are characterized by high [dTM] [33,34,49]. Consequently, the BS stations showed signs of mixed water masses [49] with intermediate temperatures, salinity values and [dTM] (Table 1). Since only one station was sampled in the AS, this area is not further discussed as a differentiable region. However, the southernmost station 98 showed very cold and saline water that was characterized by high [dTM], probably as result of TM input from icebergs, sediments and glaciers [50] (Table 1). In line with the significant differences of [dTM] between both regions, the on average lower photophysiological efficiency (F_v/F_m, $p = 0.095$) offshore was paired with a significantly higher functional absorption cross section of PSII (σPSII, $p = 0.045$). This observation agrees with values published for a similar region in summer [25].

The described differences between the two regions in autumn can be interpreted as the remnants of a strong inshore/offshore gradient observed during summer [8,25]. This gradient was however, far less significant in this study, which could be explained by a storm driven mixing of the water column and thus an increase of the mixed layer depth [8], resulting in an alleviation of Fe stress in the offshore regions in autumn.

Representative low biomass autumn plankton communities

Austral autumn marks the end of the SO growing season, when phytoplankton stocks decrease, with some species keeping up a small pelagic standing stock over winter [24]. In fact, we observed low concentrations of Chl a, POC and PP, being indicative for an autumn community, which most probably experienced light limitation. Generally, [Chl a] values measured during this study (Figure 2A) fit the few published values in the literature for nearshore stations at the WAP between April and early May and ranged mainly between 0.4 and 0.8 µg L^{-1} [19,20,23,26]. In comparison to the summer season, our measured inshore BS values were low. Trimborn et al. 2015 reported summer inshore [Chl a] values as high as 28.7 µg L^{-1}, while their summer offshore values resembled this study's inshore values, ranging

between 0.1 and 0.8 µg L^{-1} [25]. Based on the size fractionation, autotrophic cells of the LSF, presumably diatoms, were dominant at the DP stations, particularly at stations 26 and 31 (100 ± 10.7%, 91 ± 7% respectively, Figure 2A). Large heavily silicified diatoms are typical for the TM depleted SO HNLC waters [51,52] which could also explain the comparably low [Si] at the offshore DP stations. Low offshore [Si] values were already observed in summer [25], stressing that the Si-depletion may accumulate during the year.

Similar to Chl a, the [POC] values obtained during this cruise, ranging between 50 and 525 µg L^{-1} (Figure 2B), resembled the only measured autumn values of 38-398 µg L^{-1} from the Palmer Basin and the shelf off Marguerite Bay (calculated from Chl a and carbon:Chl a ratios in Vernet et al., 2012). In comparison, the summer [POC] at the WAP can reach higher values, yielding up to ~1000 µg L^{-1} inshore, and up to 140 µg L^{-1} offshore [25]. PP values, ranging between 2 and 27 µg C L^{-1} d^{-1} (Figure 2C) during this study, were higher than the published model results of 0.3-2 µg C L^{-1} d^{-1} during autumn 2001 and 2002 in the Palmer Basin and the shelf off Marguerite Bay [23]. Inshore summer values, however, were reported to be as high as 183 ± 33 µg C L^{-1} d^{-1}, while offshore values ranged between 3 and 9 µg C L^{-1} d^{-1} [25]. Interestingly, although the SSF clearly accounted for the smaller share of Chl a (median of 31%, Figure 2A), dFe uptake (median of 32%, Figure 3A) and dZn uptake (median of 37%, Figure 4A) it contributed almost half of the PP (median of 41%, Figure 2C) and even more than half of the POC (median of 60%, Figure 2B). This is possible because small cells procreate fast [53,54] and show lower TM requirements than larger cells [55], explaining the high PP and low dTM uptake. The discrepancy between the SSF's share in Chl a and POC could be explained by heterotrophic bacteria, small dead particles or transparent exopolymer particles that can contribute significantly to [POC] [56–58] but do not contribute to the Chl a.

In summation, while patches of production and comparatively high biomass still existed during this study (stations 17, 25 and 120; Figure 2), the plankton community showed strong evidence of reaching the end of its growth period in all sampled areas, which is consistent with previously published data [11].

Likely no Zn- or Fe-limitation

Generally, Fe is often discussed as growth limiting in the open HNLC areas of the SO [15], where seasonally low [dFe] prevail and the species adapted to low dFe input [59–61]. In this study, 7 out of 10 stations were located on the shelf, close to dFe input from shore, upwelling and ice. Although significant correlations between the dFe uptake by large phytoplankton (LSF) with other parameters existed ([POC], DIN:PO$_4$, [PO$_4$]; Supplementary Figure 1), an Fe limitation of offshore stations is unlikely for 2 reasons. First, although only 2 valid [dFe] were measured at the offshore DP stations (31 and 61), both values were comparatively high relative to the published early autumn (2/12 – 3/24) values averaging at 0.12 ± 0.03 nmol L^{-1} integrated over the top 100 m of the water column [21]. Since the sampling of this study took place approximately one month later, autumn storms possibly already increased the mixed layer depth, increasing [dFe] at the surface. Fe limitation has been reported at [dFe] of <0.1 – 0.2 nM [62–64] up to 0.2 - 0.5 nM [65], while a concentration of 0.7 -1.2 nM was reported as exceeding saturation for phytoplankton growth [65]. While station 61 fell into this range of possible Fe-limitation, station 31 showed a [dFe] exceeding the saturation range. High [dFe] fit the season and region very well, since in autumn storms increase the mixing of the water column and dFe is transported from the depth to the surface, particularly in the shallow shelf regions. Values in a range between 1.6 up to 100 nM dFe have been reported for inshore WAP waters in summer [49,50,66] and authors clearly state, that an Fe limitation in onshore WAP waters is unlikely [50].

The second observation that makes a dFe-limitation even at the offshore stations unlikely are the high Fe:C uptake rates (^{55}Fe uptake divided by ^{14}C uptake) in our study (28-496 µmol Fe mol C^{-1}, Figure 3C).

Much lower PP normalized Fe:C uptake rates were estimated from the DP during winter (3.0-14.3 μmol Fe mol C^{-1} in the DP [67]) and summer (mean 27 ± 4 μmol Fe mol C^{-1}, Trimborn et al., 2017). Similar low values were determined in spring on the Kerguelen-Plateau (3.7-22.9 μmol Fe mol C^{-1} [69]). Even at the offshore stations 31 and 61, Fe:C uptake rates exceed these ranges (152 and 54 μmol Fe mol C^{-1} respectively, Figure 3C) and were more similar to values from the bottom of Antarctic sea ice in summer (5.8-230 μmol Fe mol C^{-1} reported by Lannuzel et al., 2023). During the presented study, 3 Fe:C uptake ratios were measured (stations 20, 55 and 106) that even exceeded the published range of ice algae (Figure 3C). Particularly intriguing is that the highest and the lowest values were measured at stations 55 and 120 which are located almost at the same position (Figure 1), but samplings lay 19 days apart. The turnover times of the dFe pool ranged between 8-80 days at stations 61 and 98 respectively. This range spans from within published values (1-15 days [70]) from a low Fe region in the North Pacific subtropical gyre to significantly exceeding it, which is probably a result of the high [dFe]. Based on the high Fe:C uptake rates, dFe was efficiently incorporated into the cells and can thus not have been limiting. Comparing the PP normalized dFe uptake to the POC normalized dFe uptake (Figure 3), it is striking that the former parameter values show a large variance between stations (SD = 89%), while the latter are more similar (SD = 37%). It is possible that heterotrophic dFe assimilation (accounted for by the normalization to POC, but not by the normalization to carbon uptake) decreased the gap in the autotrophic dFe uptake between stations (Figure 3), as suggested by Lannuzel et al., 2023. The values of POC normalized Fe uptake ranged between 3.5 ± 2 and 17.8 ± 2 μmol Fe mol C^{-1} (Figure 3B) and are thusly in accordance with published values from the western Weddell sea (~11 μmol Fe mol C^{-1}) [7], but lower than values from the open ACC in summer, which reached 27 ± 4 μmol Fe mol POC^{-1} [68]. Exclusively at station 17 both parameters were low (Figure 3B and 3C), suggesting an either relatively inactive community (by far highest Chl a and POC values, but only second highest PP value) or a particulate organic matter that comprised already dead matter. It is possible that the comparatively low activity in PP and uptake of both measured dTM (Figures 3 and 4) hints towards a large community in the process of collapsing under light limitation.

TM limitations have been found to reduce F_v/F_m values as well as increase σ_{PSII} [71–73]. Significantly higher σ_{PSII} at the offshore DP stations ($p = 0.045$) and a particularly low F_v/F_m value at station 26 (0.181 ± 0.02, Supplementary Table 1) indicate that phytoplankton may have exhibited TM stress in the DP, but not in the BS. For station 26, [dFe] and therefore Fe:C uptake ratios were invalid, hence the causal chain making Fe limitation at the other stations unlikely, does not apply to station 26. However, besides a possible Fe-limitation at station 26, the spatial differences in photophysiological parameters observed in the entire dataset may also be a result from low [dMn]. dMn shares many of its sources with dFe [74,75] and has been discussed as limiting or co-limiting in the literature [76,77]. Hence, it is not surprising that the 3 lowest [dMn] were found at the 3 northernmost open ocean stations, with the smallest value reaching as low as 0.09 ± 0.01 nmol L^{-1}. The Mn deficiency coefficient (Mn*) [78] indicated a possible Mn deficiency with respect to the [dFe] at stations 20 and 31 (-0.43 and -0.33 respectively) by markedly falling below the published values of Mn* in Fe/Mn co-limitation scenarios (-0.02 to 0.06,[77,78]). The observation of high [dFe] paired with low [dMn] is different to the summer conditions, where usually a strong limitation by Fe together with Mn can be observed in DP waters relative to the TM-rich onshore waters [16,25].

Zn is used as a co-factor in many enzymes, which are all essential for photosynthesis and biomass production. Carbonic anhydrase mitigating, the conversion of bicarbonate to carbon dioxide, key enzymes in the nucleic acid metabolism such as RNA polymerase, tRNA synthase and reverse transcriptase, as well as superoxide dismutase, mitigating the results of oxidative stress by oxygen radicals all rely on Zn as a cofactor [79]. In line with published studies, [dZn] was high at all our sampled stations [80,81]. [dZn] were between 1.6 and 11.4 times higher than [dFe]. While the physiological demand

as expressed in the TM:C ratio is similar for both metals in the microplankton of the SO (Fe:C: 6-69 µmol:mol and Zn:C: 18-70 µmol:mol; [82,83]) the PP normalized dZn uptake ratio in the new production of microplankton in this study ranged from within this range to significantly exceeding it (Zn:C 28-119 µmol mol^{-1}, Figure 4C), also indicating that Zn was in ample supply. In contrast to the published values, the POC normalized Fe-uptake ratios were markedly higher than the POC normalized Zn-uptake ratios (Figure 3B and 4B) suggesting that more Fe than Zn was assimilated in the biomass. The total Zn-uptake (11-72 pmol L^{-1} d^{-1}, Figure 4A) was similar, but lower than the reported >100 pmol L^{-1} d^{-1} [84]. The, in comparison to [dFe], higher [dZn] paired with lower uptake rates, resulted in turnover times for dZn spanning from 64 days to over one year. As opposed to a limitation scenario, the close correlation of the LSF dZn-uptake to the [Chl a] and PP (Supplementary Figure 1) is more likely the result of a LSF community that incorporated the exact amount they needed for PP production, possibly due to a commonly abundant dZn supply in polar waters.

Conclusion

This study presents rare dTM uptake rate measurements (Fe and Zn) from the WAP in austral autumn. It highlights that in autumn the limiting influence of Fe availability decreases and suggests that light limitation increasingly determines the system. Furthermore, hints were detected that Mn limitation could influence phytoplankton growth at few sampled stations. Generally, the analysis of 41 measured and calculated parameters contributes significantly to enlarging the limited dataset of biogeochemical measurements from the WAP region during austral fall. The encountered community was identified as typical for this region and season based on low PP rates and low standing stocks of POC as well as Chl a in comparison to summer values. Although spatial differentiation between oceanic regions was less pronounced than in summer, two distinct regions were identified by physical and biogeochemical parameters: The offshore DP stations under the influence of the ACC and the nearshore stations mostly located in the BS.

References

1. Meredith, M. P., Stefels, J. & van Leeuwe, M. Marine studies at the western Antarctic Peninsula: Priorities, progress and prognosis. *Deep Sea Research Part II: Topical Studies in Oceanography* **139**, 1–8 (2017).

2. Steinberg, D., Martinson, D. & Costa, D. Two Decades of Pelagic Ecology of the Western Antarctic Peninsula. *Oceanography* **25**, 56–67 (2012).

3. Vernet, M. & Smith, R. C. Measuring and modelling primary production in marine pelagic ecosystems. in *LTER Net Primary Production Methods* (eds. Fahey, J. & Knapp, A.) (Oxford University Press, Oxford, 2006).

4. Ducklow, H. W. *et al.* Marine pelagic ecosystems: The West Antarctic Peninsula. *Philosophical Transactions of the Royal Society B: Biological Sciences* **362**, 67–94 (2007).

5. Vaughan, D. G. *et al.* Recent rapid regional warming on the Antarctic Peninsula. *Climate Change* **60**, 243–274 (2003).

6. van Leeuwe, M. A. *et al.* Annual patterns in phytoplankton phenology in Antarctic coastal waters explained by environmental drivers. *Limnol Oceanogr* **65**, 1651–1668 (2020).

7. Lannuzel, D. *et al.* First report on biological iron uptake in the Antarctic sea-ice environment. *Polar Biol* **46**, 339–355 (2023).

8. Garibotti, I. A., Vernet, M., Smith, R. C. & Ferrario, M. E. Interannual variability in the distribution of the phytoplankton standing stock across the seasonal sea-ice zone west of the Antarctic Peninsula. *J Plankton Res* **27**, 825–843 (2005).

9. Vernet, M. *et al.* Primary production within the sea-ice zone west of the Antarctic Peninsula: I-Sea ice, summer mixed layer, and irradiance. *Deep Sea Res 2 Top Stud Oceanogr* **55**, 2068–2085 (2008).

10. Boyd, P. W. Environmental factors controlling phytoplankton processes in the Southern Ocean. *J Phycol* **38**, 844–861 (2002).

11. Ferreira, A. *et al.* Climate change is associated with higher phytoplankton biomass and longer blooms in the West Antarctic Peninsula. *Nat Commun* **15**, (2024).

12. Turner, J. S. *et al.* Changing phytoplankton phenology in the marginal ice zone west of the Antarctic Peninsula. *Marine Ecology Progress Series* **734**, 1–21 (2024).

13. Plum, C. *et al.* Mesozooplankton trait distribution in relation to environmental conditions and the presence of krill and salps along the northern Antarctic Peninsula. *J Plankton Res* **43**, 927–944 (2021).

14. de Jong, J. *et al.* Natural iron fertilization of the Atlantic sector of the Southern Ocean by continental shelf sources of the Antarctic Peninsula. *J Geophys Res Biogeosci* **117**, 1–25 (2012).

15. Martin, J. H. Glacial-interglacial CO2 change: The Iron Hypothesis. *Paleoceanography* **5**, 1–13 (1990).

16. Balaguer, J., Koch, F., Hassler, C. & Trimborn, S. Iron and manganese co-limit the growth of two phytoplankton groups dominant at two locations of the Drake Passage. *Commun Biol* **5**, 1–12 (2022).

17. von Bodungen, B. Phytoplankton growth and krill grazing during spring in the Bransfield Strait, Antarctica - Implications from sediment trap collections. *Polar Biology* **6**, 153–160 (1986).

18. Lange, P. K., Ligowski, R. & Tenenbaum, D. R. Phytoplankton in the embayments of King George Island (Antarctic Peninsula): A review with emphasis on diatoms. *Polar Record* **54**, 158–175 (2018).

19. Trefault, N. *et al.* Annual phytoplankton dynamics in coastal waters from Fildes Bay, Western Antarctic Peninsula. *Scientific Reports* **11**, 1–16 (2021).

20. Lipski, M. Variations of physical conditions, nutrients and chlorophyll a contents in Admiralty Bay (King George Island, South Shetland islands, 1979). *Polish Polar Research* **8**, 307–332 (1987).

21. Selph, K. E. *et al.* Phytoplankton distributions in the Shackleton Fracture Zone/Elephant Island region of the Drake Passage in February-March 2004. *Deep-Sea Research Part II: Topical Studies in Oceanography* **90**, 55–67 (2013).

22. Kopczynska, E. E. Annual study of phytoplankton in Admiralty Bay, King George Island, Antarctica. *Polish Polar Research* **17**, 151–164 (1996).

23. Vernet, M. *et al.* Primary production throughout austral fall, during a time of decreasing daylength in the western Antarctic Peninsula. *Marine Ecology Progress Series* **452**, 45–61 (2012).

24. Pan, B. J. *et al.* Environmental drivers of phytoplankton taxonomic composition in an Antarctic fjord. *Progress in Oceanography* **183**, 102295 (2020).

25. Trimborn, S., Hoppe, C. J. M., Taylor, B. B., Bracher, A. & Hassler, C. Physiological characteristics of open ocean and coastal phytoplankton communities of Western Antarctic Peninsula and Drake Passage waters. *Deep Sea Res 1 Oceanogr Res Pap* **98**, 115–124 (2015).

26. Yilmaz, I. N. *et al.* Effects of Different Commercial Feeds and Enrichments on Biochemical Composition and Fatty Acid Profile of Rotifer (Brachionus Plicatilis, Müller 1786) and Artemia Franciscana. *Turkish Journal of Fisheries and Aquatic Sciences* **18**, 81–90 (2018).

27. Henley, S. F. *et al.* Macronutrient supply, uptake and recycling in the coastal ocean of the west Antarctic Peninsula. *Deep-Sea Research Part II: Topical Studies in Oceanography* **139**, 58–76 (2017).

28. Bown, J. *et al.* Bioactive trace metal time series during Austral summer in Ryder Bay, Western Antarctic Peninsula. *Deep-Sea Research Part II: Topical Studies in Oceanography* **139**, 103–119 (2017).

29. Panzeca, C. *et al.* Distributions of dissolved vitamin B12 and Co in coastal and open-ocean environments. *Estuarine, Coastal and Shelf Science* **85**, 223–230 (2009).

30. Panzeca, C. *et al.* B vitamins as regulators of phytoplankton dynamics. *Eos* **87**, 2–4 (2006).

31. Cabanes, D. J. E. *et al.* Using Fe chemistry to predict Fe uptake rates for natural plankton assemblages from the Southern Ocean. *Marine Chemistry* **225**, 103853 (2020).

32. Böckmann, S. *et al.* Salp fecal pellets release more bioavailable iron to Southern Ocean phytoplankton than krill fecal pellets. *Current Biology* **31**, 1–10 (2021).

33. Zhou, M., Niiler, P. P., Zhu, Y. & Dorland, R. D. The western boundary current in the Bransfield Strait, Antarctica. *Deep-Sea Research Part I: Oceanographic Research Papers* **53**, 1244–1252 (2006).

34. Zhou, X., Zhu, G. & Hu, S. Influence of tides on mass transport in the Bransfield Strait and the adjacent areas, Antarctic. *Polar Science* **23**, 100506 (2020).

35. Sangrà, P. *et al.* The Bransfield current system. *Deep Sea Res 1 Oceanogr Res Pap* **58**, 390–402 (2011).

36. Pausch, F. *et al.* Responses of a Natural Phytoplankton Community From the Drake Passage to Two Predicted Climate Change Scenarios. *Frontiers in Marine Science* **9**, 1–18 (2022).

37. *Methods of Seawater Analysis*. (Wiley-VCH Verlag GmbH, D-69469 Weinheim, 1999).

38. Holmes, R. M., Aminot, A., Kérouel, R., Hooker, B. A. & Peterson, B. J. A simple and precise method for measuring ammonium in marine and freshwater ecosystems. *Canadian Journal of Fisheries and Aquatic Sciences* **56**, 1801–1808 (1999).

39. Welschmeyer, N. A. Fluorometric analysis of chlorophyll a in the presence of chlorophyll b and pheopigments. *Limnology and Oceanography* **39**, 1985–1992 (1994).

40. Koch, F. *et al.* The effect of vitamin B 12 on phytoplankton growth and community structure in the Gulf of Alaska. *Limnology and Oceanography* **56**, 1023–1034 (2011).

41. UNESCO. Ocean Flux Study (Jgofs) Protocols for the Joint Global Core Measurements. 181 (1994).

42. Kirchman, D., K'nees, E. & Hodson, R. Leucine incorporation and its potential as a measure of protein synthesis by bacteria in natural aquatic systems. *Applied and Environmental Microbiology* **49**, 599–607 (1985).

43. Smith, D. C. & Azam, F. A simple , economical method for measuring bacterial protein synthesis rates in seawater using 3H-leucine. *Marine Microbial Food Webs* **6**, 107–114 (1992).

44. Fourquez, M. *et al.* Microbial Competition in the Subpolar Southern Ocean: An Fe–C Co-limitation Experiment. *Frontiers in Marine Science* **6**, 1–15 (2020).

45. Koch, F., Sañudo-Wilhelmy, S. A., Fisher, N. S. & Gobler, C. J. Effect of vitamins B1 and B12 on bloom dynamics of the harmful brown tide alga, Aureococcus anophagefferens (Pelagophyceae). *Limnology and Oceanography* **58**, 1761–1774 (2013).

46. Hassler, C. S., Schoemann, V., Nichols, C. M., Butler, E. C. V. & Boyd, P. W. Saccharides enhance iron bioavailability to Southern Ocean phytoplankton. *Proceedings of the National Academy of Sciences* **108**, 1076–1081 (2011).

47. Zubkov, M. V., Holland, R. J., Burkill, P. H., Croudace, I. W. & Warwick, P. E. Microbial abundance, activity and iron uptake in vicinity of the Crozet Isles in November 2004-January 2005. *Deep-Sea Research Part II: Topical Studies in Oceanography* **54**, 2126–2137 (2007).

48. Martin, J. H., Fitzwater, S. E. & Gordon, R. M. Iron deficiency limits phytoplankton growth in Antarctic waters. *Global Biogeochem Cycles* **4**, 5–12 (1990).

49. Ardelan, M. V. *et al.* Natural iron enrichment around the Antarctic Peninsula in the Southern Ocean. *Biogeosciences* **7**, 11–25 (2010).

50. Annett, A. L. *et al.* Comparative roles of upwelling and glacial iron sources in Ryder Bay, coastal western Antarctic Peninsula. *Mar Chem* **176**, 21–33 (2015).

51. Smetacek, V., Assmy, P. & Henjes, J. The role of grazing in structuring Southern Ocean pelagic ecosystems and biogeochemical cycles. *Antarct Sci* **16**, 541–558 (2004).

52. Assmy, P. *et al.* Thick-shelled, grazer-protected diatoms decouple ocean carbon and silicon cycles in the iron-limited Antarctic Circumpolar Current. *Proc Natl Acad Sci U S A* **110**, 20633–20638 (2013).

53. Jardillier, L., Zubkov, M. V., Pearman, J. & Scanlan, D. J. Significant CO2 fixation by small prymnesiophytes in the subtropical and tropical northeast Atlantic Ocean. *ISME Journal* **4**, 1180–1192 (2010).

54. Irion, S., Christaki, U., Berthelot, H., L'Helguen, S. & Jardillier, L. Small phytoplankton contribute greatly to CO2-fixation after the diatom bloom in the Southern Ocean. *ISME Journal* **15**, 2509–2522 (2021).

55. Morel, F. M. M., Rueter, J. G. & Price, N. M. Iron nutrition of phytoplankton and its possible importance in the ecology of ocean regions with high nutrient and low biomass. *Oceanography* **4**, 56–61 (1991).

56. Passow, U. Production of transparent exopolymer particles (TEP) by phyto- and bacterioplankton. *Marine Ecology Progress Series* **236**, 1–12 (2002).

57. Engel, A. & Passow, U. Carbon and nitrogen content of transparent exopolymer particles (TEP) in relation to their Alcian Blue adsorption. *Mar Ecol Prog Ser* **219**, 1–10 (2001).

58. Mari, X. Carbon content and C:N ratio of transparent exopolymeric particles (TEP) produced by bubbling exudates of diatoms. *Mar Ecol Prog Ser* **183**, 59–71 (1999).

59. Lommer, M. *et al.* Genome and low-iron response of an oceanic diatom adapted to chronic iron limitation. *Genome Biology* **13**, (2012).

60. Sunda, W. G., Swift, D. G. & Huntsman, S. A. Low iron requirement for growth in oceanic phytoplankton. *Nature* **351**, 55–57 (1991).

61. Strzepek, R. F., Hunter, K. A., Frew, R. D., Harrison, P. J. & Boyd, P. W. Iron-light interactions differ in Southern Ocean phytoplankton. *Limnology and Oceanography* **57**, 1182–1200 (2012).

62. Boyd, P. W. *et al.* A mesoscale phytoplankton bloom in the polar Southern Ocean stimulated by iron fertilization. *Nature* **407**, 695–702 (2000).

63. Gervais, F., Riebesell, U. & Gorbunov, M. Y. Changes in primary productivity and chlorophyll a in response to iron fertilization in the Southern Polar Frontal Zone. *Limnology and Oceanography* **47**, 1324–1335 (2002).

64. Hoffmann, L. J., Peeken, I., Lochte, K., Assmy, P. & Veldhuis, M. Different reactions of Southern Ocean phytoplankton size classes to iron fertilization. *Limnology and Oceanography* **51**, 1217–1229 (2006).

65. Coale, K. H. *et al.* Southern ocean iron enrichment experiment: Carbon cycling in high and low Si waters. *Science* **304**, 408–14 (2004).

66. Sañudo-Wilhelmy, S. A., Olsen, K. A., Scelfo, J. M., Foster, T. D. & Flegal, A. R. Trace metal distributions off the antarctic peninsula in the weddell sea. *Marine Chemistry* **77**, 157–170 (2002).

67. Hopkinson, B. M. *et al.* Planktonic C: Fe ratios and carrying capacity in the southern Drake Passage. *Deep Sea Res 2 Top Stud Oceanogr* **90**, 102–111 (2013).

68. Trimborn, S. *et al.* Iron sources alter the response of Southern Ocean phytoplankton to ocean acidification. *Marine Ecology Progress Series* **578**, 35–50 (2017).

69. Fourquez, M., Obernosterer, I., Davies, D. M., Trull, T. W. & Blain, S. Microbial iron uptake in the naturally fertilized waters in the vicinity of the Kerguelen Islands: Phytoplankton-bacteria interactions. *Biogeosciences* **12**, 1893–1906 (2015).

70. Hawco, N. J. *et al.* Recycling of dissolved iron in the North Pacific Subtropical Gyre. *Limnology and Oceanography* **67**, 2448–2465 (2022).

71. Greene, R. M., Geider, R. J. & Falkowski, P. G. Effect of iron limitation on photosynthesis in a marine diatom. *Limnol Oceanogr* **36**, 1772–1782 (1991).

72. Greene, R. M., Geider, R. J., Kolber, Z. & Falkowski, P. G. Iron-induced changes in light harvesting and photochemical energy conversion processes in eukaryotic marine algae. *Plant Physiol* **100**, 565–575 (1992).

73. Strzepek, R. F., Hunter, K. A., Frew, R. D., Harrison, P. J. & Boyd, P. W. Iron-light interactions differ in Southern Ocean phytoplankton. *Limnol Oceanogr* **57**, 1182–1200 (2012).

74. Van Hulten, M. *et al.* Manganese in the west Atlantic Ocean in the context of the first global ocean circulation model of manganese. *Biogeosciences* **14**, 1123–1152 (2017).

75. Anugerahanti, P. & Tagliabue, A. Process controlling iron-manganese regulation of the Southern Ocean biological carbon pump. *Philosophical Transactions of the Royal Society A: Mathematical, Physical and Engineering Sciences* **381**, (2023).

76. Balaguer, J., Koch, F., Hassler, C. & Trimborn, S. Iron and manganese co-limit the growth of two phytoplankton groups dominant at two locations of the Drake Passage. *Commun Biol* **5**, 1–12 (2022).

77. Balaguer, J. *et al.* Iron and manganese availability drives primary production and carbon export in the Weddell Sea. *Current Biology* **33**, 4405-4414.e4 (2023).

78. Browning, T. J., Achterberg, E. P., Engel, A. & Mawji, E. Manganese co-limitation of phytoplankton growth and major nutrient drawdown in the Southern Ocean. *Nat Commun* **12**, 1–9 (2021).

79. Twining, B. S. & Baines, S. B. The Trace Metal Composition of Marine Phytoplankton. *Annual Review of Marine Science* **5**, 191–215 (2013).

80. Baars, O. & Croot, P. L. The speciation of dissolved zinc in the Atlantic sector of the Southern Ocean. *Deep-Sea Research Part II: Topical Studies in Oceanography* **58**, 2720–2732 (2011).

81. Hawco, N. J., Tagliabue, A. & Twining, B. S. Manganese Limitation of Phytoplankton Physiology and Productivity in the Southern Ocean. *Global Biogeochem Cycles* **36**, (2022).

82. Twining, B. S., Baines, S. B. & Fisher, N. S. Element stoichiometries of individual plankton cells collected during the Southern Ocean Iron Experiment (SOFeX). *Limnology and Oceanography* **49**, 2115–2128 (2004).

83. Boyd, P. W. *et al.* Mesoscale iron enrichment experiments 1993-2005: Synthesis and future directions. *Science* **315**, 612–617 (2007).

84. Kell, R. M. *et al.* High metabolic zinc demand within native Amundsen and Ross Sea phytoplankton communities determined by stable isotope uptake rate measurements. *EGUsphere* (2024) doi:https://doi.org/10.5194/egusphere-2024-2085.

Supplementary Material

Out of the 561 possible correlations between 34 tested parameters included in this analysis, 106 (19%) were significant (Supplementary Figure 1).
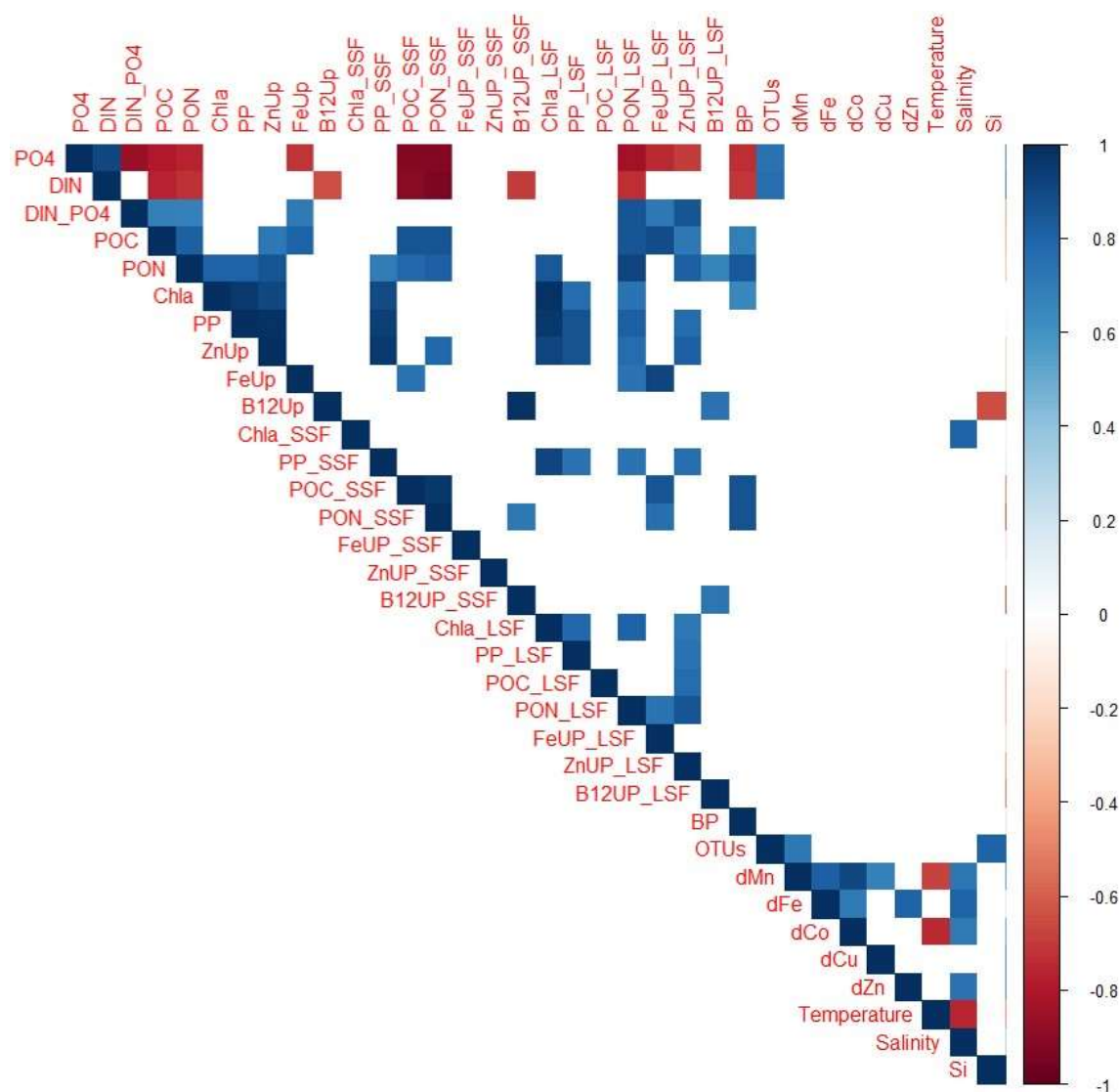
Supplement Figure 1 Correlations between parameters. Phosphate (PO4), dissolved inorganic nitrogen (DIN), DIN:PO4 ratio (DIN_PO4), particulate organic carbon (POC), particulate organic nitrogen (PON), chlorophyll a (Chla), primary production (PP), zinc uptake entire community (ZnUP), iron uptake entire community (FeUP), vitamin B$_{12}$ uptake entire community (B12UP), small size fraction (SSF), large size fraction (LSF), bacterial production (BP), bacterial operational taxonomic units (OTUs), dissolved manganese (dMn), dissolved iron (dFe), dissolved cobalt (dCo) dissolved copper (dCu), dissolved zinc (dZn), silicate (Si). Shades of blue indicate positive correlation coefficients, shades of red negative correlation coefficients. Only correlations that were significant at the p=0.05 significance threshold are indicated as colored squares.
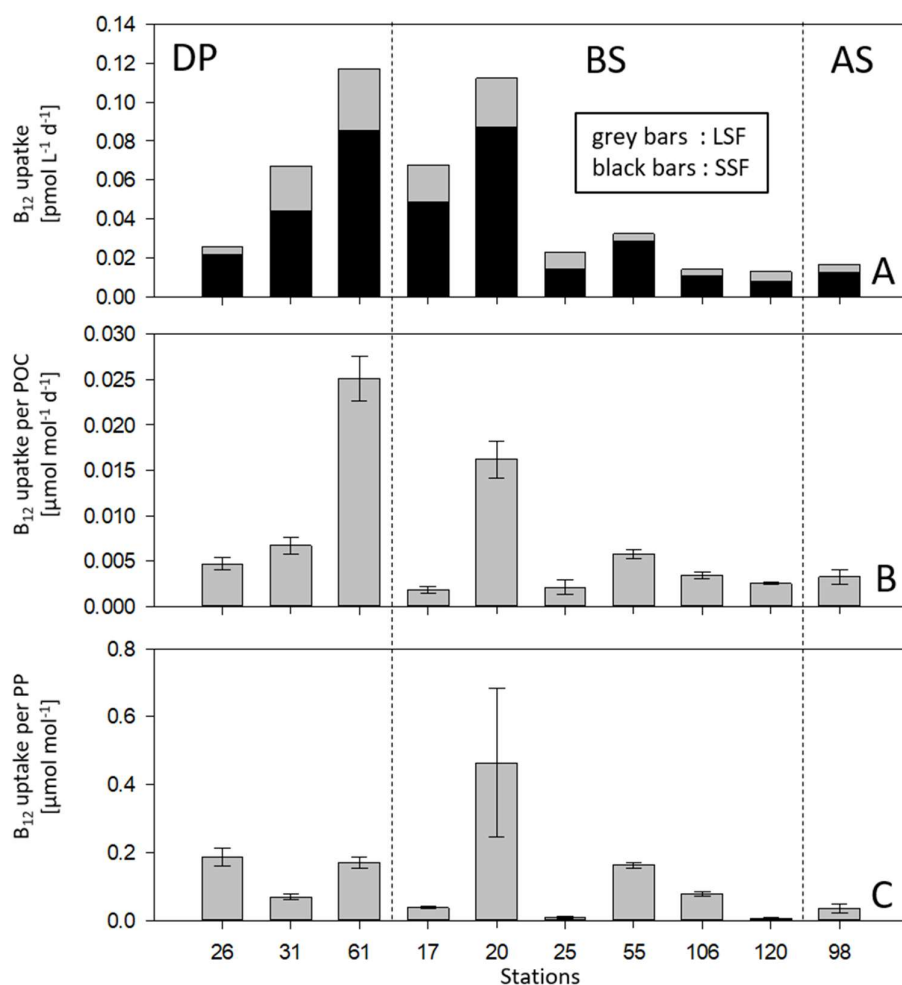
Supplementary Figure 2 Vitamin B$_{12}$-uptake rates in Drake Passage (DP), Bransfield Strait (BS) and Antarctic Sound (AS): Size fractionated (A), normalized to POC (B) and normalized to PP (C). A small size fraction <2 µm (SSF, black bars) and a large size fraction >2 µm (LSF, grey bars) were differentiated. Values in panel A are shown as means of 3 replicates. Values in panels B and C are shown as means of 3 replicates ± standard deviation. n.d. = no data.

Supplementary Table 1 Photophysiology and bacterial production data. Photochemical efficiency (F$_v$/F$_m$), functional absorption cross section of PSII (σ$_{PSII}$), bacterial production (BP) given in µC L^{-1} d^{-1}. All data are given as means of 3 replicates ± standard deviation (SD).

Station	F$_v$/F$_m$	SD F$_v$/F$_m$	σ$_{PSII}$	SD σ$_{PSII}$	BP	SD BP
26	0.181	0.020	7.201	1.277	0.06	0.003
31	0.324	0.007	5.955	0.141	0.15	0.016
61	0.346	0.019	3.840	0.131	0.28	0.023
17	0.555	0.008	5.002	0.048	0.59	0.024
20	0.370	0.011	2.842	0.047	0.36	0.083
25	0.537	0.016	2.925	0.063	0.90	0.194
55	0.269	0.017	3.122	0.320	0.19	0.015
106	0.396	0.007	3.163	0.091	0.05	0.007
120	0.415	0.015	n.d.	n.d.	0.07	0.004
98	0.204	0.015	2.483	0.240	0.04	0.005

3

PUBLICATION 2

GRAZING BY NANO- AND MICROZOOPLANKTON ON
HETEROTROPHIC PICOPLANKTON DOMINATES THE
BIOLOGICAL CARBON CYCLING AROUND THE
WESTERN ANTARCTIC PENINSULA

Published in Polar Biology

RESEARCH

Grazing by nano- and microzooplankton on heterotrophic picoplankton dominates the biological carbon cycling around the Western Antarctic Peninsula

Sebastian Böckmann[1,2] · Scarlett Trimborn[2] · Hendrik Schubert[3] · Florian Koch[2,4]

Abstract

Over the past 40 years, the significance of microzooplankton grazing in oceanic carbon cycling has been highlighted with the help of dilution experiments. The ecologically relevant Western Antarctic Peninsula (WAP) ecosystem in the Southern Ocean (SO), however, has not been well studied. Here we present data from dilution experiments, performed at three stations around the northern tip of the WAP to determine grazing rates of small zooplankton (hetero- and mixotrophic members of the 0.2–200 µm size fraction, SZP) on auto- and heterotrophic members of the < 200 µm plankton community as well as their gross growth. While variable impacts of SZP grazing on carbon cycling were measured, particulate organic carbon, not the traditionally used parameter chlorophyll a, provided the best interpretable results. Our results suggested that heterotrophic picoplankton played a significant role in the carbon turnover at all stations. Finally, a comparison of two stations with diverging characteristics highlights that SZP grazing eliminated 56–119% of gross particulate organic carbon production from the particulate fraction. Thus, SZP grazing eliminated 20–50 times more carbon from the particulate fraction compared to what was exported to depth, therefore significantly affecting the efficiency of the biological carbon pump at these SO sites.

Keywords Microzooplankton grazing · POC · Southern Ocean · Dilution experiment · Carbon cycle

Introduction

In vast areas of the Southern Ocean (SO) phytoplankton growth is controlled by 'bottom up' factors such as trace metal concentrations (mainly iron), and/or light availability (Martin et al. 1990; Boyd 2002). Top-down regulation by micro- and nanozooplankton grazing on the plankton community, has not received much attention (Tsuda and Kawaguchi 1997; Garzio et al. 2013). However, both factors crucially define the fate of photosynthetically fixed carbon (~50 Pg annually in the world ocean (Field et al. 1998)), which can have large implications on global carbon cycling. In contrast to phytoplankton cells sedimenting directly to depth, the majority of global primary production (PP) is remineralized between 0 and 200 m depth (Henson et al. 2012), often facilitated by heterotrophic grazers. Consumption of PP occurs either via short, efficient food chains (Ryther 1969), resulting in fecal pellets or carcasses which export a fraction of the originally bound carbon to depth (Turner 2015), or, conversely, the PP is recycled and respired to dissolved organic and inorganic carbon in the microbial loop (Azam et al. 1983; Calbet and Landry 2004; Turner 2015). The composition and activity of the microbial loop community thus has a large influence on the sequestration potential of the greenhouse gas CO_2 in the ocean (McNair et al. 2021).

The microplankton is a diverse community (Steinberg and Landry 2017) and ranges in size from 20 to 200 µm (Dussart 1965), which includes herbivorous protists (Paffenhöfer 1998) such as ciliates and dinoflagellates (Sherr and Sherr 2002). Microzooplankton grazing constitutes the largest

✉ Sebastian Böckmann
  sebastian.boeckmann@awi.de

1   Department of Marine Botany, University of Bremen, Bremen, Germany

2   Department of Ecological Chemistry, Helmholtz Center for Polar and Marine Research, Alfred Wegener Institute, Bremerhaven, Germany

3   Chair of Aquatic Ecology, Institute for Biosciences, University of Rostock, Rostock, Germany

4   Fachbereich 2, Hochschule Bremerhaven, Bremerhaven, Germany

Springer

phytoplankton biomass sink in the oceans (Calbet and Landry 2004; Schmoker et al. 2013), exceeding in numbers larger mesozooplankton like copepods (Calbet and Landry 2004; Löder et al. 2011). While in the North Sea grazing by microzooplankton can occasionally exceed PP rates and thus reduces the standing stock biomass of phytoplankton (Löder et al. 2011), in polar waters the median percentage of PP grazed by microzooplankton is 53–57% (Schmoker et al. 2013). Hence, assuming a respiratory cost of ~50% (Calbet and Landry 2004), microzooplankton in polar waters can reduce carbon export to depth by 26.5–28.5%, even after only one trophic transfer (Calbet and Landry 2004; Schmoker et al. 2013). In addition to its daily consumption of PP, microzooplankton organisms also provide food for larger heterotrophs by secondary production, partially sustained by feeding on particle sizes too small for the former to graze upon (Berk et al. 1977; Calbet and Saiz 2005; Schmidt et al. 2006). Thus, selective grazing of dominant microzooplankton species can influence the ecosystem by allowing less-grazed phytoplankton species to bloom (Löder et al. 2011).

One approach to estimate the impacts of microzooplankton grazing in the field is the dilution technique (Landry and Hassett 1982). This approach assumes that for small protists, even motile ones, grazing is governed by the encounter rates between predator and prey. This is due to the fact that small plankton operates at low Reynolds numbers and the forces of viscosity dominate over those of inertia (Orchard et al. 2016). Thus, if the encounter rate between predator and prey is reduced via serial dilution, less grazing will occur. This method is not undisputed. Results deviating from the typical linear regression with a negative slope are difficult to interpret, and may occur due to selective feeding, saturated grazers, complex nutrient recycling, mixotrophy, toxic substances or trophic cascades inside the incubation bottles (Teixeira and Figueiras 2009; Calbet et al. 2011, 2012; Calbet and Saiz 2013). Nonetheless, it represents the best approach for estimating microzooplankton grazing and gross growth rates available. Since its first publication in 1982, numerous dilution studies have been conducted worldwide, but only 16 studies were conducted in the SO, of which only three papers (Burkill et al. 1995; Tsuda and Kawaguchi 1997; Garzio et al. 2013) and one dissertation (Price 2012) focused on the Western Antarctic Peninsula (WAP) region. Even though the latter four studies agree that microzooplankton is an important sink for primary and secondary production at the WAP, large fluctuations between sampling sites exist. The WAP is one of the most biologically diverse and productive parts of Antarctica (Meredith et al. 2017) and supports seasonally high PP (Steinberg et al. 2012) and large numbers of grazers like krill and salps, as well as top predators like seabirds and marine mammals (Ducklow et al. 2007; Steinberg et al. 2012). Additionally,

with a 3.4–5.7 °C increase in mean annual air temperature per century (Vaughan et al. 2003) the WAP is one of the fastest warming regions on the planet and this change is expected to influence the dynamics of zooplankton predator/prey relationships (Steinberg and Landry 2017). Böckmann et al. 2021 for example, described how a shift from krill to salp dominance already being observed in the SO (Atkinson et al. 2004, 2019) affects the bioavailability of the essential trace metal iron to phytoplankton and thus influences PP (Böckmann et al. 2021). The WAP's ecological relevance and climatic vulnerability, combined with the lack of data on microzooplankton grazing (Price 2012), necessitates a closer investigation of microzooplankton grazing and its role in the biological pump. While former dilution studies presented grazing rates as solely from microzooplankton, grazing by nanozooplankton indisputably also takes place (Agis et al. 2007). Hence, this study speaks of 'small zooplankton' (SZP) comprising all heterotrophic and mixotrophic organisms from 0.2 to 200 μm, as opposed to microzooplankton, defined as 20–200 μm.

The objective of this study was to elucidate the importance of SZP grazing in the carbon cycling of the upper water column at three locations around the WAP. While previous studies relied on chlorophyll a (Chl a) as a measure of phytoplankton biomass, this study investigated SZP grazing on a wide array of parameters and plankton groups, including particulate organic carbon (POC), particulate organic nitrogen (PON) and cell abundances of heterotrophic bacteria as well as autotrophic pico- and nanoeukaryotes (PE and NE respectively).

Material and Methods

This study was performed in the framework of the POSER project (Population shift and ecosystem response—krill vs. salps), aboard RV Polarstern (PS112) between March and May 2018. Dilution experiments were performed at stations in the Drake Passage (PS112_26: LAT − 62°14.19|LONG − 64°33.44), Scotia Sea (PS112_61: LAT − 60°41.80|LONG − 54°34.25) and Bransfield Strait (PS112_106: LAT − 61°59.25|LONG − 53°59.37; Fig. 1), hereafter referred to as 26, 61 and 106 respectively. Using a polyethylene line connected to an ALMATEC membrane pump, Antarctic seawater was sampled carefully (laminar flow, 3–6 L min^{-1}, bubble free bottle filling) using trace metal clean techniques, successfully used since 2014 (Cabanes et al. 2020; Böckmann et al. 2021; Balaguer et al. 2022). Microscopic analysis of the collected water was conducted to ensure that the plankton community was intact. Water was sampled from a depth of 25 m at stations 26, 61 and 106 near the WAP (Fig. 1) at a surface temperature of 1.2 °C, 1.4 °C and 0.9 °C respectively. The seawater was pumped directly into a trace

Fig. 1 Sampling sites of three dilution experiments: PS112 stations 26 in the Drake Passage, 61 in the Scotia Sea and 106 in the Bransfield Strait
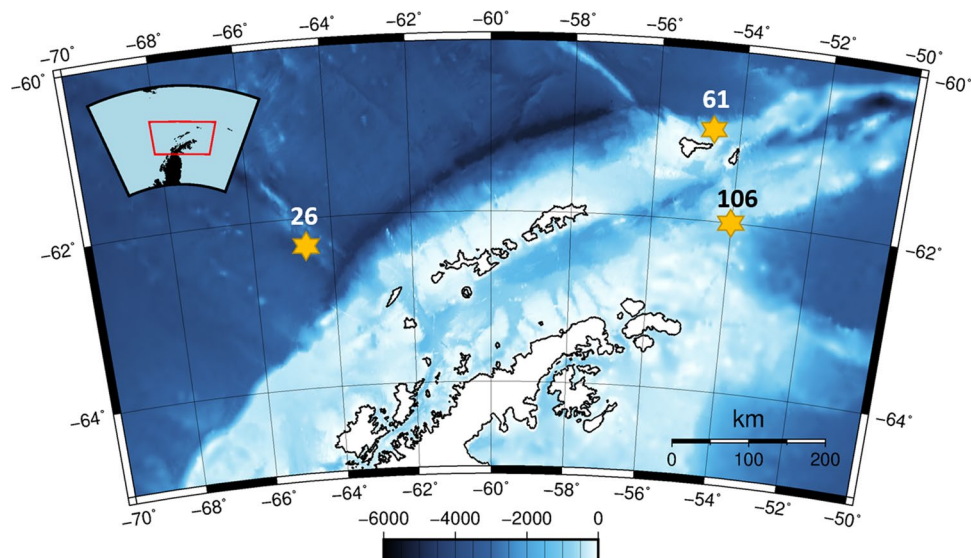
metal free laboratory container. The seawater was then filtered through a 200 µm mesh in order to exclude larger mesozooplankton grazers as described in Balaguer et al. 2022.

Experimental setup

At each sampling site, initial samples were taken to characterize the ambient plankton community, including POC, PON, Chl a, abundance of autotrophic and heterotrophic pico- and nanoplankton and macronutrients. A serial dilution was then set up by filling triplicate 2 L polycarbonate bottles with either 100% whole seawater (1.0 dilution), or diluting them to 75, 50 and 25% whole seawater (0.75, 0.5 and 0.25 dilution respectively) with 0.2 µm filtered seawater (Acropak capsule, PALL) from the same station. All bottles were incubated in front of full spectrum growth light set to a light intensity of 30 µmol photons m^{-2} s^{-1} under a light–dark cycle of 10:14 h at 2 °C, mimicking in situ conditions. The incubations lasted three days (Caron et al. 2000; Garzio et al. 2013), during which the bottles were mixed by gentle turning at least once per day. The experiments were terminated by sampling for plankton community composition, including POC, PON, Chl a, and macronutrients.

POC & PON

POC and PON were sampled, by filtering whole water (POC_{all} and PON_{all}) and 2 µm filtrate ($POC_{<2 \mu m}$ and $PON_{<2 \mu m}$) onto precombusted (15 h, 500 °C) glass fiber filters (GF/F, pore size ~0.6 µm, Whatman). The filters were stored at −20 °C and dried for > 12 h at 60 °C prior to sample preparation. The analysis was performed using a Euro Vector CHNS-O elemental analyzer (Euro Elemental Analyzer 3000, HEKAtech GmbH, Wegberg, Germany) and by

utilization of the Callidus 5.1 software. Contents of POC and PON were corrected for blank measurements and normalized to filtered volume.

Chl a and PP

Chl a samples were collected by filtering samples onto glass fiber filters (GF/F, pore size ~0.6 µm, Whatman). These filters were stored frozen until subsequent analysis via standard fluorometric methods (Welschmeyer 1994) on a Trilogy Fluorometer (Turner Designs) using the non-acidification module. PP measurements were carried out according to Koch et al. 2011. Briefly: 0.37 MBq of ^{14}C-bicarbonate (Perkin Elmer) was added to triplicate bottles and incubated in an on deck incubator, allowing for ambient temperature and light conditions. Incubations were terminated after 24 h by filtering up to 100 mL from each bottle onto 0.2 µm pore size polycarbonate filters. At the beginning and end of the incubation, a 250 µL aliquot of each bottle was removed to quantify total activity. After degassing the filters to remove any left over ^{14}C-bicarbonate and adding scintillation cocktail, samples were measured with a scintillation counter (PackardCarb2100TR) and rates calculated according to JGOFS (UNESCO 1994).

Abundance of autotrophic and heterotrophic pico- and nanoplankton

Light microscopy samples (200 mL unfiltered seawater) were taken to qualitatively determine the initial microplankton community. The samples were preserved with Lugol (1% final concentration). Preserved samples were stored at 4 °C in the dark until further analysis by inverted light microscopy (Axio Observer.D1 microscope, Zeiss).

After transfer of an appropriate amount of sample (volume based on the present Chl a at the different stations) into the Hydrobios sedimentation chambers for the three stations (50 mL, 10 mL and 25 mL for stations 26, 61 and 106, respectively) and settling of the cells for 24 h, taxonomic groups were enumerated according to the method of Utermöhl, following the recommendations of Edler (Utermöhl 1958; Edler 1979).

Samples for flow cytometric determination of heterotrophic- and cyanobacteria, as well as nano- and picoeukaryotes were taken at each station and from each treatment bottle, fixed with phosphate buffered formalin (final concentration 1%), shock frozen in liquid nitrogen and stored in the dark at − 80 °C. For measurement on a BD Accuri™ C6 Flow Cytometer, (Becton Dickinson) samples were defrosted in a water bath of ambient temperature (20 °C) and 2.11 μm rainbow fluorescent glass beads (Spherotech) were added to each sample. Fluorescence was induced by laser excitations at 488 nm and 640 nm and light emissions were detected in the following four wavelengths: FL1 533/30 nm, FL2 585/40 nm, FL3 > 670 nm, FL4 675/25 nm. In a first run, autofluorescent nano- and picoeukaryotes as well as cyanobacteria were determined. Afterwards, 2 μL of SYBR™ Green II solution (ThermoFisher) was added, samples were allowed to incubate for 10 min in a dark fridge and were then analyzed a second time for abundance of heterotrophic bacteria. The analysis of the results was performed using the BD Accuri C6 software and resulted in the characterization of 4 populations of autotrophic picoeukaryotes < 2 μm, which were differentiated by increasing size (PE 1–4) and one population of autotrophic nanoeukaryotes (> 2 μm, NE), which represent a subset of all nanoflagellates in the size spectrum of 2–5 μm, counted under the microscope. Cyanobacteria as well as high- and low DNA containing heterotrophic bacteria (Gasol et al. 1999) (HDNA bacteria and LDNA bacteria, respectively) were also characterized and counted. Additionally, two group parameters were calculated from these data: bacteria all and PE all.

Dissolved inorganic nutrients

Samples for inorganic macronutrients were taken by filtering 10 mL samples from all treatments through a 0.2 μm syringe filter (ThermoFisher Scientific) into a 15 mL polyethylene sample vial (Falcon). Samples were stored at − 20 °C until analysis. The inorganic nutrients were measured on an Evolution III autoanalyser (Alliance Instruments GmbH, Salzburg, Austria). Methods were modified after Grasshoff et al., 1999 and manufacturer's instructions (Seal Analytical, https://seal-analytical.com, accessed June 27, 2019) (Grasshoff et al. 1999). Ammonium was determined with a slightly modified method after Holmes et al. 1999.

Definition of terms

Coefficients that are measured/calculated during dilution experiments have been assigned multiple and sometimes confusing abbreviations in the existing body of literature. To avoid confusion, we have compiled all definitions in the supplementary material (Online resource 1). Particularly, we define the term 'gross absolute POC production' as the rate of gross POC increase per day. In comparison to PP, which is autotrophic POC production from dissolved inorganic carbon, gross absolute POC production comprises all POC production, including the POC production of heterotrophic organisms from dissolved organic carbon (DOC). Furthermore, by using the term small zooplankton (SZP, 0.2–200 μm) grazing instead of the commonly used microzooplankton grazing, we acknowledge that inside dilution experiments, grazers of both, the nanoplankton and the microplankton, exert grazing pressure on the community (Agis et al. 2007).

Data calculation and statistics

Apparent growth rates (r) for all 12 defined groups were calculated for each parameter and each individual bottle using Eq. 1 from Landry and Hassett 1982:

$$r = \frac{LN\left(\frac{P_t}{P_0 * f_d}\right)}{t} \tag{1}$$

where t is the time of the incubation in days, f_d is the dilution factor in decimal writing, P_t is the value of a given measured parameter after the incubation, and P_0 is the respective initial value of a given parameter, before the incubation. A simple linear regression (Altman and Krzywinski 2015) was performed, in which the deviation of the regression's slope (grazing mortality, g) from 0 was tested at the $p = 0.050$ significance threshold with the r-values of the respective experiments plotted against the decimal dilution factors. 95% confidence bands, grazing induced mortality rate (g) and the gross growth rate of the respective parameter (k = y-intercept), as well as their respective uncertainties were calculated using SigmaPlot (Systat Software GmbH) and plotted into each graph. Normality statistics for sample sizes < 5000 (Shapiro–Wilk) as well as constant variance tests were performed at the $p = 0.050$ significance threshold. All published data passed the tests. Net growth rates (μ) in the ambient seawater of all parameters yielding significant regressions were calculated by subtracting the grazing mortality (g) from the gross growth rate (k) with standard errors (SE) propagated.

Absolute rates for parameters with determinable k, g and μ (k_{abs}, g_{abs}, and μ_{abs}) were determined by using Eqs. 2, 3 and 4

$$k_{abs} = (P_0 * e^{k*t} - P_0) * \frac{1}{t} \qquad (2)$$

$$g_{abs} = (P_0 * e^{g*t} - P_0) * \frac{1}{t} \qquad (3)$$

$$\mu_{abs} = (P_0 * e^{\mu*t} - P_0) * \frac{1}{t} \qquad (4)$$

where P_0 is the respective initial value of a given parameter and t is the smallest calculable time interval in days ($= 10^{-12}$ d, Microsoft Excel). t was chosen to be so small, because in exponential functions the slope increases with the increasing independent variable. Since formula 2 assumes a system in which no grazing occurs and formula 3 assumes a system in which no growth occurs, the errors of both models increase with increasing t. Hence, t is chosen small to obtain realistic k_{abs}, g_{abs} and μ_{abs} for a very short time interval, which is then multiplied with 1/t to calculate a close approximation of the true value for the period of 1 day in order to achieve comparability with other sources. Residence times of the parameters were determined by dividing the initial pool by the g_{abs} with standard deviations propagated.

Results

Initial plankton communities

Dissolved inorganic macronutrient concentrations were high throughout the study region, indicative of HNLC waters (Table 1). Dissolved phosphate (PO_4^-) and dissolved inorganic nitrogen (NO_x) were close to Redfield ratios (Redfield et al. 1963; Martiny et al. 2014) at all stations and throughout all dilution steps (Table 1). The biggest differences were detected in dissolved silicate, with concentrations at stations 61 and 106 being ~2 and 3 times higher than at station 26, respectively. While particulate organic carbon measured for the entire community (POC_{all}) was highest at station 26, followed by stations 61 and 106 (Table 1), the community's particulate organic nitrogen (PON_{all}) was similar at stations 26 and 61 and markedly higher than at station 106 (Table 1). This resulted in $C:N_{all}$ ratios almost matching the Redfield ratio at station 61 (6.4 mol:mol) and exceeding this ratio at stations 26 and 106 (7.8 and 9.4 mol:mol, respectively). Interestingly, the C:N ratio of the < 2 μm size fraction of the plankton ($C:N_{<2 \mu m}$) was markedly higher than the community's ($C:N_{all}$) at all three stations (Table 1). In contrast to

Table 1 Initial characterization of the ambient seawater sampled at the 3 stations (26: Drake Passage, 61: Scotia Sea, 106: Bransfield Strait) before performance of the dilution experiments

Parameter	26	n	61	n	106	n
NO_X [μmol L^{-1}]	26.9 ± 0.18	2	29.2 ± 0.08	2	29.7 ± 0.10	2
PO_4 [μmol L^{-1}]	1.7 ± 0.02	2	1.9 ± 0.00	2	1.9 ± 0.00	2
N:P [mol mol^{-1}]	15.7 ± 0.31	2	15.9 ± 0.84	2	16.1 ± 0.55	2
Si [μmol L^{-1}]	23.5 ± 0.18	2	58.5 ± 1.09	2	77.5 ± 0.29	2
POC_{all} [μg L^{-1}]	65.8 ± 2.7	3	55.9 ± 3.3	3	48.9 ± 3.1	2
PON_{all} [μg L^{-1}]	9.8 ± 0.39	3	10.2 ± 0.16	3	5.9 ± 0.27	3
$C:N_{all}$ [mol mol^{-1}]	7.8 ± 0.3	3	6.4 ± 0.3	3	9.4 ± 0.4	2
$C:N_{<2 \mu m}$ [mol mol^{-1}]	12.7 ± 0.2	2	7.7 ± 0.6	3	12.4 ± 0.1	2
Chl a [μg L^{-1}]	0.09 ± 0.01	3	0.53 ± 0.03	3	0.36 ± 0.05	2
POC:Chl a [μg μg^{-1}]	731 ± 30.4	3	105 ± 6.2	3	136 ± 8.5	2
Nanoflagellates 2–5 μm [cells mL^{-1}]	1026	1	2132	1	803	1
NE [cells mL^{-1}]	106 ± 24	3	29 ± 5	2	87 ± 2	2
PE_{all} [cells mL^{-1}]	1429 ± 105	3	2099 ± 198	3	844 ± 49	3
$Bacteria_{all} * 10^3$ [cells mL^{-1}]	391 ± 13.7	3	433 ± 8.9	3	219 ± 12.7	3
$Bacteria_{HDNA} * 10^3$ [cells mL^{-1}]	216 ± 3.7	3	215 ± 7.9	2	156 ± 12.3	3
$Bacteria_{LDNA} * 10^3$ [cells mL^{-1}]	175 ± 10.0	3	220 ± 1.9	3	63 ± 3.2	3
PP [μg C L^{-1} d^{-1}]	1.65 ± 0.08	3	8.21 ± 0.52	3	2.16 ± 0.02	3

Respective sample size given in column (*n*). Sum of nitrate, nitrite and ammonia (NOx), phosphate (PO₄), ratio of dissolved NO_x and PO_4 (N:P), dissolved silicate (Si), particulate organic carbon of entire community (POC_{all}), particulate organic nitrogen of entire community (PON_{all}), ratio of POC:PON for whole community ($C:N_{all}$) and for the < 2 μm size fraction ($C:N_{<2 \mu m}$), chlorophyll a (Chl a), ratio of POC:Chl a and cell numbers of nanoflagellates in size range 2–5 μm, autotrophic nanoeukaryotes (NE), autotrophic picoeukaryotes all size fractions (PE_{all}), all heterotrophic bacteria ($Bacteria_{all}$), high DNA heterotrophic bacteria ($Bacteria_{HDNA}$), low DNA heterotrophic bacteria ($Bacteria_{LDNA}$) and primary production (PP). Please note that bacterial cell numbers need to be multiplied with 10^3. All values are given as means ± SD. N:P ratio represents the mean ± standard deviation (SD) of the initial samples and measurements from all dilution steps. For nanoflagellates 2–5 μm one sample was counted, therefore no SD

POC and PON, the Chl a was lowest at station 26, followed by 106 and highest at 61 (Table 1) resulting in POC:Chl a ratios which were lower at stations 61 and 106 than at 26 (Table 1).

At all 3 stations the nanoplankton community (2–20 µm) was dominated numerically by nanoflagellates (2–5 µm), with this group contributing > 80% of the total cells > 2 µm at all stations (Table 1). Low numbers of NE, identified by their Chl a fluorescence, in comparison to the absolute number of nanoflagellates in the size range of 2–5 µm counted under the microscope at a magnification of 640x (both shown in Table 1) suggested an abundant community of heterotrophic nanoflagellates (data accessible via PANGAEA). The total number of heterotrophic bacteria was highest at station 61 and lowest at 106. PE were most abundant at station 61 (Table 1). PP was highest at station 61 and lowest at station 26 (Table 1).

This study focuses on POC since using this parameter constitutes a novel approach for dilution experiments and measurements of this parameter were more reliable and consistent compared to Chl a. Moreover, calculated POC net growth from the dilution series were nearly identical with net growth in the 100% bottles, which represented in situ conditions. To stress the value of the dataset, the parameters Chl a, PON and bacterial numbers were closely examined focusing on their consistency with the POC values. Results of PE and NE, wherever their apparent growth rates were

significantly correlated to the dilution factor, are listed in the supplements (Online resource 2).

Growth and grazing mortality

At least three or more groups/parameters at all three stations responded to the dilution treatment and are shown in Table 2 and online resource 2, meaning that a significant regression ($p < 0.050$) between the decimal dilution factor and the apparent growth rate (r), of a parameter was observed. At station 26, 83% of the 12 parameters showed a significant response to SZP grazing, while at stations 61 and 106 fewer parameters were affected (25% and 50%, respectively). In addition, the net growth rate (µ), calculated from the grazer induced mortality rate (g) and the gross growth rate (k) of each parameter matched the measured apparent growth rate (r) in the raw, undiluted seawater (1.0 dilution) bottles, validating our calculations (Table 2 and online resource 2). Due to low concentrations of Chl a in the 0.5 bottles of station 106, this treatment was excluded from the dataset.

POC & PON

Concentrations of POC and PON integrate all autotrophic and heterotrophic organisms > 0.6 µm. The apparent growth rate of POC ($r_{POC\ all}$) was significantly correlated to the different dilutions at each station. At station 26, the grazer

Table 2 Net growth rate (µ), grazer induced mortality (g), gross growth rate (k) and residence time for the parameters: community particulate organic carbon (POC$_{all}$), community particulate organic nitrogen (PON$_{all}$), Chlorophyll a (Chl a), heterotrophic low DNA Bacteria (Bacteria$_{LDNA}$), heterotrophic high DNA bacteria (Bacteria$_{HDNA}$), all heterotrophic bacteria (Bacteria$_{all}$) at the three locations (Drake Passage (26), Scotia Sea (61) and Bransfield Strait (106)) that showed a significant correlation between dilution and apparent growth rate (r)

Station	Parameter	µ [d^{-1}]	g [d^{-1}]	k [d^{-1}]	r$_{100\%\ bottles}$ [d^{-1}]	Residence time [d]	R^2	p	n
26	POC$_{all}$	-0.09 ± 0.07	0.54 ± 0.06	0.45 ± 0.04	-0.06 ± 0.03	1.8 ± 0.2	0.908	< 0.0001	11
26	PON$_{all}$	-0.12 ± 0.03	0.22 ± 0.03	0.09 ± 0.02	-0.11 ± 0.02	4.6 ± 0.7	0.875	< 0.0001	11
26	Chl a	0.14 ± 0.04	0.08 ± 0.03	0.22 ± 0.02	0.12 ± 0.02	12.3 ± 4.6	0.486	0.0546	8
26	Bacteria$_{LDNA}$	0.05 ± 0.08	0.64 ± 0.07	0.68 ± 0.05	0.07 ± 0.01	1.6 ± 0.1	0.903	< 0.0001	12
26	Bacteria$_{HDNA}$	0.02 ± 0.04	0.28 ± 0.03	0.30 ± 0.02	0.01 ± 0.01	3.5 ± 0.5	0.901	< 0.0001	11
26	Bacteria$_{all}$	0.03 ± 0.09	0.52 ± 0.06	0.54 ± 0.04	0.03 ± 0.01	2.5 ± 0.3	0.872	< 0.0001	12
61	POC$_{all}$	0.22 ± 0.06	0.28 ± 0.05	0.50 ± 0.04	0.25 ± 0.04	3.5 ± 0.7	0.753	0.0003	12
61	Bacteria$_{LDNA}$	0.04 ± 0.09	0.41 ± 0.07	0.45 ± 0.05	0.07 ± 0.03	2.5 ± 0.5	0.797	0.0005	10
61	Bacteria$_{all}$	0.19 ± 0.08	0.25 ± 0.06	0.44 ± 0.05	0.23 ± 0.03	4.0 ± 1.1	0.627	0.0037	11
106	POC$_{all}$	0.16 ± 0.08	0.30 ± 0.06	0.46 ± 0.04	0.19 ± 0.05	3.3 ± 0.6	0.703	0.0007	12
106	Chl a	0.12 ± 0.05	0.11 ± 0.04	0.23 ± 0.03	0.12 ± 0.04	9.1 ± 3.8	0.580	0.0281	8
106	Bacteria$_{LDNA}$	0.07 ± 0.08	0.46 ± 0.07	0.53 ± 0.05	0.11 ± 0.01	2.2 ± 0.3	0.842	0.0002	10
106	Bacteria$_{HDNA}$	0.13 ± 0.02	0.16 ± 0.02	0.29 ± 0.01	0.13 ± 0.02	6.3 ± 0.9	0.863	< 0.0001	12
106	Bacteria$_{all}$	0.12 ± 0.04	0.22 ± 0.03	0.34 ± 0.02	0.13 ± 0.00	4.5 ± 0.8	0.814	< 0.0001	12

µ was calculated from k-g. µ and the growth measured in the 100% bottles ($r_{100\%\ bottles}$) showed overlapping standard errors (SE) in all cases, underlining the consistency of the dataset. Number of replicates in analysis (n), coefficient of determination (R^2), significance of regression slope (p). k, g, µ and $r_{100\%\ bottles}$ values given as means $\pm$ SE and in the unit d^{-1}. The residence time is given as mean $\pm$ standard deviation and in the unit d

induced mortality of POC ($g_{POC\ all}$) was higher than the gross growth rate ($k_{POC\ all}$) yielding a negative net growth of POC ($\mu_{POC\ all}$). At stations 61 and 106, the $k_{POC\ all}$ was higher than the $g_{POC\ all}$ resulting in positive $\mu_{POC\ all}$. It is noteworthy that the $k_{POC\ all}$ was similar at all stations (overlapping standard errors), but at 26 the $g_{POC\ all}$ was almost twice as high as at the other two stations. The $r_{PON\ all}$ was only correlated significantly to the dilution at station 26, yielding here a $k_{PON\ all}$ and $g_{PON\ all}$ that resulted in a negative $\mu_{PON\ all}$ (Table 2). Direct comparison of k and g for PON_{all} of station 26 with the other two locations is not possible, since the dilution experiments did not yield significant regressions for the measured $r_{PON\ all}$ values with the dilution factor at 61 and 106. Most interestingly the $C:N_{all}$ ratios in all experiments significantly ($n=31$, $p<0.0001$) increased with increasing dilution, resulting in $>100\%$ higher ratios than in the initials (Fig. 2).

Chl a

Chl a values integrate all autotrophic organisms >0.2 μm present in the incubation bottles, including pico- nano- and microphytoplankton. The $r_{Chl\ a}$ values were correlated significantly to the dilutions at stations 26 and 106 (Table 2). At both stations, the $k_{Chl\ a}$ and $g_{Chl\ a}$ were similar (overlapping SE) but resulted in positive $\mu_{Chl\ a}$.

Bacteria

$r_{LDNA\ bacteria}$ values showed a significant correlation to the dilution factor at all stations, while $r_{HDNA\ bacteria}$ values were only significantly correlated to the dilution factor at stations 26 and 106 (Table 2, Fig. 3b and f). At station 26, both k and g were higher for LDNA bacteria compared to HDNA bacteria. The $k_{bacteria\ all}$ ranged from 0.34 ± 0.02 at station 106 to 0.54 ± 0.04 at station 26. The $g_{bacteria\ all}$, however, was much higher at station 26 in comparison to the other two stations. This resulted in a very low, but still positive $\mu_{bacteria\ all}$ at station 26 (Table 2) in comparison to 6 and 4 times higher $\mu_{bacteria\ all}$ at 61 and 106, respectively.

Discussion

The dilution method has previously been applied successfully in numerous studies (Schmoker et al. 2013) and proven to be a powerful tool for estimating SZP grazing in aquatic systems. A significant negative correlation ($p<0.050$) between the apparent growth rate (r) and the dilution factor is accepted as an 'interpretable result'. This implies that during the experiment, grazing and growth on the respective parameters occurred in the incubation bottles and that the increase of growth due to a decrease of grazing was proportional to the dilution. Criticism on the method (Calbet and Saiz 2013) mostly revolves around challenging results such as graph shapes and the underestimation of the SZP grazing impact (Calbet et al. 2011). In contrast to this reasonable criticism, this study's results suggest a dominant SZP grazing impact at all investigated stations (Table 2 Fig. 3).

Three contrasting stations

During this study, the investigated parameters responded very differently to the dilutions at the 3 stations. At off-shelf station 26, a strong grazing pressure of SZP, particularly on heterotrophic organisms was observed, due to i) the high number of parameters (83%) resulting in significant regressions, ii) the 2 times higher g_{POC} at station 26 in comparison to the other 2 stations (Table 2), iii) the losses from the initial samples relative to the undiluted seawater (1.0 dilution, data accessible via PANGAEA) after the experiment and iv) the 8 times higher g_{POC} than $g_{Chl\ a}$ (Table 2).

Compared to 26, at station 61, SZP grazing played only a minor role, since only 25% of all measured and calculated parameters resulted in significant regressions (Table 2), although growth of several parameters was observed via an increase in the undiluted seawater bottles (1.0 dilution) compared to the initials. Though weaker than at the other two stations, SZP grazing still accounted for $>50\%$ of POC loss (Fig. 4b) at station 61, possibly due to the disproportionately strong grazing pressure on the bacterial population (Table 2). Like at the other 2 stations, the g_{LDNA} was the highest measured g among all parameters at station 61.
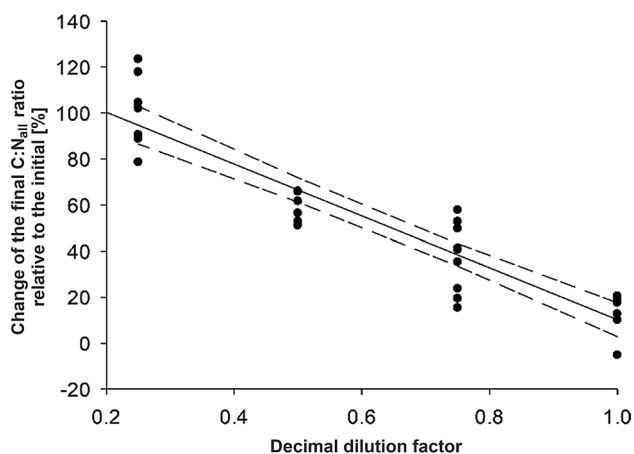

Fig. 2 The change of the final, relative to the initial $C:N_{all}$ ratio versus the decimal dilution factor. Data shown was pooled from all 3 experiments. 1.0 corresponds to undiluted seawater. The regression (solid line) was highly significant ($n=31$, $p<0.0001$). Dashed lines indicate 95% confidence intervals. An increase of $C:N_{all}$ ratios with increasing dilution of $>100\%$ (right to left) was observed. Please note that the x-axis terminates at 0.2

Fig. 3 Result of dilution series at the three stations 26 (**a**, **b**), 61 (**c**, **d**) and 106 (**e**, f) for low DNA (LDNA) and high DNA (HDNA) bacteria. Apparent growth rates (r) on abscissa, dilution factor on ordinate. 1.0 corresponds to undiluted seawater. Slope = grazer induced mortality (g), y-intercept = gross growth rate (k). Significant results obtained for LDNA bacteria at all stations and for HDNA bacteria at stations 26 and 106. Solid lines signify regression, dotted lines 95% confidence bands. Respective n values given in Table 2
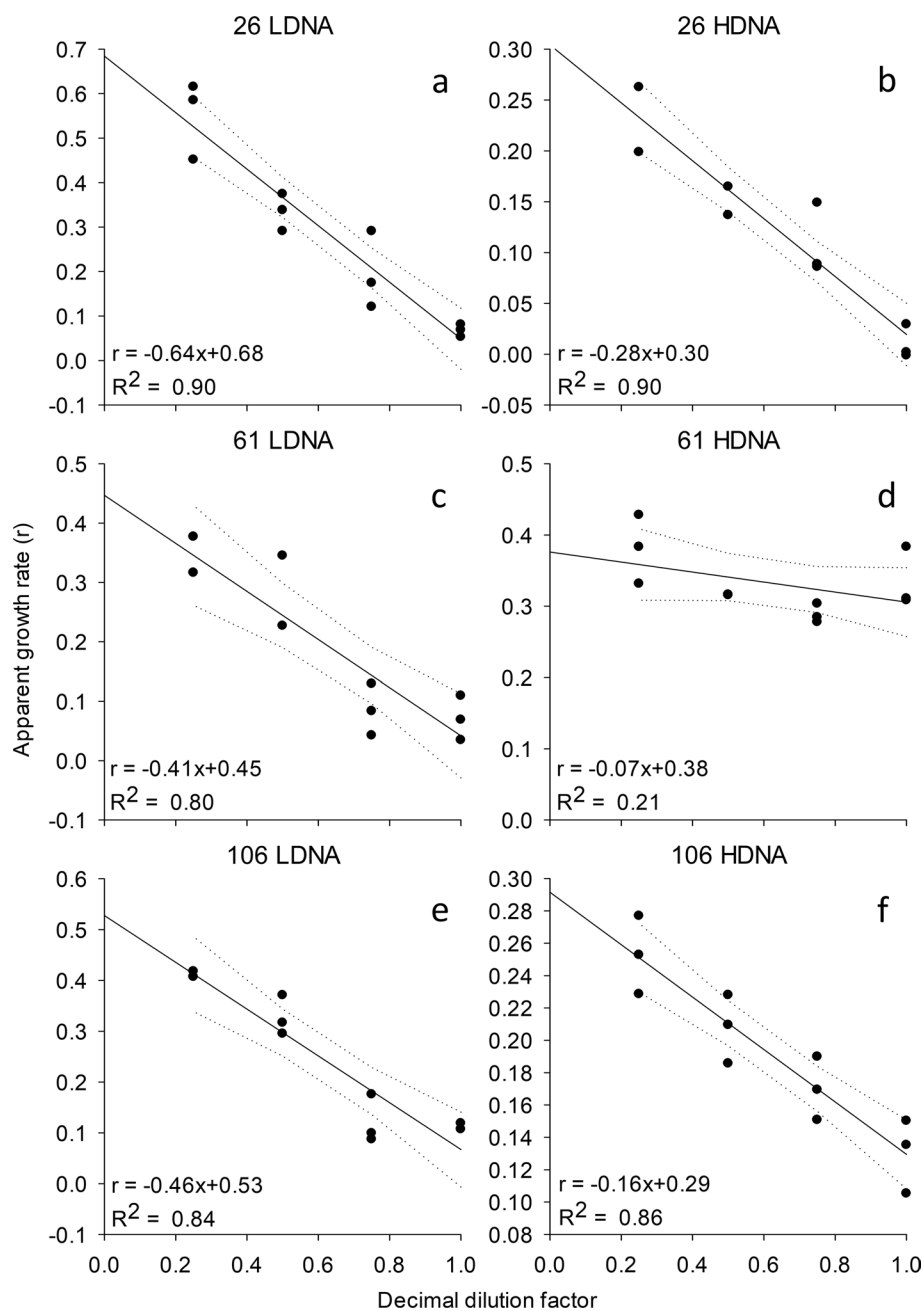
At the on-shelf station 106, SZP grazing had a moderate influence on the plankton community, with 50% of measured and calculated parameters yielding significant regressions with the dilution factor. Similar to station 26, a higher μ_{POC} than $\mu_{Chl\ a}$ was observed, suggesting an important contribution of heterotrophic organisms to POC_{all}. In line with this observation and similar to station 26, the LDNA bacteria were the main drivers of the bacterial turnover and carbon cycling at station 106. Overall 66% of the gross absolute POC production was eliminated from the particulate pool by SZP grazing at station 106.

SZP grazing reduced C:N of particulate organic matter

A relieve of SZP grazing pressure resulted in a highly significant increase of the $C:N_{all}$ ratio of the total particulate organic matter (integrating living cells and dead particles) of > 100% (Fig. 2). Such a change could be the result of either an increase of POC by growth, or a decrease of PON by remineralization. A remineralization of PON, however, would not be dependent on the dilution factor, since it would likely be happening to the particulate organic matter
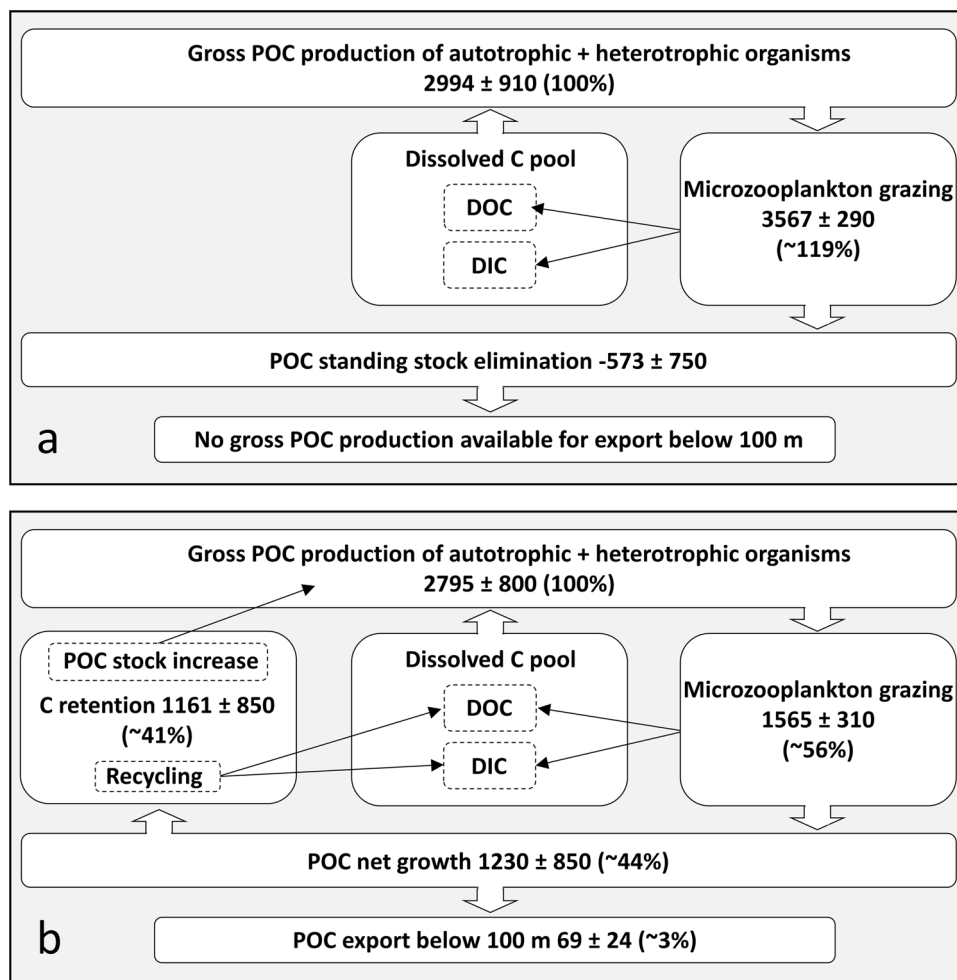
Fig. 4 Budget for particulate organic carbon (POC) integrated over the upper 100 m of the water column at station 26 (**A**) and 61 (**B**). Carbon (**C**), dissolved organic carbon (DOC), dissolved inorganic carbon (DIC). All numbers are given as means ± standard deviation and in mg C m^{-2} d^{-1}. Percentages reflect the share in gross absolute POC production rates. At station 26 more than the gross absolute POC production rate was lost by microzooplankton grazing hence, the POC standing stock was diminished and no POC production remained for export to depth. At station 61, microzooplankton still constituted the biggest loss term of gross absolute POC production in the water column, but after microzooplankton grazing, a net absolute POC production remained. Only ~3% of the original gross absolute POC production was lost from the upper 100 m by sedimentation, mostly in form of krill and salp fecal pellets (Pauli et al. 2021a). The lion's share of net absolute POC production therefore must have remained in the upper 100 m, likely either due to consumption and recycling, or as an addition to the POC standing stock

in all treatments to the same extend. The opposite was observed here (Fig. 2). Furthermore, while targeted nitrogen remineralization in a system that was high in dissolved nitrogen (Table 1) is not likely, a remineralization of nitrogen from dead particles to an extend that could yield such a C:N shift would likely have to entail a decrease of PON in the particulate organic matter, which was not observed. Relative to the initial samples and taking the dilution factor of each treatment into consideration, POC and PON increased in 32 and 25 out of 36 bottles, respectively (3 experiments times 12 bottles each, data accessible via PANGAEA). Hence, an increase of POC is the more probable reason for the C:N shift. Two likely scenarios exist

for this observation, both focusing on the < 2 μm plankton community:

High C:N picoplankton growth

It is possible that the increase of the C:N$_{all}$ ratio was due to the growth of very small (< 2 μm), fast reproducing cells with high C:N ratio. At all three stations, size-fractionated initial POC:PON values revealed that the C:N ratio in the < 2 μm size fraction was 20–63% higher than the C:N$_{all}$ ratio of the whole community (Table 1, statistically significant only at station 26 ($n = 3$, $p = 0.0017$)). It is important to keep in mind that this community of pico-cells is still

a diverse mixture of different bacteria and picoeukaryotes with variable C:N ratios. LDNA bacteria outgrew all other measured parameters at stations 26 and 106 when grazing pressure was relieved. Although bacteria are known to have low C:N ratios of 3.6–6.8 (Fagerbakke et al. 1996; Fukuda et al. 1998) the sources do not discriminate between HDNA and LDNA bacteria. According to Geider and La Roche 2002, DNA, RNA and proteins are characterized by a particularly low C:N ratio (2.6, 2.5 and 3.8 respectively) and can contribute significantly to the cells' biomass (0.5–3%, 3–15% and 30–65%, respectively) of phytoplankton and cyanobacteria. The C:N ratio of an organism containing low ratios of these compounds would therefore be driven by compounds with a high carbon content, such as lipids, carbohydrates and phosphoglycerides and consequently exhibit a high C:N ratio. Consistent with this, the highest growth– and mortality rates measured in all three experiments were those of POC and LDNA bacteria, which by definition carry low quantities of DNA. The fast gross growth rates of LDNA bacteria were countered by almost equally high grazing rates at all stations, resulting in balanced µ values in the undiluted seawater (1.0 dilution) bottles. With increasing dilution however, the gross growth rate of every parameter remained unaltered, while the SZP grazing pressure decreased sequentially from the undiluted (1.0 dilution) to the strongly diluted (0.25 dilution) bottles. Since the community's POC:Chl a ratio also increased with increasing dilutions at all three stations by a factor of ~ 2.1, ~ 3.1 and ~ 2.3 at stations 26, 61 and 106, respectively (comparison between the stations' initial samples and the strongly diluted 0.25 bottles yielded increases of 26: 731 ± 30 to 1523 ± 303 µg µg^{-1}, 61: 105 ± 6 to 326 ± 38 µg µg^{-1} and 106: 136 ± 9 to 317 ± 28 µg µg^{-1}), it can be assumed that mainly heterotrophic organisms were responsible for the shift of the communities C:N$_{all}$ ratio. Therefore, it is plausible that heterotrophic bacteria and potentially other groups of heterotrophic picoplankton with high growth rates and putatively very high cellular C:N ratios thrived, once grazing pressure was released, thus leading to the observed increase in C:N$_{all}$ of the whole community.

Transparent exopolymer particles

Conversely, the increasing C:N ratio with increasing dilution could be explained by the production of transparent exopolymer particles (TEP). TEP can contribute to the POC concentration equally to conventional particles (Mari 1999; Engel and Passow 2001). Furthermore, TEP have a C:N of 26 (Engel and Passow 2001) which is 4.3 times higher than the expected C:N ratio of phytoplankton in eutrophic polar waters (C:N:P of 78:13:1 equals C:N of 6 (Martiny et al. 2013)). The possibly high concentration of TEP in concert with their high C:N ratio, generally enables them to influence the C:N ratio significantly,

as was observed in this study with increasing dilution. Bacteria increase TEP concentrations in multiple ways, even in concert with phytoplankton. First, bacteria produce TEP themselves (Sugimoto et al. 2007). While the appearance of TEP in situ is usually best explained by the amount of Chl a (Zamanillo et al. 2019), bacteria are the second most important group to explain TEP occurrence (Corzo et al. 2005) particularly under the mixed layer (Ortega-Retuerta et al. 2009). Second bacteria have been observed to indirectly mediate TEP production on a scale that exceeded total bacterial carbon utilization by 1–twofold (Sugimoto et al. 2007). And third bacteria have been observed to induce TEP production in phytoplankton (Van Oostende et al. 2013).

Since TEP are routinely measured by filtering samples on a 0.4 µm polycarbonate filter (Passow and Alldredge 1995), a significant share of TEP would have been retained by the GF/F filters (pore size ~0.6 µm) used in this study. High gross growth rates of bacteria were observed in the experiments at all 3 stations. Therefore, it is plausible that bacteria increased POC far beyond their own incorporation of DOC into bacterial biomass by direct formation of TEP, the mediation of the TEP-precursors' aggregation to TEP and the induction of TEP formation in the present phytoplankton. The observed strong increase of POC with increasing dilution, in comparison with the only moderate increase of PON is in line with this argumentation.

TEP themselves, which can reach up to 100 µm in size (Passow and Alldredge 1995), aggregates bound by TEP (Larsson et al. 2022) as well as their dissolved precursors can be directly utilized as a carbon source by heterotrophic grazers (Tranvik et al. 1993; Passow and Alldredge 1999). There is no reason to believe that the TEP production rate was affected by the dilution itself. Consequently, it appears plausible that TEP have characteristic features of a prey item in the context of a dilution experiment and that with decreasing grazer concentration more TEP could prevail. As a side effect, the increasing dilution thusly also increased the C:N ratio of the particulate organic matter. Furthermore, the ecological role of TEP is far more complex than serving as prey for heterotrophic organisms. TEP constitute substrate for bacteria (Corzo et al. 2005) and as a coagulation agent (Engel and Passow 2001; Larsson et al. 2022), amplify the sedimentation of particulate organic matter. If indeed TEP significantly reacted to the dilution in these experiments, the presence of SZP grazers reduced the potential for carbon sequestration far beyond the direct disintegration of living cells into DOC and DIC by a direct consumption of TEP.

Assessing the use of POC for dilution experiments— Carbon complements Chl a

Dilution studies conducted in general, and around the WAP in particular (Burkill et al. 1995; Tsuda and Kawaguchi

1997; Garzio et al. 2013), rarely reported carbon based results (Calbet and Landry 2004) and instead relied on Chl a and cell counts. However, our results underline that it is important to include POC into the set of measured parameters for several reasons: POC provided significant correlations with the dilution factor more reliably than Chl a. While Chl a only yielded interpretable results for stations 26 and 106, POC was interpretable at all three stations. POC measurements also allowed for a direct assessment of carbon dynamics, independent of Chl a/carbon conversion factors. Former studies either calculated total PP, or the percentage of PP grazed by SZP (Calbet and Landry 2004; Pearce et al. 2008) based on Chl a results. However, it is crucial to keep in mind that this Chl a derived PP only represents a share of the total POC production in the system. The size of this share may be highly variable in between stations, as shown in this study, where the gross growth rate of POC was approximately twice as high as the gross growth rate of Chl a at station 26. Furthermore, depending on the stations characteristics, the actual share of grazed carbon may not be depicted with certainty based on Chl a derived carbon values alone. As seen at station 26 the share of SZP grazing induced mortality of Chl a in the gross Chl a production ($g_{Chl a}$:$k_{Chl a}$) amounted to only $36 \pm 16\%$ (calculated from g and k numbers in Table 2). If Chl a represented the carbon dynamics accurately, the 1.0 dilution bottles should show an increase in POC after the experiment, something that was not consistent with the 16% less POC at the end of the experiment. In contrast, the share of grazed POC in the gross POC production (g_{POC}:k_{POC}), amounted to $119 \pm 16\%$ at station 26 and thus may explain the loss of POC in the 1.0 dilution bottles. This difference between measured Chl a and carbon dynamics is crucial for the determination of the POC's fate in the context of SZP grazing. Also, it is important to note that POC included heterotrophic organisms, not just Chl a containing phototrophs and that especially in HNLC regions of the SO, where phytoplankton are Fe-limited, Chl a may not necessarily be a good indicator of phytoplankton biomass or changes thereof (Twining and Baines 2013). Additionally, the production and consumption of TEP would not be included if only Chl a based growth rates were used.

As a general remark, the results suggested that ^{14}C PP measurements should be interpreted cautiously in the context of dilution experiments, since the ^{14}C PP measurements in this study showed increasing gaps to the gross absolute POC production rate ($\mu_{abs POC}$) with increasing grazing intensity. At station 61, PP (Table 1) accounted for ~67% of the $\mu_{abs POC}$ (Fig. 4b), at station 106 only for ~28% of the $\mu_{abs POC}$ (763 ± 745 mg C m^{-2} d^{-1}) and at station 26, the PP (Table 1) was positive, while the $\mu_{abs POC}$ (Fig. 4a) was negative. Since phytoplankton and SZP are inseparable by filtration, phytoplankton growth and SZP grazing occur simultaneously in the bottles of the ^{14}C assay, with the latter

possibly affecting the former (Moigis 1999; Marra et al. 2012). ^{14}C is fixed, grazed, incorporated into SZP biomass, respired into the DIC pool and egested into the DOC pool all at the same time. While some studies dismiss grazing as a significant factor for ^{14}C uptake assays (Calbet and Landry 2004; Mosby and Smith 2015), published discussion on the topic and our results, suggest that respiration and DOC excretion may constitute a significant sink of particulate ^{14}C, especially when the grazing activity is high, potentially decreasing the measured PP. Together, our results suggest that the addition of POC to the set of measured parameters in dilution experiments leads to much better interpretation of SZP grazing activity.

SZP grazing recycled 20–50 times more carbon than was exported to depth

Upon relieve of grazing pressure, the observed increase of the C:N$_{all}$ ratios in the plankton communities at all three stations (Fig. 2) suggested that SZP might either prey on cells with a comparatively high POC content, or on TEP, which have a high C:N ratio, indicated by the 2.5 times higher g_{POC} in comparison to the g_{PON} (g values from station 26). However, whether this was a result of the SZP targeting these high carbon, low nitrogen particles, or an effect of cells with a low C:N ratio being better protected against grazing remains unresolved. Calbet & Landry (2004) postulated a 50% loss of carbon ingested by microzooplankton due to respiration. Taking this into account it can be assumed that an additional share of POC in the dilution experiments was converted to DOC and excreted. In addition to the carbon released from particles egested by the microplankton, organisms with a low C:N ratio may have been avoided, leading to species with predominantly low C:N being transferred to higher grazers, which then form fecal pellets which facilitate carbon export. Thus via these two processes, SZP may attenuate or even impede carbon export to depth. Thusly, the higher the SZP's consumption of POC production, the lower the potential carbon export to depth.

Comparing all 3 stations investigated during this study, the absolute SZP grazing on POC calculated from Eq. 3 was highest at station 26 and lowest at 61. Figure 4 shows a comparison of these two contrasting stations, assuming a relatively well-mixed upper water column to a depth of 100 m. The observations made at the two stations are not intended to represent general regional characteristic features, but attempt to highlight the variable influence SZP grazing can have on the plankton community in the SO. At station 26, 119% (3567 ± 290 mg C m^{-2} d^{-1}, Eq. 3) of the gross absolute POC produced was eliminated from the POC pool by SZP grazing (Fig. 4a) leaving no POC production for export to depth and resulting in a turnover time of 1.8 ± 0.2 days for the total POC pool (Table 2). In contrast, at station 61 only

56% (1565 ± 310 mg C m^{-2} d^{-1}) of the gross POC production (Fig. 4b) was eliminated from the particulate pool by SZP grazing. This value represents the middle of a range of grazing values calculated from Chl a, by Burkill et al. 1995. Consequently, 44% (1230 ± 850 mg C m^{-2} d^{-1}) of gross absolute POC produced was left for net POC production. Pauli et al. 2021a, b reported a particulate carbon flux of 69 ± 24 mg C m^{-2} d^{-1} (Pauli et al. 2021a) at a depth of 100 m during PS112 off Elephant Island, that predominantly consisted of krill and salp fecal pellets, meaning only < 3% of produced POC at station 61 was exported. Furthermore, 20 times more POC was eliminated from the particulate pool by SZP grazing than by carbon export at station 61 and at station 26, 50 times more POC was eliminated by SZP grazing than was exported at station 61. The remaining 41% of gross absolute POC production at station 61 must therefore have been retained in the upper 100 m, possibly due to the activity of mesozooplankton grazers (Iversen et al. 2017) or as an addition to the standing stock particulate carbon pool.

In line with previous studies, our work demonstrates that SZP plays a dominant role in the carbon cycling of the upper SO (Tsuda and Kawaguchi 1997; Schmoker et al. 2013). Interestingly, across all 3 stations, SZP grazing was further evidenced by the short residence times of POC, which ranged between 2 and 3 days (Table 2). Since the residence times of LDNA bacteria at stations 26 and 106, were ~7.7 and ~4.1 times lower than the residence times of Chl a, respectively (Table 2), it is likely that a significant portion of POC recycling encompassed the growth and consumption of small heterotrophic organisms in contrast to Chl a containing autotrophs. Furthermore, the significance of SZP in POC recycling raises the question, if their grazing activity might also significantly contribute to the recycling of other potentially limiting nutrients and trace elements like iron and manganese (Balaguer et al. 2022) or vitamins (Koch et al. 2011), as suggested in the literature (Sarthou et al. 2008).

Possible factors influencing microzooplankton grazing induced mortality

In line with previous studies (Garrison 1991; Garzio et al. 2013), which assessed the role of microzooplankton in the SO, SZP abundance and grazing induced mortality rates on the plankton community differed at the three stations. This can be explained by the following aspects:

Top down: microzooplankton abundance

During this study, heterotrophic microplankton (including heterotrophic dinoflagellates, tintinnids, aloricate ciliates and micrometazoans) showed a heterogeneous distribution, varying greatly in abundance in the South Shetland area (3–84 individuals L^{-1}) and around Elephant island (4–81

individuals L^{-1}), areas close to all stations in this study (Monti-Birkenmeier et al. 2021). Although not measured it is plausible, that the density and activity of higher consumers capable of feeding on microzooplankton influenced their abundance. The mesozooplankton community composition also differed greatly between the chosen experimental stations (26: 889 individuals m^{-3}, 106: 68 individuals m^{-3}) and over time (61: 496 and 2539 individuals m^{-3} within a sampling period of 18 days) (Plum et al. 2021). Salps (von Harbou et al. 2011; Pauli et al. 2021b) and Krill (Wickham and Berninger 2007; Siegel 2016; Pauli et al. 2021b) graze on members of the micro- and mesozooplankton and occur as dense swarms capable of locally grazing down the phytoplankton community with high efficiency, outcompeting other zooplankton (Perissinotto and Pakhomov 1998; Siegel 2016). However, during the PS112 expedition, both grazers had a patchy distribution (Pauli et al. 2021a), with salps ranging from 3 to 4750 ind. 1000 m^{-3}, 47–2707 ind. 1000 m^{-3} and 0–251 ind. 1000 m^{-3} close to stations 26, 61 and 106, respectively (R. Driscoll, Bremerhaven, personal communication). In comparison, adult krill was much less abundant, but also patchy, with densities of 0–8 ind. 1000 m^{-3}, 0–147 ind. 1000 m^{-3} and 0–112 ind. 1000 m^{-3} at stations 26, 61 and 106, respectively (R. Driscoll, Bremerhaven, personal communication).

Hence, the group-specific influences that different grazers imposed on the system at the time it was sampled were likely very different, even within a comparably small area. Therefore, the presence of higher consumers are one aspect that may explain the patchiness of SZP grazing rates, illustrated by the differences between the investigated stations. The focus of historical studies on mesozooplankton grazing combined with a lack of studies examining SZP activity have resulted in a general disregard of the importance of the microbial loop in the tertiary productivity of Antarctic ecosystems, many of which suffer from low primary productivity compared to lower latitude systems (Azam et al. 1991).

Bottom up: nutrient supply

While the dilution series method is based on the premise that only the encounter rate of predator and prey are reduced while the water chemistry remains the same, it does result in reduced demand for resources in the highly diluted treatments compared to the undiluted control. Some dilution studies thus add dissolved inorganic macronutrients to the incubations (nitrate, phosphate, silicate), in order to prevent nutrient limitation from reducing the apparent growth rates (r) of the undiluted treatments. Nutrient limitation of the undiluted bottles could increase the slope of the regression, thus overestimating the SZP grazing induced mortality (g). This was not done in this study for three main reasons: (i) Macronutrient amendments are necessary in coastal regions,

which harbor high biomass and where macronutrients, especially dissolved inorganic nitrogen, often limit phytoplankton production. In contrast, in the SO, where macronutrients are generally high and biomass is low (Table 1) those amendments are not necessary. (ii) 11 of the published 16 dilution studies performed in the Southern Ocean (Burkill et al. 1995; Froneman and Perissinotto 1996a, b; Tsuda and Kawaguchi 1997; Li et al. 2001; Froneman 2004; Safi et al. 2007; Pearce et al. 2008, 2010; Mosby and Smith 2015; Christaki et al. 2021) did not add nutrients. (iii) The original method instructs that it is important to not artificially increase growth factors during the incubation (Landry and Hassett 1982). Therefore, no trace metals were added since iron limitation at these SO ocean sites was expected. An addition of iron in this context would have entailed the risk to fertilize the experimental bottles, and thereby deviate from the ambient conditions in the ocean, resulting in artificially increased r and significantly underestimated g values. The fact that the measured g values in this study even fall in the lower range of values published in the literature for the SO (Table 2 in Garzio et al. 2013), validates the decision not to add iron. Some studies have suggested that heterotrophic bacteria in the SO may be limited by the availability of carbon, rather than iron (Fourquez et al. 2020). Since DOC was not monitored during the experiments, we cannot rule out that DOC limitation may have acted together with SZP grazing to influence the mortality rates of bacteria ($g_{bacteria\ all}$) in the undiluted bottles. However, it is worth noting that in those bottles more DOC was likely produced by higher absolute grazing intensity (Pearce et al. 2010) and that the $g_{bacteria\ all}$ in this study fell well into the range of bacterial g values published in the literature for the Southern Ocean (Table 3 in Garzio et al. 2013) strengthening the validity of the measured values of this study.

Conclusion

Our study highlights the regionally variable influence of SZP grazing on carbon cycling, by characterizing 3 very different systems. The study suggests that POC can be a valuable addition to Chl a measurements in the context of dilution experiments. Relatively short geographic distances between stations were enough to alter the influence of SZP grazing dramatically, likely due to the patchy distribution of SZP organisms and higher grazers. However, the strong overall contribution of SZP grazing to the loss of gross absolute POC production (56%-119%) suggests that SZP plays an important role in the carbon cycling at these SO sites. Furthermore, it was found that in the absence of SZP grazing, community C:N ratio rose significantly. Remineralization of carbon in the top 100 m was responsible for 20–50 times more POC recycling than was exported to depth. Thus,

SZP grazing is an important removal factor to consider in global carbon cycle models since it may drastically impede the amount of carbon being exported to depth. The rates presented here fall within the range of the previously published 0.03–0.52 d^{-1} for the SO and corroborates previously published work, which showed that SZP grazing is highly variable in the SO in general (Schmoker et al. 2013) and around the WAP in particular. As a result, the WAP region is characterized by a high degree of patchiness and adaptability to short-term change (Tsuda and Kawaguchi 1997), such as phytoplankton bloom events due to episodic iron inputs. To investigate the existence and effects of reoccurring rhythms in this system, far more research is necessary than has been so far directed towards the climatically and ecologically pivotal system that is the WAP.

Author contributions FK conceived and designed research. FK conducted the field work. SB and FK analysed the data. All authors contributed to writing, review and editing. Funding was acquired by ST and FK This study was supervised by FK and ST.

Declarations

Competing interests The authors have no competing interests to declare that are relevant to the content of this article..

need to obtain permission directly from the copyright holder. To view a copy of this licence, visit http://creativecommons.org/licenses/by/4.0/.

References

Agis M, Granda A, Dolan JR (2007) A cautionary note: examples of possible microbial community dynamics in dilution grazing experiments. J Exp Mar Bio Ecol 341:176–183. https://doi.org/10.1016/j.jembe.2006.09.002

Altman N, Krzywinski M (2015) Simple linear regression. Nat Methods 12:999–1000. https://doi.org/10.1038/nmeth.3627

Atkinson A, Siegel V, Pakhomov E, Rothery P (2004) Long-term decline in krill stock and increase in salps within the Southern Ocean. Nature 432:100–103. https://doi.org/10.1038/nature02996

Atkinson A, Hill SL, Pakhomov EA et al (2019) Krill (*Euphausia superba*) distribution contracts southward during rapid regional warming. Nat Clim Chang 9:142–147. https://doi.org/10.1038/s41558-018-0370-z

Azam F, Fenchel T, Field J et al (1983) The ecological role of water-column microbes in the sea. Mar Ecol Prog Ser 10:257–263. https://doi.org/10.3354/meps010257

Azam F, Smith DC, Hollibaugh JT (1991) The role of the microbial loop in Antarctic pelagic ecosystems. Polar Res 10:239–244. https://doi.org/10.3402/polar.v10i1.6742

Balaguer J, Koch F, Hassler C, Trimborn S (2022) Iron and manganese co-limit the growth of two phytoplankton groups dominant at two locations of the Drake Passage. Commun Biol 5:1–12. https://doi.org/10.1038/s42003-022-03148-8

Berk SG, Brownlee DC, Heinle DR et al (1977) Ciliates as a food source for marine planktonic copepods. Microb Ecol 4:27–40. https://doi.org/10.1007/BF02010427

Böckmann S, Koch F, Meyer B et al (2021) Salp fecal pellets release more bioavailable iron to Southern Ocean phytoplankton than krill fecal pellets. Curr Biol 31:1–10. https://doi.org/10.1016/j.cub.2021.02.033

Boyd PW (2002) Environmental factors controlling phytoplankton processes in the Southern Ocean. J Phycol 38:844–861. https://doi.org/10.1046/j.1529-8817.2002.t01-1-01203.x

Burkill PH, Edwards ES, Sleight MA (1995) Microzooplankton and their role in controlling phytoplankton growth in the marginal ice zone of the Bellingshausen Sea. Deep Sea Res Part II Top Stud Oceanogr 42:1277–1290. https://doi.org/10.1016/0967-0645(95)00060-4

Cabanes DJE, Blanco-Ameijeiras S, Bergin K et al (2020) Using Fe chemistry to predict Fe uptake rates for natural plankton assemblages from the Southern Ocean. Mar Chem 225:103853. https://doi.org/10.1016/j.marchem.2020.103853

Calbet A, Landry MR (2004) Phytoplankton growth, microzooplankton grazing, and carbon cycling in marine systems. Limnol Oceanogr 49:51–57. https://doi.org/10.4319/lo.2004.49.1.0051

Calbet A, Saiz E (2005) The ciliate-copepod link in marine ecosystems. Aquat Microb Ecol 38:157–167. https://doi.org/10.3354/ame038157

Calbet A, Saiz E (2013) Effects of trophic cascades in dilution grazing experiments: from artificial saturated feeding responses to positive slopes. J Plankton Res 35:1183–1191. https://doi.org/10.1093/plankt/fbt067

Calbet A, Saiz E, Almeda R et al (2011) Low microzooplankton grazing rates in the Arctic Ocean during a *Phaeocystis pouchetii* bloom (Summer 2007): fact or artifact of the dilution technique? J Plankton Res 33:687–701. https://doi.org/10.1093/plankt/fbq142

Calbet A, Martínez RA, Isari S et al (2012) Effects of light availability on mixotrophy and microzooplankton grazing in an oligotrophic plankton food web: evidences from a mesocosm study in Eastern Mediterranean waters. J Exp Mar Bio Ecol 424–425:66–77. https://doi.org/10.1016/j.jembe.2012.05.005

Caron DA, Dennett MR, Lonsdale DJ et al (2000) Microzooplankton herbivory in the Ross Sea, Antarctica. Deep Sea Res Part II Top Stud Oceanogr 47:3249–3272. https://doi.org/10.1016/S0967-0645(00)00067-9

Christaki U, Skouroliakou ID, Delegrange A et al (2021) Microzooplankton diversity and potential role in carbon cycling of contrasting Southern Ocean productivity regimes. J Mar Syst. https://doi.org/10.1016/j.jmarsys.2021.103531

Corzo A, Rodríguez-Gálvez S, Lubian L et al (2005) Spatial distribution of transparent exopolymer particles in the Bransfield Strait, Antarctica. J Plankton Res 27:635–646. https://doi.org/10.1093/plankt/fbi038

Ducklow HW, Baker K, Martinson DG et al (2007) Marine pelagic ecosystems: the West Antarctic Peninsula. Philos Trans R Soc B Biol Sci 362:67–94. https://doi.org/10.1098/rstb.2006.1955

Dussart BH (1965) Les différentes catégories de plancton. Hydrobiologia 26:72–74. https://doi.org/10.1007/BF00142255

Edler L (1979) Recommendations on methods for marine biological studies in the Baltic Sea. Phytoplankton and chlorophyll. Balt Mar Biol Publ 5:1–38

Engel A, Passow U (2001) Carbon and nitrogen content of transparent exopolymer particles (TEP) in relation to their Alcian Blue adsorption. Mar Ecol Prog Ser 219:1–10. https://doi.org/10.3354/meps219001

Fagerbakke K, Heldal M, Norland S (1996) Content of carbon, nitrogen, oxygen, sulfur and phosphorus in native aquatic and cultured bacteria. Aquat Microb Ecol 10:15–27. https://doi.org/10.3354/ame010015

Field CB, Behrenfeld MJ, Randerson JT, Falkowski P (1998) Primary production of the biosphere: integrating terrestrial and oceanic components. Science 281:237–240. https://doi.org/10.1126/science.281.5374.237

Fourquez M, Bressac M, Deppeler SL et al (2020) Microbial competition in the subpolar Southern Ocean: an Fe–C Co-limitation experiment. Front Mar Sci 6:1–15. https://doi.org/10.3389/fmars.2019.00776

Froneman PW (2004) Protozooplankton community structure and grazing impact in the eastern Atlantic sector of the Southern Ocean in austral summer 1998. Deep Res Part II Top Stud Oceanogr 51:2633–2643. https://doi.org/10.1016/j.dsr2.2004.09.001

Froneman P, Perissinotto R (1996a) Microzooplankton grazing in the Southern Ocean: implications for the carbon cycle. Mar Ecol 17:99–115. https://doi.org/10.1111/j.1439-0485.1996.tb00493.x

Froneman PW, Perissinotto R (1996b) Microzooplankton grazing and protozooplankton community structure in the South Atlantic and in the Atlantic sector of the Southern Ocean. Deep Res Part I Oceanogr Res Pap 43:703–721. https://doi.org/10.1016/0967-0637(96)00010-6

Fukuda R, Ogawa H, Nagata T, Koike I (1998) Direct determination of carbon and nitrogen contents of natural bacterial assemblages in marine environments. Appl Environ Microbiol 64:3352–3358. https://doi.org/10.1128/AEM.64.9.3352-3358.1998

Garrison DL (1991) An overview of the abundance and role of protozooplankton in Antarctic waters. J Mar Syst 2:317–331. https://doi.org/10.1016/0924-7963(91)90039-W

Garzio L, Steinberg D, Erickson M, Ducklow H (2013) Microzooplankton grazing along the Western Antarctic Peninsula. Aquat Microb Ecol 70:215–232. https://doi.org/10.3354/ame01655

Gasol JM, Zweifel UL, Peters F et al (1999) Significance of size and nucleic acid content heterogeneity as measured by flow cytometry

in natural planktonic bacteria. Appl Environ Microbiol 65:4475–4483. https://doi.org/10.1128/AEM.65.10.4475-4483.1999

Geider R, La Roche J (2002) Redfield revisited: variability of C:N:P in marine microalgae and its biochemical basis. Eur J Phycol 37:1–17. https://doi.org/10.1017/S0967026201003456

Grasshoff K, Ehrhardt M, Kremling K (eds) (1999) Methods of seawater analysis. Wiley-VCH Verlag GmbH, Weinheim

Henson SA, Sanders R, Madsen E (2012) Global patterns in efficiency of particulate organic carbon export and transfer to the deep ocean. Global Biogeochem Cycles. https://doi.org/10.1029/2011GB004099

Holmes RM, Aminot A, Kérouel R et al (1999) A simple and precise method for measuring ammonium in marine and freshwater ecosystems. Can J Fish Aquat Sci 56:1801–1808. https://doi.org/10.1139/f99-128

Iversen MH, Pakhomov EA, Hunt BPV et al (2017) Sinkers or floaters? Contribution from salp pellets to the export flux during a large bloom event in the Southern Ocean. Deep Sea Res Part II Top Stud Oceanogr 138:116–125. https://doi.org/10.1016/j.dsr2.2016.12.004

Koch F, Marcoval MA, Panzeca C et al (2011) The effect of vitamin B_{12} on phytoplankton growth and community structure in the Gulf of Alaska. Limnol Oceanogr 56:1023–1034. https://doi.org/10.4319/lo.2011.56.3.1023

Landry MR, Hassett RP (1982) Estimating the grazing impact of marine micro-zooplankton. Mar Biol 67:283–288. https://doi.org/10.1007/BF00397668

Larsson ME, Bramucci AR, Collins S et al (2022) Mucospheres produced by a mixotrophic protist impact ocean carbon cycling. Nat Commun 13:1–15. https://doi.org/10.1038/s41467-022-28867-8

Li C, Sun S, Zhang G, Ji P (2001) Summer feeding activities of zooplankton in Prydz Bay, Antarctica. Polar Biol 24:892–900. https://doi.org/10.1007/s003000100292

Löder MGJ, Meunier C, Wiltshire KH et al (2011) The role of ciliates, heterotrophic dinoflagellates and copepods in structuring spring plankton communities at Helgoland Roads, North Sea. Mar Biol 158:1551–1580. https://doi.org/10.1007/s00227-011-1670-2

Mari X (1999) Carbon content and C: N ratio of transparent exopolymeric particles (TEP) produced by bubbling exudates of diatoms. Mar Ecol Prog Ser 183:59–71. https://doi.org/10.3354/meps183059

Marra J, Capuzzo E, Montecino V (2012) Potential grazing effects in incubations with ^{14}C. Aquat Biol 14:283–288. https://doi.org/10.3354/ab00403

Martin JH, Fitzwater SE, Gordon RM (1990) Iron deficiency limits phytoplankton growth in Antarctic waters. Global Biogeochem Cycles 4:5–12. https://doi.org/10.1029/GB004i001p00005

Martiny AC, Pham CTA, Primeau FW et al (2013) Strong latitudinal patterns in the elemental ratios of marine plankton and organic matter. Nat Geosci 6:279–283. https://doi.org/10.1038/ngeo1757

Martiny AC, Vrugt JA, Lomas MW (2014) Concentrations and ratios of particulate organic carbon, nitrogen, and phosphorus in the global ocean. Sci Data 1:140048. https://doi.org/10.1038/sdata.2014.48

McNair HM, Morison F, Graff JR et al (2021) Microzooplankton grazing constrains pathways of carbon export in the subarctic North Pacific. Limnol Oceanogr 66:2697–2711. https://doi.org/10.1002/lno.11783

Meredith MP, Stefels J, van Leeuwe M (2017) Marine studies at the western Antarctic Peninsula: priorities, progress and prognosis. Deep Sea Res Part II Top Stud Oceanogr 139:1–8. https://doi.org/10.1016/j.dsr2.2017.02.002

Moigis AG (1999) Photosynthetic rates in the surface waters of the Red Sea: the radiocarbon versus the non-isotopic dilution method. J Plankton Res 22:713–727. https://doi.org/10.1093/plankt/22.4.713

Monti-Birkenmeier M, Diociaiuti T, Badewien TH et al (2021) Spatial distribution of microzooplankton in different areas of the northern Antarctic Peninsula region, with an emphasis on tintinnids. Polar Biol 44:1749–1764. https://doi.org/10.1007/s00300-021-02910-8

Mosby AF, Smith WO (2015) Phytoplankton growth rates in the Ross Sea, Antarctica. Aquat Microb Ecol 74:157–171. https://doi.org/10.3354/ame01733

Orchard MJ, Humphries S, Schuech R, Menden-Deuer S (2016) The influence of viscosity on the motility and sensory ability of the dinoflagellate *Heterocapsa triquetra*. J Plankton Res 38:1062–1076. https://doi.org/10.1093/plankt/fbw004

Ortega-Retuerta E, Reche I, Pulido-Villena E et al (2009) Uncoupled distributions of transparent exopolymer particles (TEP) and dissolved carbohydrates in the Southern Ocean. Mar Chem 115:59–65. https://doi.org/10.1016/j.marchem.2009.06.004

Paffenhöfer G-A (1998) Heterotrophic protozoa and small metazoa: feeding rates and prey-consumer interactions. J Plankton Res 20:121–133. https://doi.org/10.1093/plankt/20.1.121

Passow U, Alldredge AL (1995) A dye-binding assay for the spectrophotometric measurement of transparent exopolymer particles (TEP). Limnol Oceanogr 40:1326–1335. https://doi.org/10.4319/lo.1995.40.7.1326

Passow U, Alldredge AL (1999) Do transparent exopolymer particles (TEP) inhibit grazing by the euphausiid *Euphausia pacifica*? J Plankton Res 21:2203–2217. https://doi.org/10.1093/plankt/21.11.2203

Pauli N-C, Flintrop CM, Konrad C et al (2021a) Krill and salp faecal pellets contribute equally to the carbon flux at the Antarctic Peninsula. Nat Commun 12:7168. https://doi.org/10.1038/s41467-021-27436-9

Pauli N-C, Metfies K, Pakhomov EA et al (2021b) Selective feeding in Southern Ocean key grazers—diet composition of krill and salps. Commun Biol 4:1061. https://doi.org/10.1038/s42003-021-02581-5

Pearce I, Davidson AT, Wright S, Van Den Enden R (2008) Seasonal changes in phytoplankton growth and microzooplankton grazing at an Antarctic coastal site. Aquat Microb Ecol 50:157–167. https://doi.org/10.3354/ame01149

Pearce I, Davidson AT, Thomson PG et al (2010) Marine microbial ecology off East Antarctica (30–80°E): rates of bacterial and phytoplankton growth and grazing by heterotrophic protists. Deep Res Part II Top Stud Oceanogr 57:849–862. https://doi.org/10.1016/j.dsr2.2008.04.039

Perissinotto RA, Pakhomov E (1998) The trophic role of the tunicate *Salpa thompsoni* in the Antarctic marine ecosystem. J Mar Syst 17:361–374. https://doi.org/10.1016/S0924-7963(98)00049-9

Plum C, Cornils A, Driscoll R et al (2021) Mesozooplankton trait distribution in relation to environmental conditions and the presence of krill and salps along the northern Antarctic Peninsula. J Plankton Res 43:927–944. https://doi.org/10.1093/plankt/fbab068

Price LM (2012) Microzooplankton Community Structure and Grazing Impact Along the Western Antarctic Peninsula. College of William and Mary

Redfield AC, Ketchum BH, Richards FA (1963) The influence of organisms on the composition of sea-water. In: Hill MN (ed) In The Sea. Ideas and observations on progress in the study of the sea. Wiley Interscience, New York, pp 26–77

Ryther JH (1969) Photosynthesis and fish production in the sea. Science 166:72–76. https://doi.org/10.1126/science.166.3901.72

Safi KA, Brian Griffiths F, Hall JA (2007) Microzooplankton composition, biomass and grazing rates along the WOCE SR3 line between Tasmania and Antarctica. Deep Res Part I Oceanogr Res Pap 54:1025–1041. https://doi.org/10.1016/j.dsr.2007.05.003

Sarthou G, Vincent D, Christaki U et al (2008) The fate of biogenic iron during a phytoplankton bloom induced by natural fertilisation:

impact of copepod grazing. Deep Res Part II Top Stud Oceanogr 55:734–751. https://doi.org/10.1016/j.dsr2.2007.12.033

Schmidt K, Atkinson A, Petzke K-J et al (2006) Protozoans as a food source for Antarctic krill, *Euphausia superba*: complementary insights from stomach content, fatty acids, and stable isotopes. Limnol Oceanogr 51:2409–2427. https://doi.org/10.4319/lo.2006.51.5.2409

Schmoker C, Hernández-León S, Calbet A (2013) Microzooplankton grazing in the oceans: impacts, data variability, knowledge gaps and future directions. J Plankton Res 35:691–706. https://doi.org/10.1093/plankt/fbt023

Sherr EB, Sherr BF (2002) Significance of predation by protists in aquatic microbial food webs. Antonie Van Leeuwenhoek 81:293–308. https://doi.org/10.1023/A:1020591307260

Siegel V (2016) Biology and Ecology of Antarctic Krill, vol 1. Springer International Publishing, Berlin

Steinberg DK, Landry MR (2017) Zooplankton and the Ocean carbon cycle. Ann Rev Mar Sci 9:413–444. https://doi.org/10.1146/annurev-marine-010814-015924

Steinberg D, Martinson D, Costa D (2012) Two decades of pelagic ecology of the Western Antarctic Peninsula. Oceanography 25:56–67. https://doi.org/10.5670/oceanog.2012.75

Sugimoto K, Fukuda H, Baki MA, Koike I (2007) Bacterial contributions to formation of transparent exopolymer particles (TEP) and seasonal trends in coastal waters of Sagami Bay, Japan. Aquat Microb Ecol 46:31–41. https://doi.org/10.3354/ame046031

Teixeira IG, Figueiras FG (2009) Feeding behaviour and non-linear responses in dilution experiments in a coastal upwelling system. Aquat Microb Ecol 55:53–63. https://doi.org/10.3354/ame01281

Tranvik LJ, Sherr EB, Sherr BF (1993) Uptake and utilization of "colloidal DOM'' by heterotrophic flagellates in seawater". Mar Ecol Prog Ser 92:301–309. https://doi.org/10.3354/meps092301

Tsuda A, Kawaguchi S (1997) Microzooplankton grazing in the surface water of the Southern Ocean during an austral summer. Polar Biol 18:240–245. https://doi.org/10.1007/s003000050184

Turner JT (2015) Zooplankton fecal pellets, marine snow, phytodetritus and the ocean's biological pump. Prog Oceanogr 130:205–248. https://doi.org/10.1016/j.pocean.2014.08.005

Twining BS, Baines SB (2013) The trace metal composition of marine phytoplankton. Ann Rev Mar Sci 5:191–215. https://doi.org/10.1146/annurev-marine-121211-172322

UNESCO (1994) Ocean Flux Study (Jgofs) Protocols for the Joint Global Core Measurements. 181

Utermöhl H (1958) Zur Vervollkommnung der quantitativen Phytoplankton Methodik. Mitteilung Int Vereinigung Für Theor Und Angew Limnol 9:1–39

Van Oostende N, Moerdijk-Poortvliet TCW, Boschker HTS et al (2013) Release of dissolved carbohydrates by *Emiliania huxleyi* and formation of transparent exopolymer particles depend on algal life cycle and bacterial activity. Environ Microbiol 15:1514–1531. https://doi.org/10.1111/j.1462-2920.2012.02873.x

Vaughan DG, Marshall GJ, Connolley WM et al (2003) Recent rapid regional warming on the Antarctic Peninsula. Clim Chang 60:243–274. https://doi.org/10.1023/A:1026021217991

von Harbou L, Dubischar CD, Pakhomov EA et al (2011) Salps in the Lazarev Sea, Southern Ocean: I. Feeding Dynamics Mar Biol 158:2009–2026. https://doi.org/10.1007/s00227-011-1709-4

Welschmeyer NA (1994) Fluorometric analysis of chlorophyll a in the presence of chlorophyll b and pheopigments. Limnol Oceanogr 39:1985–1992. https://doi.org/10.4319/lo.1994.39.8.1985

Wickham SA, Berninger UG (2007) Krill larvae, copepods and the microbial food web: interactions during the Antarctic fall. Aquat Microb Ecol 46:1–13. https://doi.org/10.3354/ame046001

Zamanillo M, Ortega-Retuerta E, Nunes S et al (2019) Distribution of transparent exopolymer particles (TEP) in distinct regions of the Southern Ocean. Sci Total Environ 691:736–748. https://doi.org/10.1016/j.scitotenv.2019.06.524

4

PUBLICATION 3

SALP FECAL PELLETS RELEASE MORE
BIOAVAILABLE IRON TO SOUTHERN OCEAN
PHYTOPLANKTON THAN KRILL FECAL PELLETS

Published in Current Biology

Salp fecal pellets release more bioavailable iron to Southern Ocean phytoplankton than krill fecal pellets

Highlights

- Salps recycle iron in a more bioavailable form than krill

- Per mol fecal pellet carbon, salps release more iron than krill

- Possibly, salps increase the carbon fixation potential of the Southern Ocean

Authors

Sebastian Böckmann, Florian Koch, Bettina Meyer, ..., Luis Miguel Laglera, Christel Hassler, Scarlett Trimborn

Correspondence

sebastian.boeckmann@awi.de

In brief

Böckmann et al. show that salp fecal pellets release more iron than krill fecal pellets. Additionally, the iron recycled from salp fecal pellets is more bioavailable to Southern Ocean phytoplankton than iron recycled from krill fecal pellets. Increasing salp populations might increase the carbon fixation potential of the Southern Ocean.

CelPress

Current Biology

Article

Salp fecal pellets release more bioavailable iron to Southern Ocean phytoplankton than krill fecal pellets

Sebastian Böckmann,[1,2,11,*] Florian Koch,[2,3] Bettina Meyer,[4,5,8] Franziska Pausch,[1,2] Morten Iversen,[4,9] Ryan Driscoll,[4] Luis Miguel Laglera,[10] Christel Hassler,[6,7] and Scarlett Trimborn[1,2]

[1]Marine Botany, University of Bremen, Bibliothekstraße 1, 28359 Bremen, Germany
[2]Ecological Chemistry, Alfred Wegener Institute, Helmholtz Center for Polar and Marine Research, Am Handelshafen 12, 27570 Bremerhaven, Germany
[3]Fachbereich 2, Hochschule Bremerhaven, An der Karlstadt 8, 27568 Bremerhaven, Germany
[4]Polar Biological Oceanography, Alfred Wegener Institute, Helmholtz Center for Polar and Marine Research, Am Handelshafen 12, 27570 Bremerhaven, Germany
[5]Helmholtz Institute for Marine Functional Biodiversity, University of Oldenburg, Ammerländer Heerstraße 231, 26129 Oldenburg, Germany
[6]Department F.-A. Forel for Environmental and Aquatic Science, University of Geneva, 66, Boulevard Carl-Vogt, 1211 Geneva, Switzerland
[7]Swiss Polar Institute, Ecole Polytechnique Fédérale de Lausanne, Route Cantonale, 1015 Lausanne, Switzerland
[8]Institute for Chemistry and Biology of the Marine Environment, University of Oldenburg, Carl-von-Ossietzky-Strasse 9-11, 26111 Oldenburg, Germany
[9]Marum and University of Bremen, Leobener Strasse 13, 28359 Bremen, Germany
[10]FI-TRACE, Departamento de Química and Laboratori Interdisciplinari sobre Canvi Climatic, Universidad de las Islas Baleares, Edificio Mateu Orfila, Campus Universitario, Carretera de Valldemossa, km 7.5, Palma, Balearic Islands 07122, Spain
[11]Lead contact
*Correspondence: sebastian.boeckmann@awi.de
https://doi.org/10.1016/j.cub.2021.02.033

SUMMARY

Over the last decades, it has been reported that the habitat of the Southern Ocean (SO) key species Antarctic krill (*Euphausia superba*) has contracted to high latitudes, putatively due to reduced winter sea ice coverage, while salps as *Salpa thompsoni* have extended their dispersal to the former krill habitats. To date, the potential implications of this population shift on the biogeochemical cycling of the limiting micronutrient iron (Fe) and its bioavailability to SO phytoplankton has never been tested. Based on uptake of fecal pellet (FP)-released Fe by SO phytoplankton, this study highlights how efficiently krill and salps recycle Fe. To test this, we collected FPs of natural populations of salps and krill, added them to the same SO phytoplankton community, and measured the community's Fe uptake rates. Our results reveal that both FP additions yielded similar dissolved iron concentrations in the seawater. Per FP carbon added to the seawater, 4.8 ± 1.5 times more Fe was taken up by the same phytoplankton community from salp FP than from krill FP, suggesting that salp FP increased the Fe bioavailability, possibly through the release of ligands. With respect to the ongoing shift from krill to salps, the potential for carbon fixation of the Fe-limited SO could be strengthened in the future, representing a negative feedback to climate change.

INTRODUCTION

In vast areas of the Southern Ocean (SO), phytoplankton growth is limited by iron (Fe) availability. Fe input from *de novo* sources, including upwelling, dust deposition, melting sea ice, and resuspension of coastal sediments,[1–4] is strong in the vicinity of land. In contrast, for the open ocean, upwelling and Fe recycling in the water column is of paramount importance.[5,6] Previous studies suggested that grazers[7,8] and predators[9] contribute to the recycling of Fe in the water column. In some open ocean regions, up to 50% of the soluble Fe pool is turned over on a weekly basis, mediated by biological recycling,[10] with Antarctic krill (*Euphausia superba*), hereafter referred to as krill, being particularly important.[11] So far, few studies have quantified the amount of Fe

released by krill[8,12–14] and the dominant SO salp species *Salpa thompsoni*,[15] hereafter referred to as salps. Because krill and salps form high biomass aggregates, it is believed that both play a substantial role in Fe recycling via acidic and anaerobic digestion of phytoplankton cells.[14] Krill foraging on the seabed[16] was also identified as a vector of new Fe from abyssal depths, hence sustaining phytoplankton productivity in the euphotic zone by recycling and importing Fe from below. Maldonado et al.[17] calculated that krill and salps can release 3.4–14.4 kg Fe km^{-2} year^{-1} and 1.3–12.1 kg Fe km^{-2} year^{-1}, respectively, making them the third and fourth most important Fe recycling organisms in the SO, after microzooplankton and carnivorous zooplankton. However, the actual bioavailability of this recycled Fe to SO phytoplankton has never been tested.
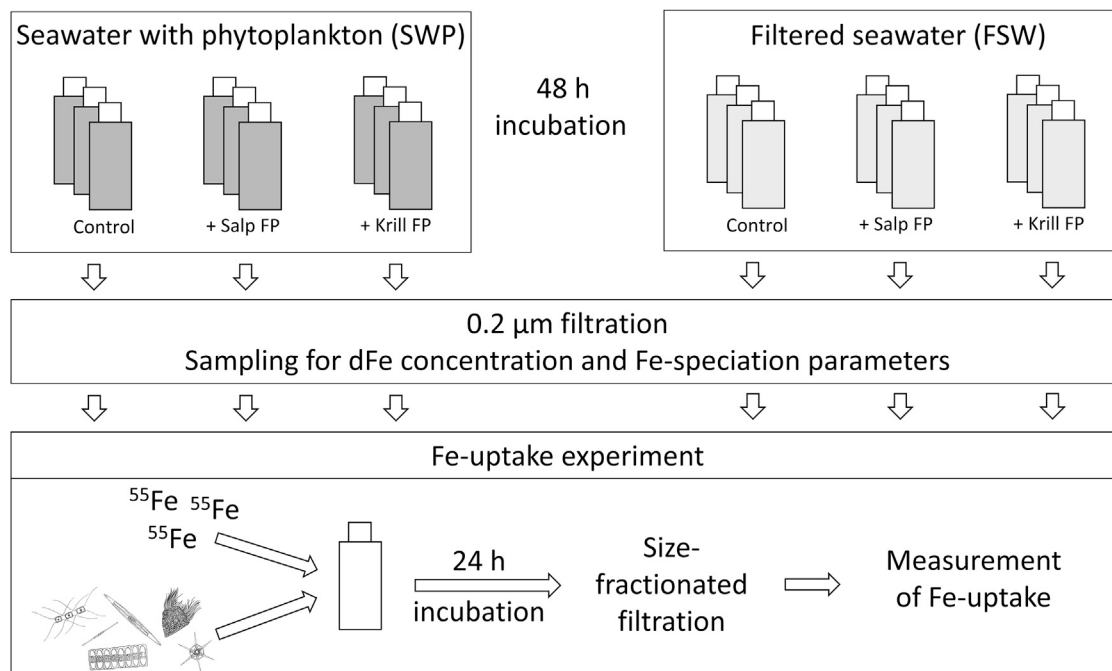
Figure 1. Experimental setup

Natural Southern Ocean seawater was filled into 18 bottles. Nine were filled with seawater that contained phytoplankton (SWP), and 9 were filled with filtered seawater (FSW). Three bottles were left untreated (controls); to 3 bottles, salp fecal pellets (salp FPs) were added, and to the other 3 bottles, krill fecal pellets (krill FPs) were added. After 48 h, all bottles were filtered through a 0.2 μm filter, and the filtrate was used to determine the dissolved iron concentration (dFe) and Fe-speciation parameters. Afterward, the filtrate from each bottle was used to determine Fe-uptake rates. A concentrated natural phytoplankton community and [55]Fe as a tracer label were added to the preconditioned water aliquots. After a 24-h incubation phase, the Fe uptake into the 0.2–2 μm fraction and the >2 μm fraction were measured in a scintillation counter.

It has been reported that, between 1926 and 2016, krill distributions shifted from the northern part of the southwest Atlantic sector of the SO to the Antarctic shelf.[18] Concurrently, Pakhomov et al.[19] reported that, due to global warming, salps increasingly inhabit krill habitats. In light of these climate-driven ecosystem changes, the biogeochemical consequences for the Fe supply from salps and krill to the SO need to be quantified.

The objective of this study was to assess the bioavailability of recycled Fe from krill and salp fecal pellets (FPs) to a natural SO plankton community. Our incubation experiment showed that the concentrations of Fe dissolved from salp and krill FPs were similar although the dissolved Fe (dFe) from salp FPs was taken up 1.7 times more effectively by phytoplankton, suggesting a higher bioavailability for dFe released from salp FPs.

RESULTS AND DISCUSSION

To investigate the role of salp and krill FPs on SO Fe biogeochemistry, a two-step incubation experiment was performed close to the Western Antarctic Peninsula (STAR Methods; Figure 1) 45 km north-east of Elephant Island, a location which experienced increasing salp and decreasing krill densities in the past 5 decades.[20]

Freshly collected FPs were added to natural seawater (including the ambient phytoplankton community; seawater with plankton [SWP]) and to 0.2 μm filtered seawater (FSW) (no phytoplankton) in concentrations matching typical *in situ*

situations during a bloom period.[20–25] Amended (salp FPs and krill FPs) and unamended (control) samples were incubated for 48 h at ambient light and temperature conditions. At the end of the experiment, dFe concentrations and the ligand complexing capacity were determined. In a second step, the Fe bioavailability was determined with [55]Fe as a tracer, by adding a concentrated, natural phytoplankton community to the 0.2 μm filtered water from the different treatments (Figure 1; STAR Methods).

FPs as a source of Fe

The amount of FP additions per liter for salps was chosen to mimic natural conditions based on reported salp densities in the Lazarev Sea of 4 individuals m^{-3} and a projected doubling of salp density every decade.[20,21] At the beginning of the experiments, an amount of 3.4 ± 0.5 μg FP C L^{-1} d^{-1} (Table 1) was added once, corresponding to the release of FP by 13.4 salps m^{-3}, defecating at a rate of ~250 μg C salp^{-1} day^{-1},[22–24] representing realistic *in situ* densities of present-day SO waters. For krill, an average density of 16–64 individuals m^{-2} at the tip of the Western Antarctic Peninsula[20] and a defecation rate of 146 μg C krill^{-1} d^{-1} (estimated from Atkinson et al.[26]) were reported. We added 9 ± 1 μg FP C L^{-1} d^{-1} (Table 1), representing a density of one individual krill in 16 L, which equals 62.5 krill individuals m^{-3}. Our krill FP addition thus exceeded the expected average krill FP density of the region but stayed well below the density of FPs estimated for krill swarms of 1.3 g C m^{-3} d^{-1}.[25]

Current Biology
Article

CellPress
OPEN ACCESS

Table 1. Iron and carbon in FP

Parameter	Unit	Salp FP treatment	Krill FP treatment
C addition by FP	$\mu g\ L^{-1}\ d^{-1}$	3.4 ± 0.5	9 ± 1
Dry weight addition by FP	$\mu g\ L^{-1}\ d^{-1}$	80 ± 0.2	142 ± 3.8
tFe in FP	$nmol\ Fe\ \mu g\ dw^{-1}$	0.73 ± 0.0004	0.75 ± 0.001
Leached dFe from total added tFe	%	0.6 ± 0.2	0.3 ± 0.03
Leached dFe per FP C	$nmol\ dFe\ \mu g\ FP\ C^{-1}\ d^{-1}$	0.1 ± 0.05	0.03 ± 0.005
Fe uptake by phytoplankton per added FP C	$nmol\ dFe\ \mu g\ FP\ C^{-1}$	0.08 ± 0.02	0.02 ± 0.004

Carbon (C) addition by fecal pellets (FPs), addition of FP dry weight, total iron content (tFe) inside the FP, leached dissolved iron (dFe) from added tFe, leached dFe per FP C, and iron (Fe) uptake into phytoplankton cells per added FP C.

Thus, measurements were obtained at conditions that represent the effect of FP material in the extended surrounding area of a krill swarm event. In order to fuel phytoplankton production, the FPs have to release the dFe in the euphotic zone. Thus, even though FPs can develop high sinking velocities,[27] it has been reported that two-thirds of salp FPs produced do not reach 100 m depth,[28] putatively because of zooplankton coprophagy (feeding of zooplankton organisms on FPs), which causes the FPs to loosen or break up. It is possible that this effect is transferable to krill FPs as well.

To our knowledge, this study is the first time that dFe release rates from FPs of these two major zooplankton species under ambient ocean conditions (without an additional acidification step) have been measured (Table 1). Irrespective of the FP type that was added, no significant differences in dFe were detected in the SWP (Figure 2A). This is in stark contrast to the FSW, where salp and krill FP additions significantly increased the dFe pool (salp FP: $p = 0.007$ and krill FP: $p = 0.021$) by 1.54- $\pm$ 0.10- and 1.45- $\pm$ 0.04-fold, respectively, indicating Fe fertilization from both FP types (Figure 2B). We hypothesize that, in the SWP treatments, the phytoplankton cells present during the 48 h of incubation removed most of the Fe leached from the FP either by absorption or adsorption to their cell surface.

It has been reported that the FP of krill contain higher concentrations of Fe than any other part of the krill's body.[12] Also, krill guts have the potential to release originally lithogenic Fe in a reactive form.[14] Furthermore, the Fe:C ratio in FPs of marine animals is generally enriched in comparison to their food, due to (1) low assimilation rates of Fe in animals and (2) the respiratory conversion of particulate organic carbon to dissolved organic and inorganic carbon.[29] Schmidt et al.[14] report an Fe content in krill FPs of 0.94 nmol Fe μg^{-1} FP dry weight^{-1},[14] which is very similar to the 0.75 nmol Fe μg^{-1} FP dry weight of this study (Table 1). For salps, the observed increase of dFe in FSW contradicts previous results by Cabanes et al.,[15] who used whole salp FP, and did not measure a significant amount of dFe leaching from them. In the study presented here, the FPs were broken up, destroying their peritrophic membrane, mimicking natural exposure to grazers (i.e., through coprophagy [ingestion of FPs], coprorhexy [fragmentation of FPs], and coprochaly [loosening of FPs]).[30,31] This activity facilitates a disintegration of the FPs into small, slow-sinking fragments.[28]

From the total Fe added in form of FP, 0.3% $\pm$ 0.03% and 0.6% $\pm$ 0.2% were released in a dissolved form for krill and salp FP, respectively (Table 1). These values lie at the low end of a previously reported range of 0.05%–6.33% as leachable particulate Fe in krill FPs[13] and krill stomachs.[32] The latter two studies, however, measured the leachable Fe fraction by acidification with a 25% acetic acid solution and a NH_4Ac buffer, respectively, therefore reaching a lower pH than in our study. Similarly, Cabanes et al.[15] acidified their salp FPs to pH = 2 in order to measure leachable Fe. No study so far has measured dFe release from FPs under natural conditions without an additional acidification step. It is therefore not surprising that all previous studies report dFe release values, which differ from our study. What is consistent across all (this study and Schlosser et al.,[13] Cabanes et al.,[15] and Schmidt et al.[32]) is that <7% of the total Fe content was leached from the FPs, suggesting that most of the Fe was refractory.

Even though the amount of krill FPs added (FP C given in μg of carbon) was 2.6 times higher than the amount of salp FP C added (Table 1), both additions increased the dFe concentration similarly in the FSW treatments (Figure 2B). Furthermore, normalized to FP C, the salp FPs released 3.3 times as much dFe as the krill FPs (Table 1). This higher leachability could be explained as follows: in contrast to krill FPs, salp FPs are fragile,[28] less dense than those of pelagic crustaceans,[33] and lack a peritrophic membrane.[34] In contrast, krill FPs are known to be dense and physically robust.[26] Salp FPs disintegrate easier than krill FPs, which results in a larger surface area to volume ratio of the FP fragments. Thus, an increased probability for exchange with seawater and naturally present Fe binding ligands exists, facilitating remineralization, both by leaching and microbial degradation.[35] Additionally, pH and the presence of oxygen inside the animal's guts as well as diet composition and amount[36,37] have been proposed as factors influencing Fe release in copepods. Also, the microbial community composition has been reported as an important factor governing the mobilization of particulate Fe from sinking biogenic particles.[6] Measurements of pH, oxygen, and microbial community compositions inside krill and salp guts are lacking, but it is evident that the two animals rely on different digestion strategies. Although krill cut and grind food items with their mandibles and their stomach before the food enters
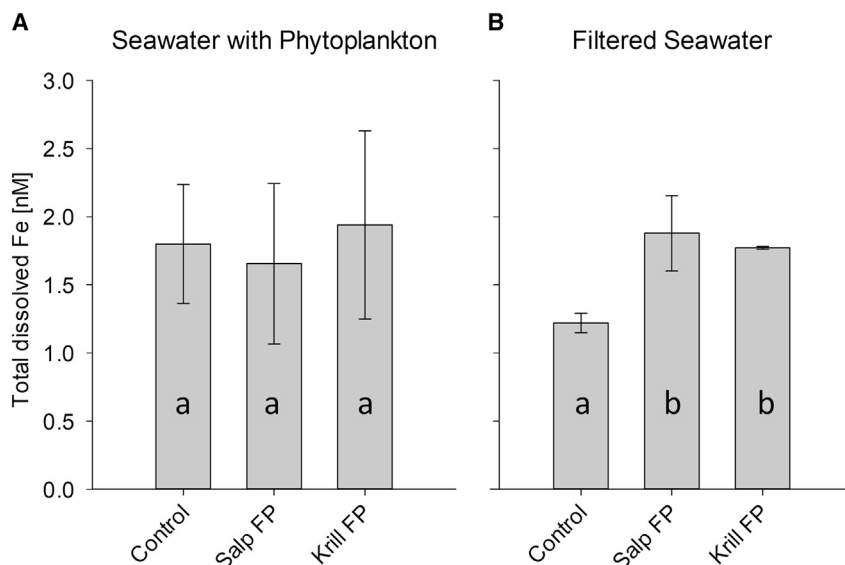
CellPress
OPEN ACCESS

Current Biology
Article

Figure 2. FPs as a source of iron

Total dissolved Fe contents were determined after 48 h of incubation. SWP FP treatments and un-treated control (A) and FSW FP treatments and un-treated control (B) are shown. Significant differences (p < 0.05) among treatments were tested using the Fisher-least significant difference (LSD) post hoc test and are indicated by small letters (a and b). n = 3 except for (A): krill FP as well as control and (B): krill FP (n = 2). Values represent means ± SD.

the digestive gland,[38] salps have no mechanical apparatus to disintegrate their food before digestions[39] and rely only on chemical and enzymatic digestion. It is possible that, compared to krill, salp guts maintain a lower pH in order to compensate for less mechanical breakdown of the food. A lower pH inside a salp gut would enhance the dissolution of colloidal Fe into the dFe pool[14,40] compared to a krill gut. Any one of these factors could be responsible for salp FP leaching more dFe than krill FP, as reflected by our data (Table 1). Our data suggest that, due to the projected climate-change-driven population shift from krill to salps in the SO, more dFe could be released in surface waters, thereby potentially enhancing phytoplankton productivity and impacting the strength of the biological pump.

Bioavailability of released Fe

In order to assess the bioavailability of the Fe released from krill versus salp FPs, each treatment bottle was filtered (0.2 μm) after the initial 48 h of incubation and amended with a preconcentrated, natural plankton community. After 24 h incubation in the presence of 0.03 nM ^{55}Fe, size fractionated (0.2–2 μm and >2 μm) intracellular Fe uptake rates (Figure 1; STAR Methods) were measured. dFe concentrations for each treatment were considered in the calculation of the Fe uptake rates, enabling a direct comparison among treatments.

In all SWP treatments, Fe uptake rates of the two size classes (0.2–2 μm and >2 μm) were not significantly different (Figures 3A, 3C, and 3E), likely due to regeneration and recycling of Fe and organic ligands during the initial incubation, as has been previously reported for diatoms[41] and bacteria.[42] Flowcytometric analysis revealed that the bulk of the 0.2–2 μm size fraction consisted of heterotrophic bacteria, with less than 1% being photoautotrophic picoplankton (data not shown). In the FSW treatment, where no Fe recycling during the incubation occurred, the total Fe uptake in the salp FP treatment was significantly higher than in the krill FP and the control treatments (p = 0.011 and 0.041, respectively; Figure 3B). Surprisingly, in comparison to the FSW salp FP treatment and the FSW control, the picoplankton fraction (0.2–2 μm;

Figure 3E) that mainly consisted of hetero-trophic bacteria in the FSW krill FP treatment took up two orders of magnitude less Fe. This implies that the lower amounts of Fe released from krill FP compared to salp FP were even less bioavailable to picoplankton than to nano- and microplankton, likely due to changing chemical speciation. The enhanced total Fe uptake rates in the filtrates of the FSW salp FP treatment in comparison to the FSW krill FP treatment cannot be explained by differences in the dFe concentrations of the treatments because the dFe concentrations were similar in both treatments (Figure 2B). Rather, they must be related to the presence of highly bioavailable inorganic or labile organic Fe in the salp FP treatment.

Ligands play a significant role in the biogeochemistry of Fe in seawater[43,44] by increasing its solubility and modulating its bioavailability. In our study, we observed that salp and krill FPs released significant quantities (p = 0.004 and p = 0.028, respectively, compared to the control) of ligands into the FSW of our experiment. The complexing capacity (STAR Methods) was increased by 1.25 ± 0.38 nM and 0.78 ± 0.33 nM by the addition of salp and krill FPs, respectively, in comparison to the control, an increase of 78% and 49%, respectively. Neither the complexing capacity nor the stability constant of Fe-ligand complexes differed between the FSW salp and krill FP treatments (Supplemental information; Table S1). Nevertheless, in this study, the greatest Fe uptake was measured in the salp FP treatments, suggesting that the quality of salp-FP-associated ligands enhanced the bioavailability of Fe. Similarly, the grazing of copepods has been hypothesized to release rapidly degradable Fe-ligand complexes,[45] and bacterial exopolysaccharides,[46] as well as the monosaccharide glucuronic acid and polysaccharide dextran,[47] have been reported to act as ligands that enhance Fe bioavailability.

In laboratory experiments, unchelated Fe showed the highest bioavailability to phytoplankton, although the bioavailability of Fe bound to the siderophore desferrioxamine B was 1,000 times lower.[48] In the ligand soup of natural seawater, the availability of Fe to plankton lies within a narrow range (factor of four) between these two extremes.[49] Similar to our study, Fe bioavailability did not clearly correlate with dFe concentrations, Fe-binding ligand concentrations, or their stability constants.[49] However, the bioavailability may depend on the specific chemical nature of ligands and environment interactions inside the natural ligand soup.[48] The ligand species inside a FP are likely
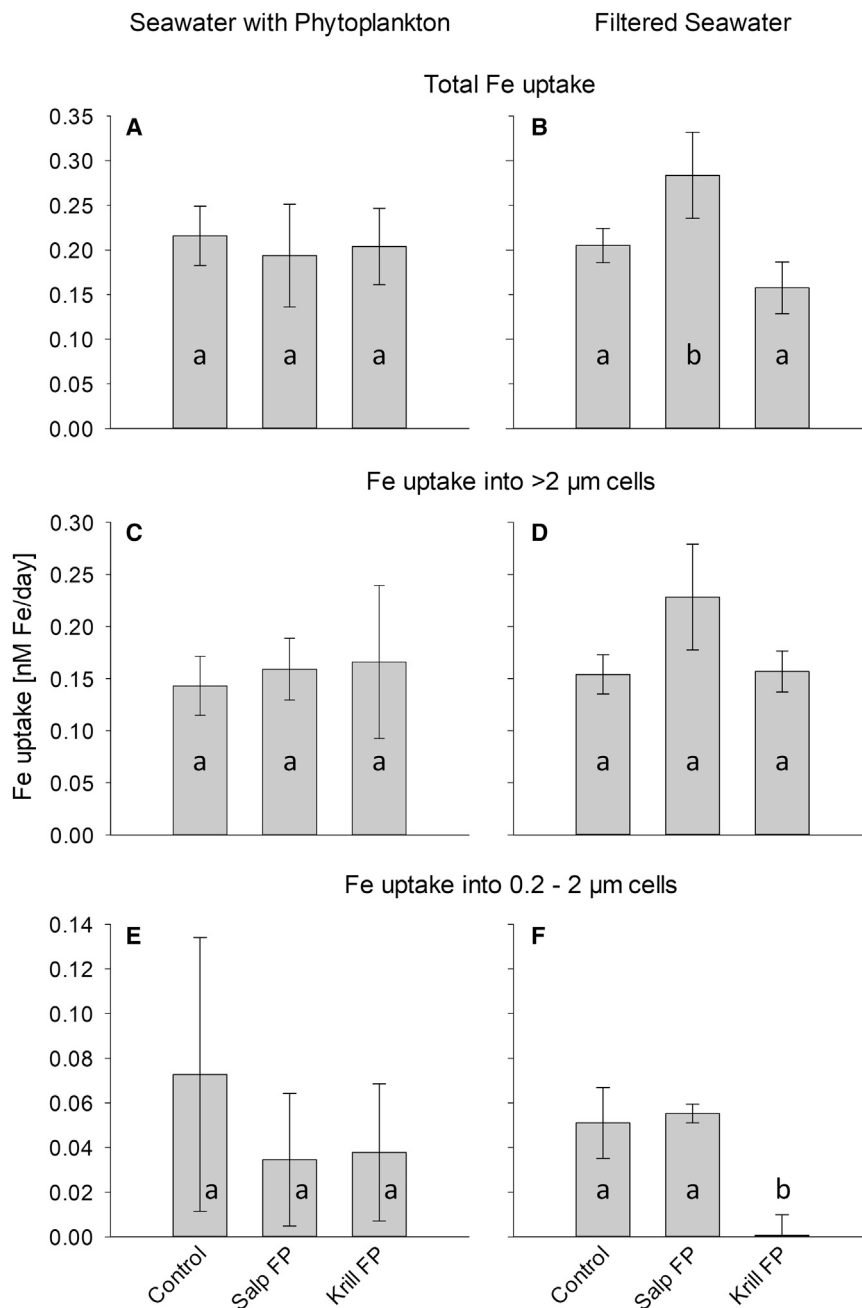
Current Biology
Article

CellPress
OPEN ACCESS

Figure 3. Bioavailability of released iron
Fe uptake rates were determined for all cells (A and B), for large cells ($>2~\mu m$; C and D), and for small cells ($0.2-2~\mu m$; E and F) from the filtrate of SWP (A, C, and E) and FSW (B, D, and F), to which no addition (control), salp, or krill FPs were given. For determination of Fe uptake, a 10 mL concentrate of the same phytoplankton community was added to each treatment. Please note that, before addition of the cell concentrate, all treatments were 0.2 μm prefiltered. Significant differences ($p < 0.05$) among treatments were tested using Fisher-LSD post hoc tests and are indicated by different small letters (a and b). n = 3 except for FSW: krill FP and SWP: control as well as krill FP (n = 2). Values represent means ± SD.

differences in their digestion mechanisms and assimilation efficiencies. Thus, in our study, it is plausible that the set of ligands leaching from the salp FPs was different from the ligands released by the krill FPs.

Krill digestion and excretion can influence the availability of dissolved organic carbon (DOC),[51] which in turn can positively influence the Fe-uptake[52] and the growth of heterotrophic bacteria.[53] Additionally, a recent study has extended the range of the known capacity for Fe storage in marine bacteria by an order of magnitude,[54] suggesting high capacities for luxury Fe uptake. In our study, heterotrophic bacteria made up the small size fraction ($0.2-2~\mu m$) of plankton. As in our study, DOC concentrations remained unaltered in any treatment over the whole experiment, being on average $49.4 \pm 2~\mu M$; this demonstrates clearly that, in our study, DOC was neither consumed nor released (data not shown).

Impacts on the ecosystem

It has been reported that the recent warming in the SO may be responsible for a 2-fold decrease of krill numbers per decade after 1976 in the sampling area of this study.[20] Additionally, between 1926 and 2003, salp numbers have increased by 2-fold per decade.[20] Increasing temperatures and reduced sea ice cover are proposed as factors negatively influencing krill egg production and the survival of larval krill[18] and in turn thought to favor salp growth. Krill spawning is closely related to the intensive diatom bloom in spring and summer,[38] which follows the seasonal retreat of sea ice, and its intensity is closely related to the duration of winter sea ice cover.[55] On the other hand, salp blooms can occur in spring and summer[56,57] and are known to be favored by diminished sea ice coverage.[19] In regions where salps and krill co-occur, salps influence krill abundance in two ways: (1) indirectly by competing for the same limited food

dependent on the animal's nutrition and digestion. Although salp and krill guts contain a similar composition of ingested food items, the content of salp and krill FPs differed significantly from each other (N.-C. Pauli, personal communication). Salp FPs were shown to contain more whole diatoms in their FPs than in their stomachs, most likely due to a lack of mandibles to destroy the diatom silica frustule (N.-C. Pauli, personal communication). Extracellular cracking of diatoms by foraminifera without any mandibles has been observed,[50] but no such mechanism has yet been described in salps. In krill, the percentage of diatoms in the stomach and in the FP was very similar (N.-C. Pauli, personal communication). This suggests

Table 2. Contribution of krill and salps to iron flux

Species	Limits	Density (ind. 1,000 m^{-3})	FP egestion rate (µg C ind.$^{-1}$ d^{-1})	dFe release (µmol Fe m^{-2} d^{-1})	Source
Krill	mean	1 ± 2	146 (Clarke et al.[25])	0.001 ± 0.001	this study
	max	5.7	146 (Clarke et al.[25])	0.005	this study
	min	0	146 (Clarke et al.[25])	0	this study
Krill	max			0.076	Ratnarajah et al.[30]
	min			0.002	Ratnarajah et al.[30]
Krill	max			0.7	Maldonado et al.[17]
	min			0.17	Maldonado et al.[17]
Salps	mean	1,385 ± 820	239 (Huntley et al.[22])	5.5 ± 4.1	this study
	max	2,707	239 (Huntley et al.[22])	10.8	this study
	min	103	239 (Huntley et al.[22])	0.4	this study
Salps	max			0.59	Maldonado et al.[17]
	min			0.06	Maldonado et al.[17]

Density of krill and salps in individuals 1,000 m^{-3} measured during this study at 8 stations in the study area northeast of Elephant Island using IKMT net trawls, assumed FP egestion rates based on literature sources, and dFe release measured in this study in comparison to the literature.

supply, phytoplankton, and thus affecting krill gonadal development[55] and (2) directly via predation by salps on krill larvae.[57] Conversely, krill have been shown to feed on salps.[58] In light of our results, a shift from a dominance of krill to a dominance of salps in some areas of the SO may have significant implications for the Fe recycling in the SO ecosystem.

Fe recycling in a salp-dominated area

Northeast of Elephant Island, between 60° to 60°44.4 S and 54° to 55°31.8 W, where this study was conducted, the abundance and distribution of salps and krill were observed as 1,385 ± 820 salps and 1 ± 2 krill per 1,000 m^3 (Table 2).

Egestion rates of 239 µg C salp^{-1} d^{-1} and of 146 µg C krill^{-1} d^{-1} (estimated from Atkinson et al.[26]) were reported.[23] Our observed dFe release of 0.1 ± 0.05 nmol dFe µg salp FP C^{-1} d^{-1} and 0.03 ± 0.005 nmol dFe µg krill FP C^{-1} d^{-1} (Table 1) was integrated over a 170-m-depth interval, resulting in a release of 0.4–10.8 µmol dFe m^{-2} d^{-1} (average 5.5 ± 4.1) by salp FPs and 0.0002–0.004 µmol dFe m^{-2} d^{-1} (average 0.001 ± 0.001) by krill FPs (Table 2). Compared to the literature on dFe release from krill,[8,17,30,32] our values are much lower (Table 2), which is not surprising for two reasons: first, our study is the first to have directly measured dFe release from krill FPs under *in situ* conditions (without acidification), which is probably why less Fe was leached from the individual FPs than in previous studies. Second, the release of dFe is strongly dependent on the amount of FP material produced. Although we measured 1 ± 2 krill individuals 1,000 m^{-3} in the study area and used this value for our calculations, other studies used higher krill biomass.[17]

Schmidt et al.[32] acidified the krill's stomach content with NH$_4$Ac buffer (pH 4.5) for 2 h, in order to analyze labile Fe, thus driving the reported higher release of dFe. Tovar-Sanchez et al.[8] used whole animals and their exudates for their experiments, which is why their values are higher than ours. For salps, on the other hand, our numbers are much higher than values previously estimated by Maldonado et al.[17] This is not surprising, because their numbers were based on mass-balanced Ecopath models, in which they used information on Fe content of sea squirts from Strohal et al.[59] as an approximation of the Fe

content of salps bodies. To our knowledge, we, for the first time ever, measured the direct release of dFe from salp FPs under ambient *in situ* conditions. According to this study, the regional dFe supply from salp FPs exceeds the lateral flux of 1.8 µmol dFe m^{-2} d^{-1} at Elephant Island that was estimated to support a production of 0.84–1.32 g C m^{-2} d^{-1}.[60] Additionally, the release of dFe into the water is no guarantee that it is bioavailable and utilized by phytoplankton cells. As we have seen in this study and the literature,[48,61,62] the chemical environment, into which the Fe is released, can affect its bioavailability greatly. Furthermore, our Fe uptake experiment allows for a calculation of the carbon (C) fixation potential generated by the Fe released from both FP types. The addition of 3.4 ± 0.5 µg salp FP C L^{-1} d^{-1} (Table 1) resulted in an increased Fe uptake of 0.08 ± 0.05 nmol Fe L^{-1} d^{-1} by phytoplankton (Figure 3B) in the salp FP treatment in comparison to the control, although the krill FP treatment did not show any significant difference. An average salp FP egestion rate of 56 273 ± 33 258 µg FP C m^{-2} d^{-1} in the sampling area is realistic, based on salp abundances and the individual egestion rate.[23] Using Equation 1 (details in STAR Methods: Quantification and statistical analysis), an estimate of the C fixation potential, assuming an Fe:C ratio of 27 ± 4 µmol Fe mol C^{-1}, which has been reported for a phytoplankton community in the SO,[63] was obtained. Salp FPs increase the C fixation potential by 0.6 ± 0.5 g C m^{-2} d^{-1} (t C km^{-2} d^{-1}), in comparison to the control, although krill FPs did not increase the dFe uptake by the plankton community (Figure 4).

$$C\ fixation\ potential = \frac{Fe\ uptake * FP\ production * molar\ mass_C}{Added\ FP\ C * Fe : C\ ratio_{phytoplankton}}$$

Effects on Fe recycling if salps replaced krill

In comparison to the already salp-dominated region around Elephant Island, in the Weddell Sea, krill dominated with 14–449 krill individuals 1,000 m^{-3} at 5 different stations between 63°39.906 S 54°38.184 W and 63°55.046 S 55°28.518 W although no salps were observed. Assuming an egestion rate of 146 µg C krill^{-1} d^{-1} (estimated from Atkinson et al.[26]) and
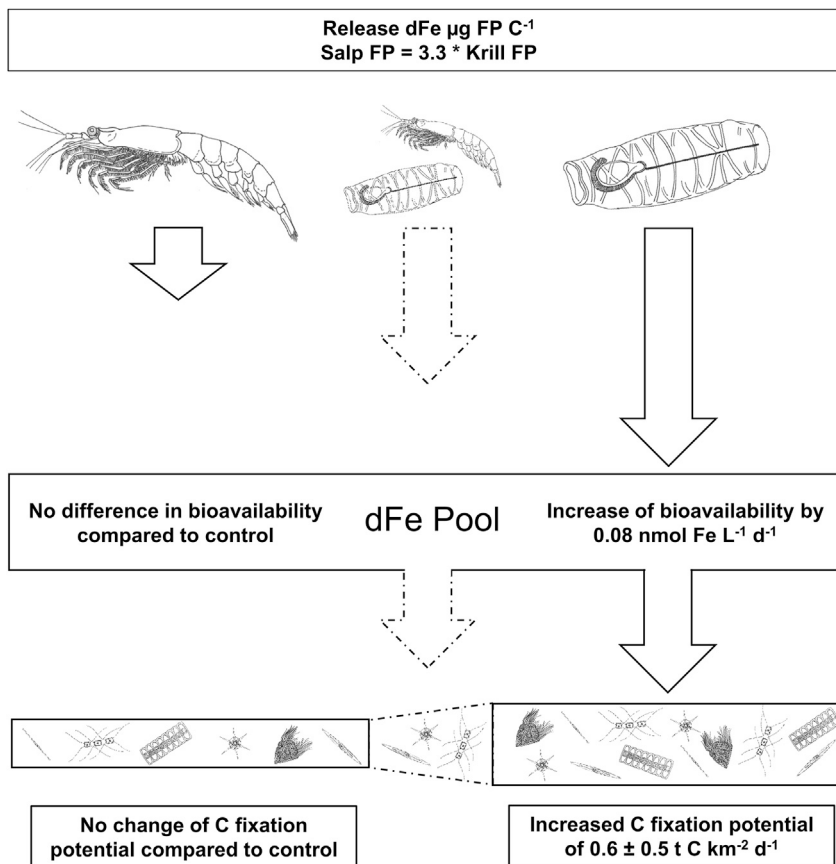
CellPress
OPEN ACCESS

Figure 4. Impact on the ecosystem

Input of dissolved iron (dFe) and changes in bioavailability of Fe to phytoplankton from krill and salp FPs, as well as calculated increase in carbon fixation potential by phytoplankton. Arrow length proportional to amount of Fe released by krill and salp FPs is shown. According to the results of this study, FPs from salps released 3.3 times more dFe μg FP C^{-1} than krill FPs. Additionally, in the dFe pool fueled by salp FPs, bioavailability of Fe to a natural phytoplankton community was increased by 0.08 nmol Fe L^{-1} d^{-1} compared to the control, although in the dFe pool fueled by krill FPs, no change in bioavailability was detected. All FPs used in this study were sampled around Elephant Island within a time frame of a few days. Based on our results, we deduce that, with a shift from a krill- to a salp-dominated community in the future, the bioavailable dFe pool as well as the production of chlorophyll and carbon fixation will increase—particularly in HNLC areas. In krill-dominated areas of the SO, the recycling of bioavailable Fe might be less efficient than in salp-dominated regions. The response of phytoplankton in areas where salp and krill populations merge requires further research (broken lines).

an integration depth of 170 m, at which krill were found, a production of 347–11 144 μg krill FP C m^{-2} d^{-1} is realistic. Given a dFe uptake into plankton of 0.02 ± 0.004 nmol dFe μg krill FP C^{-1} (Table 1), this amount of krill FP material results in a C fixation potential of 0.003 ± 0.0007 to 0.09 ± 0.02 g C m^{-2} d^{-1}. If this krill population was replaced by salps, which produced the same amount of FP C, the C fixation potential through Fe from salp FP would be 4.8 ± 1.5 times higher, reaching 0.01 ± 0.004 to 0.4 ± 0.1 g C m^{-2} d^{-1}. Although these numbers are strongly dependent on the regional salp and krill densities, it is striking how close they fall to the net air-sea carbon flux in the SO south of 44° S of 0.007–0.01 g C m^{-2} d^{-1} (estimation based on 0.16 ± 0.18 Pg $year^{-1}$ in the period between 2015 and 2017).[64] The relative increase of C fixation potential by Fe released from both salp and krill FPs by a factor of 4.8 ± 1.5, however, is not dependent on the animals' densities and likely a general phenomenon. For the majority of the Fe-poor SO south of 44° S, this increased C fixation potential is likely to strongly enhance phytoplankton biomass and carbon fixation wherever krill is replaced by salps.

Conclusions

Our study highlights that, per μg FP C added to the FSW treatments, salp FPs released 3.3 times as much dFe as krill FPs did (Table 1) and increased the bioavailability of the dFe (Figure 3). In contrast to the absolute dFe release in the study area by salp and krill FP, respectively (Table 2), which is strongly dependent

on the local FP density, we hypothesize that the relatively higher release, normalized to FP C, and the higher bioavailability could be species-specific values, influenced by the digestion capabilities and resulting ligand compositions of the animals' FPs. Therefore, the observed elevated Fe bioavailability from salp FPs in comparison to krill FPs may be applicable to other oceanic regions in a similar way. In the future, particularly in HNLC waters of the SO, the rising abundances of salps will likely increase the amount and bioavailability of recycled Fe, potentially increasing phytoplankton productivity. One could expect that a potential increase in bioavailable Fe could enhance phytoplankton biomass.[65] However, it remains unclear whether the fixed C could be transferred to higher trophic levels, potentially increasing the biomass of grazers and predators. Still, a potential increase in primary production is likely to enhance the efficiency of the biological carbon pump, thus acting in this case as a stronger sink of anthropogenically released CO_2.

STAR★METHODS

Detailed methods are provided in the online version of this paper and include the following:

- KEY RESOURCES TABLE
- RESOURCE AVAILABILITY
  - Lead contact
  - Materials availability

84

Current Biology
Article

REFERENCES

1. de Jong, J., Schoemann, V., Lannuzel, D., Croot, P., de Baar, H., and Tison, J.-L. (2012). Natural iron fertilization of the Atlantic sector of the Southern Ocean by continental shelf sources of the Antarctic Peninsula. J. Geophys. Res. Biogeosci. *117*, G01029.

2. Duce, R.A., and Tindale, N.W. (1991). Atmospheric transport of iron and its deposition in the ocean. Limnol. Oceanogr. *36*, 1715–1726.

3. Lannuzel, D., Schoemann, V., de Jong, J., Tison, J.-L., and Chou, L. (2007). Distribution and biogeochemical behaviour of iron in the East Antarctic sea ice. Mar. Chem. *106*, 18–32.

4. Moore, J.K., and Braucher, O. (2008). Sedimentary and mineral dust sources of dissolved iron to the world ocean. Biogeosciences *5*, 631–656.

5. Boyd, P.W., Law, C.S., Hutchins, D.A., Abraham, E.R., Croot, P.L., Ellwood, M., Frew, R.D., Hadfield, M., Hall, J., Handy, S., et al. (2005). FeCycle: attempting an iron biogeochemical budget from a mesoscale SF_6 tracer experiment in unperturbed low iron waters. Global Biogeochem. Cycles *19*, GB4S20.

6. Boyd, P.W., Ibisanmi, E., Sander, S.G., Hunter, K.A., and Jackson, G.A. (2010). Remineralization of upper ocean particles: implications for iron biogeochemistry. Limnol. Oceanogr. *55*, 1271–1288.

7. Nuester, J., Shema, S., Vermont, A., Fields, D.M., and Twining, B.S. (2014). The regeneration of highly bioavailable iron by meso- and micro-zooplankton. Limnol. Oceanogr. *59*, 1399–1409.

8. Tovar-Sanchez, A., Duarte, C.M., Hernández-León, S., and Sañudo-Wilhelmy, S.A. (2007). Krill as a central node for iron cycling in the Southern Ocean. Geophys. Res. Lett. *34*, L11601.

9. Wing, S.R., Jack, L., Shatova, O., Leichter, J.J., Barr, D., Frew, R.D., and Gault-Ringold, M. (2014). Seabirds and marine mammals redistribute bioavailable iron in the Southern Ocean. Mar. Ecol. Prog. Ser. *510*, 1–13.

10. Boyd, P.W., and Ellwood, M.J. (2010). The biogeochemical cycle of iron in the ocean. Nat. Geosci. *3*, 675–682.

11. Ratnarajah, L., and Bowie, A.R. (2016). Nutrient cycling: are Antarctic krill a previously overlooked source in the marine iron cycle? Curr. Biol. *26*, R884–R887.

12. Ratnarajah, L., Nicol, S., Kawaguchi, S., Townsend, A.T., Lannuzel, D., Meiners, K.M., and Bowie, A.R. (2016). Understanding the variability in the iron concentration of Antarctic krill. Limnol. Oceanogr. *61*, 1651–1660.

13. Schlosser, C., Schmidt, K., Aquilina, A., Homoky, W.B., Castrillejo, M., Mills, R.A., Patey, M.D., Fielding, S., Atkinson, A., and Achterberg, E.P. (2018). Mechanisms of dissolved and labile particulate iron supply to shelf waters and phytoplankton blooms off South Georgia, Southern Ocean. Biogeosciences *15*, 4973–4993.

14. Schmidt, K., Schlosser, C., Atkinson, A., Fielding, S., Venables, H.J., Waluda, C.M., and Achterberg, E.P. (2016). Zooplankton gut passage mobilizes lithogenic iron for ocean productivity. Curr. Biol. *26*, 2667–2673.

15. Cabanes, D.J.E., Norman, L., Santos-Echeandía, J., Iversen, M.H., Trimborn, S., Laglera, L.M., and Hassler, C.S. (2017). First evaluation of the role of salp fecal pellets on iron biogeochemistry. Front. Mar. Sci. *3*, 289.

16. Clarke, A., and Tyler, P.A. (2008). Adult Antarctic krill feeding at abyssal depths. Curr. Biol. *18*, 282–285.

17. Maldonado, M.T., Surma, S., and Pakhomov, E.A. (2016). Southern Ocean biological iron cycling in the pre-whaling and present ecosystems. Philos. Trans.- Royal Soc., Math. Phys. Eng. Sci. *374*, 20150292.

18. Atkinson, A., Hill, S.L., Pakhomov, E.A., Siegel, V., Reiss, C.S., Loeb, V.J., Steinberg, D.K., Schmidt, K., Tarling, G.A., Gerrish, L., et al. (2019). Krill (*Euphausia superba*) distribution contracts southward during rapid regional warming. Nat. Clim. Chang. *9*, 142–147.

19. Pakhomov, E.A., Froneman, P.W., and Perissinotto, R. (2002). Salp/krill interactions in the Southern Ocean: spatial segregation and implications for the carbon flux. Deep Sea Res. Part II Top. Stud. Oceanogr. *49*, 1881–1907.

20. Atkinson, A., Siegel, V., Pakhomov, E., and Rothery, P. (2004). Long-term decline in krill stock and increase in salps within the Southern Ocean. Nature *432*, 100–103.

21. Perissinotto, R., and Pakhomov, E.A. (1998). The trophic role of the tunicate *Salpa thompsoni* in the Antarctic marine ecosystem. J. Mar. Syst. *17*, 361–374.

22. Huntley, M.E., Sykes, P.F., and Marin, V. (1989). Biometry and trophodynamics of *Salpa thompsoni* foxton (Tunicata: Thaliacea) near the Antarctic Peninsula in austral summer, 1983–1984. Polar Biol. *10*, 59–70.

23. Pakhomov, E.A., Dubischar, C.D., Strass, V., Brichta, M., and Bathmann, U.V. (2006). The tunicate *Salpa thompsoni* ecology in the Southern Ocean. I. Distribution, biomass, demography and feeding ecophysiology. Mar. Biol. *149*, 609–623.

24. Phillips, B., Kremer, P., and Madin, L.P. (2009). Defecation by *Salpa thompsoni* and its contribution to vertical flux in the Southern Ocean. Mar. Biol. *156*, 455–467.

25. Clarke, A., Quetin, L.B., and Ross, R.M. (1988). Laboratory and field estimates of the rate of faecal pellet production by Antarctic krill, *Euphausia superba*. Mar. Biol. *98*, 557–563.

Current Biology
Article

CellPress
OPEN ACCESS

26. Atkinson, A., Schmidt, K., Fielding, S., Kawaguchi, S., and Geissler, P.A. (2012). Variable food absorption by Antarctic krill: relationships between diet, egestion rate and the composition and sinking rates of their fecal pellets. Deep Sea Res. Part II Top. Stud. Oceanogr. *59–60*, 147–158.

27. Turner, J.T. (2015). Zooplankton fecal pellets, marine snow, phytodetritus and the ocean's biological pump. Prog. Oceanogr. *130*, 205–248.

28. Iversen, M.H., Pakhomov, E.A., Hunt, B.P.V., van der Jagt, H., Wolf-Gladrow, D., and Klaas, C. (2017). Sinkers or floaters? Contribution from salp pellets to the export flux during a large bloom event in the Southern Ocean. Deep Sea Res. Part II Top. Stud. Oceanogr. *138*, 116–125.

29. Le Mézo, P.K., and Galbraith, E.D. (2021). The fecal iron pump: global impact of animals on the iron stoichiometry of marine sinking particles. Limnol. Oceanogr. *66*, 201–213.

30. Ratnarajah, L., Nicol, S., and Bowie, A.R. (2018). Pelagic iron recycling in the Southern Ocean: exploring the contribution of marine animals. Front. Mar. Sci. *5*, 109.

31. Cavan, E.L., Belcher, A., Atkinson, A., Hill, S.L., Kawaguchi, S., McCormack, S., Meyer, B., Nicol, S., Ratnarajah, L., Schmidt, K., et al. (2019). The importance of Antarctic krill in biogeochemical cycles. Nat. Commun. *10*, 4742.

32. Schmidt, K., Atkinson, A., Steigenberger, S., Fielding, S., Lindsay, M.C.M., Pond, D.W., Tarling, G.A., Klevjer, T.A., Allen, C.S., Nicol, S., et al. (2011). Seabed foraging by Antarctic krill: implications for stock assessment, bentho-pelagic coupling, and the vertical transfer of iron. Limnol. Oceanogr. *56*, 1411–1428.

33. Bruland, K.W., and Silver, M.W. (1981). Sinking rates of fecal pellets from gelatinous zooplankton (Salps, Pteropods, Doliolids). Mar. Biol. *63*, 295–300.

34. Caron, D.A., Madin, L.P., and Cole, J.J. (1989). Composition and degradation of salp fecal pellets: Implications for vertical flux in oceanic environments. J. Mar. Res. *47*, 829–850.

35. Giering, S.L.C., Sanders, R., Lampitt, R.S., Anderson, T.R., Tamburini, C., Boutrif, M., Zubkov, M.V., Marsay, C.M., Henson, S.A., Saw, K., et al. (2014). Reconciliation of the carbon budget in the ocean's twilight zone. Nature *507*, 480–483.

36. Pond, D.W., Harris, R.P., and Brownlee, C. (1995). A microinjection technique using a pH-sensitive dye to determine the gut pH of *Calanus helgolandicus*. Mar. Biol. *123*, 75–79.

37. Tang, K.W., Glud, R.N., Glud, A., Rysgaard, S., and Nielsen, T.G. (2011). Copepod guts as biogeochemical hotspots in the sea: evidence from microelectrode profiling of *Calanus* spp. Limnol. Oceanogr. *56*, 666–672.

38. Siegel, V. (2016). In Biology and Ecology of Antarctic Krill, *Volume 1*, V. Siegel, ed. (Springer International), pp. 203–205.

39. von Harbou, L., Dubischar, C.D., Pakhomov, E.A., Hunt, B.P.V., Hagen, W., and Bathmann, U.V. (2011). Salps in the Lazarev Sea, Southern Ocean: I. feeding dynamics. Mar. Biol. *158*, 2009–2026.

40. Liu, X., and Millero, F.J. (2002). The solubility of iron in seawater. Mar. Chem. *77*, 43–54.

41. Rijkenberg, M.J.A., Gerringa, L.J.A., Timmermans, K.R., Fischer, A.C., Kroon, K.J., Buma, A.G.J., Wolterbeek, B.T., and de Baar, H.J.W. (2008). Enhancement of the reactive iron pool by marine diatoms. Mar. Chem. *109*, 29–44.

42. Velasquez, I.B., Ibisanmi, E., Maas, E.W., Boyd, P.W., Nodder, S., and Sander, S.G. (2016). Ferrioxamine siderophores detected amongst iron binding ligands produced during the remineralization of marine particles. Front. Mar. Sci. *3*, 172.

43. Hunter, K.A., and Boyd, P.W. (2007). Iron-binding ligands and their role in the ocean biogeochemistry of iron. Environ. Chem. *4*, 221–232.

44. Hassler, C.S., Schoemann, V., Boye, M., Tagliabue, A., Rozmarynowycz, M., and McKay, R.M.L. (2012). Iron bioavailability in the Southern Ocean. Oceanogr. Mar. Biol. *50*, 1–64.

45. Laglera, L.M., Tovar-Sanchez, A., Sukekava, C.F., Naik, H., Naqvi, S.W.A., and Wolf-Gladrow, D.A. (2020). Iron organic speciation during the LOHAFEX experiment: iron ligands release under biomass control by copepod grazing. J. Mar. Syst. *207*, 103151.

46. Hassler, C.S., Norman, L., Mancuso Nichols, C.A., Clementson, L.A., Robinson, C., Schoemann, V., Watson, R.J., and Doblin, M.A. (2015). Iron associated with exopolymeric substances is highly bioavailable to oceanic phytoplankton. Mar. Chem. *173*, 136–147.

47. Hassler, C.S., Schoemann, V., Nichols, C.M., Butler, E.C.V., and Boyd, P.W. (2011). Saccharides enhance iron bioavailability to Southern Ocean phytoplankton. Proc. Natl. Acad. Sci. USA *108*, 1076–1081.

48. Lis, H., Shaked, Y., Kranzler, C., Keren, N., and Morel, F.M.M. (2015). Iron bioavailability to phytoplankton: an empirical approach. ISME J. *9*, 1003–1013.

49. Shaked, Y., Buck, K.N., Mellett, T., and Maldonado, M.T. (2020). Insights into the bioavailability of oceanic dissolved Fe from phytoplankton uptake kinetics. ISME J. *14*, 1182–1193.

50. Austin, H.A., Austin, W.E.N., and Paterson, D.M. (2005). Extracellular cracking and content removal of the benthic diatom *Pleurosigma angulatum* (Quekett) by the benthic foraminifera *Haynesina germanica* (Ehrenberg). Mar. Micropaleontol. *57*, 68–73.

51. Arístegui, J., Duarte, C.M., Reche, I., and Gómez-Pinchetti, J.L. (2014). Krill excretion boosts microbial activity in the Southern Ocean. PLoS ONE *9*, e89391.

52. Fourquez, M., Bressac, M., Deppeler, S.L., Ellwood, M., Obernosterer, I., Trull, T.W., and Boyd, P.W. (2020). Microbial competition in the subpolar Southern Ocean: an Fe–C co-limitation experiment. Front. Mar. Sci. *6*, 776.

53. Obernosterer, I., Fourquez, M., and Blain, S. (2015). Fe and C co-limitation of heterotrophic bacteria in the naturally fertilized region off the Kerguelen Islands. Biogeosciences *12*, 1983–1992.

54. Mazzotta, M.G., McIlvin, M.R., and Saito, M.A. (2020). Characterization of the Fe metalloproteome of a ubiquitous marine heterotroph, Pseudoalteromonas (BB2-AT2): multiple bacterioferritin copies enable significant Fe storage. Metallomics *12*, 654–667.

55. Siegel, V., and Loeb, V. (1995). Recruitment of Antarctic krill *Euphausia superba* and possible causes for its variability. Mar. Ecol. Prog. Ser. *123*, 45–56.

56. Loeb, V., Siegel, V., Holm-Hansen, O., Hewitt, R., Fraser, W., Trivelpiece, W., and Trivelpiece, S. (1997). Effects of sea-ice extent and krill or salp dominance on the Antarctic food web. Nature *387*, 897–900.

57. Nishikawa, J., Naganobu, M., Ichii, T., Ishii, H., Terazaki, M., and Kawaguchi, K. (1995). Distribution of salps near the South Shetland Islands during austral summer, 1990–1991 with special reference to krill distribution. Polar Biol. *15*, 31–39.

58. Kawaguchi, S., and Takahashi, Y. (1996). Antarctic krill (Euphausia superba Dana) eat salps. Polar Biol. *16*, 479–481.

59. Strohal, P., Tuta, J., and Kolar, Z. (1969). Investigations of certain microconstituents in two tunicates. Limnol. Oceanogr. *14*, 265–268.

60. Dulaiova, H., Ardelan, M.V., Henderson, P.B., and Charette, M.A. (2009). Shelf-derived iron inputs drive biological productivity in the southern Drake Passage. Global Biogeochem. Cycles *23*, GB4014.

61. Hassler, C., Cabanes, D., Blanco-Ameijeiras, S., Sander, S.G., and Benner, R. (2020). Importance of refractory ligands and their photodegradation for iron oceanic inventories and cycling. Mar. Freshw. Res. *71*, 311–320.

62. Hassler, C.S., and Schoemann, V. (2009). Bioavailability of organically bound Fe to model phytoplankton of the Southern Ocean. Biogeosciences *6*, 2281–2296.

63. Trimborn, S., Brenneis, T., Hoppe, C.J.M., Laglera, L.M., Norman, L., Santos-Echeandía, J., Völkner, C., Wolf-Gladrow, D., and Hassler, C.S. (2017). Iron sources alter the response of Southern Ocean phytoplankton to ocean acidification. Mar. Ecol. Prog. Ser. *578*, 35–50.

64. Bushinsky, S.M., Landschützer, P., Rödenbeck, C., Gray, A.R., Baker, D., Mazloff, M.R., Resplandy, L., Johnson, K.S., and Sarmiento, J.L. (2019). Reassessing Southern Ocean air-sea CO_2 flux estimates with the addition

Current Biology
Article

of biogeochemical float observations. Global Biogeochem. Cycles *33*, 1370–1388.

65. Martin, J.H., Fitzwater, S.E., and Gordon, R.M. (1990). Iron deficiency limits phytoplankton growth in Antarctic waters. Global Biogeochem. Cycles *4*, 5–12.

66. Cutter, G., Casciotti, K., Croot, P., Geibert, W., Heimbürger, L.-E., Lohan, M., Planquette, H., and van de Flierdt, T. (2017). Sampling and Sample-handling Protocols for GEOTRACES Cruises. Version 3, August 2017. https://repository.oceanbestpractices.org/handle/11329/409.

67. Koch, F., and Trimborn, S. (2019). Limitation by Fe, Zn, Co, and B$_{12}$ results in similar physiological responses in two Antarctic phytoplankton species. Front. Mar. Sci. *6*, 514.

68. Trimborn, S., Hoppe, C.J.M., Taylor, B.B., Bracher, A., and Hassler, C. (2015). Physiological characteristics of open ocean and coastal phytoplankton communities of Western Antarctic Peninsula and Drake Passage waters. Deep. Res. Part I Oceanogr. Res. Pap. *98*, 115–124.

69. Koch, F., Marcoval, M.A., Panzeca, C., Bruland, K.W., Sañudo-Wilhelmy, S.A., and Gobler, C.J. (2011). The effect of vitamin B$_{12}$ on phytoplankton growth and community structure in the Gulf of Alaska. Limnol. Oceanogr. *56*, 1023–1034.

70. Croot, P.L., and Johansson, M. (2000). Determination of iron speciation by cathodic stripping voltammetry in seawater using the competing ligand 2-(2-thiazolylazo)-*p*-cresol (TAC). Electroanalysis *12*, 565–576.

87

Current Biology
Article

CellPress
OPEN ACCESS

STAR★METHODS

KEY RESOURCES TABLE

REAGENT or RESOURCE	SOURCE	IDENTIFIER
Chemicals, peptides, and recombinant proteins		
55FeCl3	Perkin Elmer, MA, USA	LOT 021714C
2-(2-Thiazolylazo)-p-cresol	Alfa Aesar	LOT 30549
Deposited data		
Original dataset	PANGAEA	https://doi.org/10.1594/PANGAEA.931631
Software and algorithms		
SigmaPlot	Systat Software GmbH	https://systatsoftware.com/downloads/download-sigmaplot/; RRID :SCR_003210

RESOURCE AVAILABILITY

Lead contact
Further information and requests for resources and reagents should be directed to and will be fulfilled by the Lead Contact, Sebastian Böckmann (sebastian.boeckmann@awi.de).

Materials availability
This study did not generate new unique reagents.

Data and code availability
The dataset generated during this study is available at https://doi.org/10.1594/PANGAEA.931631. Complexing capacities and stability constants of the iron-ligand complexes are available in the supplementary material in Table S1.

EXPERIMENTAL MODEL AND SUBJECT DETAILS

No models or cell strains were used in this study. The study was an *in vivo* study performed with a natural community of phytoplankton.

METHOD DETAILS

In the framework of the Polarstern cruise PS112, Antarctic seawater was sampled in the vicinity of the Western Antarctic Peninsula (60° 44.455 S 54° 30.477 W, 04/11/2018) from a depth of 25 m using a polyethylene line connected to a teflon ALMATEC membrane pump. The water was pumped directly into a trace metal free laboratory container for processing. Prior to use, all lab ware was cleaned according to GEOTRACES cookbook[66] at the Alfred Wegener Institute in Bremerhaven, Germany.

Experimental set-up
Ambient untreated seawater with phytoplankton (SWP) was filtered through an acid cleaned 200 μm mesh to avoid mesozooplankton contamination, used to rinse and fill 9 acid cleaned 4.2 L polycarbonate bottles (Figure 1). 9 other bottles were rinsed and filled with 0.2 μm filtered ambient seawater (FSW) using acid cleaned Acropak capsule (PALL). 3 SWP and FSW bottles were immediately sealed and served as controls. 3 bottles of each set (SWP and FSW) were amended with homogenized salp FP, while the last 3 bottles of each set were amended with homogenized krill FP material (Table 1).

   FP material of krill and salps used in the experiment was produced by animals that had fed on an *in situ* plankton community and were caught at several stations around Elephant Island. The FP were frozen until use in experiment. The FP were rinsed once in ambient filtered seawater from the studied station and before addition to the incubation bottles, homogenized using a pipette to emulate zooplanktonic coprophagy, coprorhexy and coprochaly in the water column. To determine the carbon and Fe content of each FP material added, 1 mL of each FP suspension was kept and its Fe content determined. Using a representative amount of FP material collected in the same region as the FP used in the actual incubations, the particulate organic carbon amendments to each bottle was calculated.

88

All incubation bottles were put in front of halogen culture lamps with daylight spectrum which were set to a light intensity of 30 μmol photons m^{-2} s^{-1} under a light-dark cycle of 10:14 hours at 2°C. After 48 hours of incubation the dFe concentration of all bottles was measured. The 48 h incubation time reflects the residence time of FP material in the upper ocean after it has been loosened or broken up by zooplankton coprorhexy and coprochaly.[28] In order to assess the photophysiological efficiency (F_v/F_m) of the *in situ* phytoplankton community, an indicator of Fe stress, a fast repetition rate fluorometer (FRRF) in combination with a FastAct Laboratory system (FastOcean PTX), both from Chelsea Technologies Group ltd. was used. All measurements were taken at 2°C following a 10 min dark acclimation period, assuring that all photosystem II (PSII) reaction centers were fully oxidized and nonphotochemical quenching was relaxed.[67] Iterative algorithms for the induction and relaxation phases were applied to estimate minimum Chl *a* fluorescence (F_0) and maximum Chl *a* fluorescence (F_m).[63] The apparent maximum quantum yield of photosynthesis of PSII (F_v/F_m) could then be calculated according to the equation

$$\frac{F_v}{F_m} = \frac{F_m - F_0}{F_m}$$

The measured F_v/F_m value of 0.32 at the station was in the range of values, reported for open ocean communities in the vicinity of the Western Antarctic Peninsula.[68] The high initial dFe value of 4.11 nM together with the initial complexing capacity for Fe of 3.31 nM hints toward a saturated Fe solubility at this station.

Dissolved and particulate Fe concentrations

Samples for the determination of total dFe concentrations were taken in a clean room container. 100 mL from each treatment bottle were filtered on two trace metal clean filtration racks over a 0.2 μm filter with a negative pressure of 200 mbar applied. The filtrate was used to sample for dFe. In between samplings all equipment involved was rinsed 30 minutes in 1 M HCl and MilliQ (18.2 MΩ.cm). To determine the Fe content of the FP material, the remainder of each FP addition used in the incubation experiment was rinsed with 9 mL of MilliQ water to reduce salt content. Afterward the particulate material was transferred to a 1.5 mL Eppendorf cup and dried at 60°C in an oven over night. The FP material's dry weight was determined. After that, the material was transferred in 30 mL PTFE vials and dissolved in a mixture of 5 mL subboiled HNO_3 (distilled 65%, p.a., Merck) and 0.5 mL HF (ROTIPURAN Ultra 48%, Carl Roth) in a pressure digestion system (PicoTrace, DAS 30) at a temperature of 180°C over 16 hours. Followed by the addition of 1 mL of Milli-Q water. The volume of the FP extract was then evaporated on a 140°C hot plate and the evaporate was passed through a NaOH solution, which effectively neutralized it. 0.2 mL of subboiled HNO_3 and 0.8 mL Milli-Q water was then added and the solution was heated to 50°C for 4 hours to resuspend the FP extract before it was transferred into 10 mL trace metal cleaned polypropylene (PP) vials. Finally, 10 μL of Rh (1 mg L^{-1}) was added as an internal standard and the volume was brought up to 10 mL using Milli-Q water before subsequent analysis on a high resolution ICP-MS (Attom, Nu Instruments).

Back at AWI Bremerhaven prior to analysis, all seawater samples were acidified to pH 1.7 with sub-boiled HNO_3 (distilled 65% HNO_3, pro analysis, Merck). dFe concentrations in seawater samples were analyzed via standard addition using a SeaFAST system (Elemental Scientific) coupled to an Element2 (Thermo Scientific) mass spectrometer. Therefore, each seawater samples was separated into 4 aliquots and spiked with commercially available ICP-MS single element standards (SCP Science 1000 mg L^{-1}). Standards for external calibration were prepared from seawater spiked with commercially available ICP-MS single element standards (SCP Science; 1000 mg L^{-1}). The SeaFAST system eliminates matrix components, such as the major ions in seawater (Na, Mg, and Cl) and preconcentrates the samples by a factor of 40. This procedure reduces possible interferences by the matrix and enables to analyze expected low concentrations of elements of interest.

The Nass-7 reference material was used to validate the quality of the analysis of trace elements in seawater at the beginning and end of a batch run. Because the element concentrations of the reference material were much higher than the concentrations expected in the seawater samples, the reference material was analyzed in a 1:10 dilution. The analysis of the Nass-7 reference material (n = 6) showed good results. Certified 351 ± 26 ng Fe * L^{-1} measured 365.97 ± 14.15 ng Fe * L^{-1}.

Fe-uptake assay

In order to assess the bioavailability of the dFe pool, 50 mL from each experimental treatment was filtered over an acid cleaned 0.2 μm polycarbonate filter, removing all of the biotic and abiotic particles. A concentrate of a natural plankton community, collected at the same station from 25 m depth as the experimental water was then added into this filtrate. Briefly: 10 L of whole seawater was concentrated with gravity filtration onto a 0.2 μm polycarbonate filter (WhatmanNucleoporeTrack-EtchMembrane, 90 mm) using an acid-cleaned AMICON 8400 filtration unit (Millipore). The AMICON was used to keep the plankton community in suspension by gently mixing it during the concentration step. A small aliquot of the concentrate was then added back to the filtrate from each treatment, ensuring that the final plankton biomass matched initial sampling conditions. This permitted the exposure of the same plankton community to each treatment without diluting the conditioned water. To each bottle containing the filtered treatment water and plankton concentrate, 0.03 nmol L^{-1} (final concentration) $^{55}FeCl_3$ (150 Bq; Perkin Elmer, MA, USA) was added. After an incubation period of 24 hours at 1°C under 30 μmol photons m^{-2} s^{-1}, the cells were size fractionated by filtering them onto 0.2 and 2 μm filters, allowing for the determination of size class specific uptake of the tracer.[69] Each filter was rinsed 3 times with oxalate solution that was gravity-filtered for approx. 2 min between each rinsing step, followed by 3 rinses with natural 0.2 μm filtered seawater.[47] Finally, each filter was collected in a scintillation vial, amended with 10 mL scintillation cocktail (Ultima Gold, Perkin Elmer) and mixed thoroughly (Vortex). Counts per minute were estimated for each sample on the shipboard scintillation counter (Tri-Carb2900TR). Counts per minute were

Current Biology
Article

CellPress
OPEN ACCESS

then converted into disintegrations per minute taking into account the radioactive decay and custom quench curves. ^{55}Fe uptake was calculated taking into account the nominal ^{55}Fe concentration and the total dFe concentration (background and added). To separately infer Fe bioavailability, the Fe uptake rates were then normalized to their respective total dFe concentrations and compared among treatments.

Fe speciation

From the initially sampled seawater and at the end of both experiments, ligand concentrations and stability constants were determined by the competitive ligand exchange adsorptive cathodic stripping voltammetry method on the basis of the competitive ligand 2-(2-Thiazolylazo)-p-cresol (TAC, LOT 30549, Alfa Aesar) according to Croot and Johansson[70] on a Metrohm 663 VA stand. Defrosted samples were split into 10 mL subsamples and buffered with 5 mM EPPS to obtain a pH of 8.1. Variable amounts of a 0.75 μM Fe standard were added in order to obtain concentrations between 0 and 7 nM added Fe. After 1-2 hours of equilibration, the TAC was added and sample analysis was conducted 24 hours later on a bioanalytical system consisting of an EC epsilon potentiostat and a controlled growth mercury electrode. As a working electrode, a medium sized mercury drop was used in conjunction with the static mercury drop electrode setting, an Ag/AgCl reference electrode and a platinum wire counter electrode. The ligand concentrations and stability constants, as well as complexing capacities were calculated using the Van den Berg/Ružić linearization.

QUANTIFICATION AND STATISTICAL ANALYSIS

Statistical significance between samples were in all cases determined by the use of the computer program SigmaPlot (Systat Software). A One Way ANOVA was run for all factors and treatments (post hoc test: Fisher-LSD (Least Significant Difference) test, level of significance $p = 0.05$, pairwise comparison). Statistical significance was always tested within the same filtration mode (FSW or SWP). Relevant p values are given in the sections "FP as a source of Fe" and "Bioavailability of released Fe." Figures 2 and 3 give means ± SD. The respective n (number of values from replicate bottles) are given in the last two lines of the figure legends. Where n deviates from 3, in Figure 2 extreme values have been excluded based on a deviation from the mean by at least 5 standard deviations. These values were considered contaminations or machine errors. In Figure 3 values were excluded if a dFe value, necessary for the calculation of the dFe uptake had been excluded based on the principle of deviation from the mean by at least 5 SD.

Equation 1, calculating the carbon fixation potential through iron uptake of phytoplankton from salp or krill FP uses the following units: Carbon fixation potential [g m^{-2} d^{-1}], Fe uptake [μmol Fe L^{-1} d^{-1}], FP production [μg FP C m^{-2} d^{-1}], molar mass of carbon = 12 [g mol^{-1}], added FP carbon [μg C L^{-1} d^{-1}] and Fe:C ratio of phytoplankton [μmol Fe mol C^{-1}].

90

Supplemental Information

Salp fecal pellets release more

bioavailable iron to Southern Ocean

phytoplankton than krill fecal pellets

Sebastian Böckmann, Florian Koch, Bettina Meyer, Franziska Pausch, Morten Iversen, Ryan Driscoll, Luis Miguel Laglera, Christel Hassler, and Scarlett Trimborn

Treatment	[L] [nM]	logK'FeL	n
FSW Control	1.60 ± 0.18	11.63 ± 0.12	3
FSW Salp	2.84 ± 0.33	11.72 ± 0.17	3
FSW Krill	2.23 ± 0.24	11.54 ± 0.45	2
SWP Control	2.38 ± 0.13	11.63 ± 0.53	2
SWP Salp	3.14 ± 0.27	11.70 ± 0.53	3
SWP Krill	3.23	11.91	1

Table S1. Iron speciation parameters. Related to STAR methods.

Iron ligand concentration (L) and conditional stability constant of their iron complexes (logK$'_{Fe'L}$) determined by CLE-AdCSV in filtered seawater (FSW) and seawater with phytoplankton (SWP) treatments; standard deviations from the deviation of L and K$'_{Fe'L}$ determined in n replicates.

5

SYNTHESIS

In chapter 5, the hypotheses formulated in chapter 1 are either confirmed or rejected. First, and quasi summarizing the main findings from chapters 2-4, the biogeochemical background conditions in the study area in austral autumn are described, the grazing environment is characterized and the role of macrozooplankton grazers on the Fe recycling is discussed (chapter 5.1). In subchapter 5.2 the hypothesis is discussed that the patchy distribution of plankton biomass and PP is rooted in the interplay between regional, biogeochemical characteristics on the one hand and local grazing pressure on the other. In subchapter 5.3 the ecosystem-wide deduction is addressed that the shift from krill to salps may increase the carbon sequestration potential of the WAP ecosystem. Finally, in subchapter 5.4 future research directions are proposed.

5.1 Autumn conditions at the WAP

5.1.1 Oceanographic partitioning of the sampling area and TM utilization in autumn

High latitude ecosystems, such as the WAP, experience a strong seasonality, driven by annual variability in solar irradiance [1]. The decrease of light transmitted into the water column in autumn marks the end of the SO growth season by light limitation [2], accompanied by a storm driven deepening of the mixed layer[3]. Consequently, as discussed in chapter 2, the encountered plankton community was characterized by low concentrations of Chl a and POC as well as low PP rates compared to summer [4], and could thusly be described as typical for the season and region (chapter 2).

Furthermore, chapter 2 presents measurements of dTM concentrations as well as rare Fe, Zn and vitamin B_{12} uptake rates into plankton organisms from the WAP in austral autumn. In the sampled area, a TM limitation would be expected at the offshore DP stations in summer[5,6], while inshore stations are usually not limited by low dTM values[7]. Our autumn measurements of PP normalized Fe- and Zn-uptake rates suggest that both TM were sufficiently abundant and bioavailable at all stations in the study area, including the offshore DP stations. Since no reliable dFe and Fe uptake values are available for station 26, as discussed in chapter 2, a Fe-limitation at this station cannot be ruled out. At DP stations 31 and 61 however, the PP normalized Fe-uptake rates were high (152 and 54 µmol Fe mol C^{-1} respectively, Figure 3C in chapter 2) in comparison to the literature[8,9], which suggests that the limiting influence of Fe availability, dominant in summer, decreased in autumn. Wind driven deep mixing of the water column on the one hand replenishes the dFe concentrations in the surface waters, which fits the high dFe value at station 31 (1.31 ± 0.31 nmol L^{-1}, Table 1 chapter 2), as well as increases light limitation[10], supporting the idea that light was the determining factor during the sampling period. In contrast to this argumentation, hints were detected that Mn limitation could have influenced phytoplankton growth and could even have been limiting at offshore DP station 31. Generally it was observed that at the offshore stations the F_v/F_m values were lower (however not significant) and the functional absorption cross

section values of PSII (σ_{PSII}) were significantly higher (both common signs of TM limitation[11–13]) than at the inshore stations. Mn has been discussed as limiting or co-limiting (with Fe and light) in the literature[6,14,15]. The 3 lowest [dMn] were found at the 3 open ocean DP stations (Table 1 in chapter 2). The Mn deficiency coefficient (Mn*)[16] indicated a possible Mn deficiency with respect to the dFe concentration at stations 20 and 31 (-0.43 and -0.33 respectively) by falling below the published values of Mn* in Fe/Mn co-limitation scenarios (-0.02 to 0.06,[14,16]). It has been described that under suboptimal light conditions (in autumn decreasing light due to reduced day length and reduced incidence angle[1,17]) and sufficient Fe supply, Mn limitation can develop, for example due to an increased demand for Mn-intensive photosystem II [15]. In this strain of argumentation however, deep mixing appears irrelevant since it seems unlikely that deep mixing replenished the dFe concentrations in the surface waters, while leaving the dMn concentrations unaltered. During this study, no experiments were performed to directly determine the limiting factors in the sampled region. However, an overall light deficiency, coupled to a possible Mn limitation at station 31 appear to be promising candidates

Finally, as discussed in chapter 2, the sampling area exhibited differences in oceanographic characteristics, allowing for a differentiation of at least two distinct study areas (Figure 1): The offshore DP stations in the ACC-influence zone (stations 26, 31 and 61) and the nearshore stations in the BC influence zone (stations 17, 20, 25, 55, 106 and 120). A comparison between both regions generally hinted towards warmer and less saline waters with lower dissolved trace metal concentrations to the northern offshore waters (Table 1 in chapter 2), which is typical for the ACC [4,5,18] (statistically significant for the dMn and dCu concentrations). Within the biological parameters, only the σ_{PSII} showed significant differences between the defined regions. Although values of the total biomass and production indicators Chl a and POC, as well as PP were strongly inhomogeneous among stations, the lowest Chl a concentrations and PP were measured among the northern offshore stations, while the highest Chl a, the three highest PP and the two highest POC values were measured inshore in the influence zone of the BC (Figure 2 in chapter 2). Low biomass values are typical for the waters off-shore the WAP in the ACC [19–21] and in summer, higher biomass concentrations are found inshore[4], hinting towards an existing, but strongly weakened inshore/offshore gradient in autumn. Also, the data hinted towards taxonomical differences between the defined regions. Although not directly measured, an importance of heavily silicified diatom species at the offshore DP stations typical for the region [22,23], as opposed to the BS stations was indicated by several parameters. First, at the offshore DP stations large shares of the phytoplankton's large size fraction (>2 µm) in PP (66-79%) and Chl a (64-100%) were observed (Figure 2 in chapter 2), suggesting that picoplankton cells were less active at the DP stations than at the BS stations. Second, low dissolved silicate concentrations (Table 1 in chapter 2), indicating a strong utilization of dissolved silicate in the north, further support the influence of heavily silicified diatom species at the DP stations. At station 26 the low silicate concentrations resulted in a low Si:DIN ratio (0.9 ± 0.01 mol mol^{-1}, data calculated from Si and DIN concentrations in chapter 2) reaching the threshold of silicate limitation for diatoms (Si:DIN <1;[24]).

With respect to hypothesis 1, hard evidence for a partitioning of the sampled region in a northern DP area under the influence of the ACC and a southern BS area under the influence of the BC can only be derived from the distribution of Mn and Cu concentrations as well as the σ_{PSII} values. Knowing that in summer a strong inshore/offshore gradient in the sampled area exists, it is tempting to accept the value distribution of many other parameters such as salinity, temperature, concentrations of Chl a and POC as well as PP as clues pointing towards the persistence of this gradient into autumn, however in a markedly weaker form. Hence, hypothesis 1 can be tentatively accepted.

5.1.2 Autumn SZP grazing environment

The SZP community of the microbial loop constitutes the largest phytoplankton biomass sink in the oceans [25,26]. While this paradigm is also applicable to the SO[27], little SZP grazing data from the WAP so far exists[28–31], and none of the published studies focus on autumn. In our study, with the help of 3 dilution experiments based on POC in addition to the classically investigated Chl a (for methodology see chapter 3), the summer observation was confirmed, and grazing pressure by SZP was found to be significant at all sampled stations, also in autumn. This is illustrated by the result that more than half of the gross POC production (56%) was eliminated by SZP grazing from the particulate fraction at the station with the lowest SZP grazing rate (station 61, off Elephant Island). While grazing on POC and grazing on PP are not exactly identical parameters, this value from our study coincides with the narrow range published for grazing on PP in polar waters (53–57%) [26]. At offshore station 26 in the DP the SZP grazing was strongest and eliminated more POC from the particulate fraction than was produced (119%), thusly decreasing the standing stock biomass. This value falls into the published range of cases, reporting extreme SZP grazing on PP in the SO of between 100% [32,33] and up to 762% [34]. The observation that at offshore station 26 (where TM limitation could not be ruled out with certainty based on the results in chapter 2) high SZP grazing was detected is in accordance with the report that the constantly regenerating, complex microbial communities of the microbial loop [35] play an important role in the typically Fe-depleted offshore HNLC areas [36]. In contrast, in inshore Fe replete regions diatom blooms occur, supplying the 'food chain of the giants' (diatom – krill - vertebrate predator) [22,36,37].

Surprisingly, it was observed that SZP grazing resulted in a highly significant increase of the C:N ratio of up to 100% between the undiluted and the highly diluted treatments, which was consistent across all 3 experiments (Figure 2 in chapter 3). To explain this observation, 2 possible scenarios are discussed in chapter 3. First, it was observed that the small size fraction <2 μm showed an up to 1.6 times higher initial C:N ratio than the whole community at all stations (chapter 3). In addition, heterotrophic bacteria belonging to this size fraction showed the highest gross growth and grazing rates of all measured groups and parameters in the experiments. With decreasing grazing pressure by serial dilution it is possible that a species or group with a particularly high C:N ratio thrived, increasing the C:N ratio of the entire community. However, bacterial C:N ratios are usually low (3.6–6.8 [38,39]). To increase the C:N ratio of the entire community so substantially, a very high C:N ratio in the group in question would have been

necessary. The second hypothesis revolves around transparent exopolymer particles (TEP). TEP have a 4.3 times higher C:N ratio (26) [40] than phytoplankton in eutrophic polar waters (C:N:P of 78:13:1 = C:N of 6:1 [41]). Furthermore, TEP have been shown to occasionally contribute to the POC concentration equally to conventional particles [40,42]. Direct TEP production has been documented for bacteria and phytoplankton individually[43–46], but bacteria have also been shown to indirectly mediate TEP formation [43] and induce TEP production in phytoplankton[47]. Since TEP themselves[48], particles aggregated by TEP [49] or their dissolved precursors can be directly utilized as a carbon source by heterotrophic grazers [50,51] it is possible that TEP constituted a regular prey item during the dilution experiments, resulting in a significant increase of TEP upon serial dilution. A strong increase of high-C:N TEP would thusly explain the C:N increase in the entire community.

The dilution method used in chapter 3 is not undisputed[52,53], but has been successfully applied since 1982 [54]. Therefore, the alterations we made, need to be justified. In the endeavor to broaden the perspective of the Chl a based dilution method [54], our study presents and discusses an extended approach, in which grazing on, and production of POC was measured directly, additionally to the classic parameter Chl a. The result were shown to be useful and reliable. We chose this approach because the measurement of POC represented carbon dynamics in the particulate fraction outright and, as a result, back calculations of the carbon from Chl a could be dispensed with. This seemed advantageous, because data based on Chl a is necessarily limited to representing growth of and grazing on autotrophic organisms. Thusly, the carbon dynamic in the possibly large share of heterotrophic organisms (reported to reach as high as ~half of the biomass) [55] evades detection, which may lead to an incorrect depiction of SZP grazing influence, as discussed for station 26 in chapter 3. Furthermore, so far published studies used the term microzooplankton grazing instead of the term SZP grazing in this study. We decided in favor of SZP grazing, since grazing by microzooplankton and nanozooplankton is not differentiable in the dilution experiment and the term SZP accounts for the grazing pressure of both size classes.

Based on all results in chapter 3, hypothesis 2 can be accepted. While different intensities of SZP grazing were detected among stations, SZP grazing was the dominant loss term of POC production at all investigated sites.

5.1.3 Macrozooplankton grazers and Fe recycling

The published literature suggests that grazers mediate Fe recycling [56–58] in form of dFe release from their FP. While Fe is a growth limiting nutrient for primary producers in ~30% of the world's ocean [57], including vast areas of the SO, adult animals do not require all Fe accumulated in their prey and excrete the superfluous Fe ingested [58]. Particularly the Fe release of krill has been investigated before and was found to be substantial [56,58,59]. It has been reported that with increasing sea surface temperature the habitat of krill contracts southward, while salps spread in the vacated regions[60,61]. The implications of this population shift on the biogeochemical cycling of the limiting micronutrient Fe, as well as its

bioavailability to SO phytoplankton has not been investigated yet [62]. To close this knowledge gap, chapter 4 reports an experiment in which we collected FPs of natural populations of salps and krill, added them to the same SO phytoplankton community, and measured the community's Fe uptake rates (for detailed methodology please see chapter 4). In accordance with the published literature, Fe release from krill and salp FP could be detected during the experiment presented in chapter 4. Furthermore, supporting previous studies, the fraction of leachable Fe in the presented study remained < 7% of the total Fe in all of the FP [63–65]. In contrast to the previously published studies however[65], the release of dFe from salp FP was higher in our study. Furthermore, normalized to the amount of FP carbon added, salp FP released 3.3 times more dFe than krill FP. We observed that disregarding this difference in dFe release per FP carbon, the amount of both FP additions were balanced resulting in similar dFe concentrations in the treatment bottles (Figure 2 in chapter 4). However, per FP carbon added, 4.8 ± 1.5 times more Fe was taken up by the same phytoplankton community from salp FP than from krill FP, suggesting that salp FP increased the Fe bioavailability, possibly through the release of ligands. We calculated that a shift from krill to salp dominance could increase the carbon fixation potential in the investigated region by $0.6 \pm 0.5 \, t \, C \, km^{-2} \, d^{-1}$ by the supply of additional bioavailable Fe to phytoplankton.

Based on all results in chapter 4, hypothesis 3 must be rejected. Salp FP proved more beneficial for the recycling of bioavailable Fe than krill FP.

5.2 Patchy occurrence of grazers likely led to patchy biomass distribution

The availability of the bottom-up factors light and dissolved trace metals shape the SO [2] on an ecosystem scale. These factors determine the margin within which PP can take place, and thereby set the stage for all effects observed downstream the food chain, such as secondary and tertiary production, as well as carbon export to depth. However, based on this frame of bottom-up factors alone, the actual patchiness of biological parameters encountered at the different stations, as obvious from the results in chapter 2, cannot be explained for two reasons. First, stations on similar latitudes, and therefore similar day lengths and solar angles, showed very different values of biomass (station pair 17|20), PP (station pairs 20|25, 26|31 or 55|120), or micronutrient utilization (station pairs 20|25 or 31|106) (Chapter 2, Table 1 and Figures 2, 3 and 4). Second, the concentrations of trace metals were not correlated significantly with any growth- or biomass parameters in the entire dataset (Chapter 2, Supplementary Figure 1). Thusly, although these abiotic bottom-up factors certainly shape the ecosystem as a whole, the locally patchy structure of biomass parameters was likely dependent on the highly complex interplay of grazing and predation, even further gaining in complexity through advection between geographic locations in the complex BC system [66,67].

5.2.1 Distribution and grazing pressure of planktonic grazers in the sampled area

In chapter 3, a highly significant, but inhomogeneous grazing pressure of SZP organisms among stations was described. Since SZP grazing is generally considered the largest biomass sink in the oceans [25,26], exceeding even the impact of mesozooplankton [25,68], it is probable that the individual SZP abundance and grazing activity at the different stations contributed to the patchiness of the sampling area with respect to the biological parameters Chl a, POC, PP and micronutrient utilization. The abundance and taxonomic composition of the microzooplankton community (which is a subset of the SZP) showed pronounced differences between different areas in the study region [69]. Although the study's resolution [69] is not sufficient to allow for a direct comparison between SZP abundance at individual stations with the here presented results, a connection between patchy SZP abundance, -taxonomy or -activity and the measured patchy biological parameters is likely. Climbing up the trophic ladder, mesozooplankton (0.2-20 mm [70]) is an important group of consumers (19-34% of PP consumption [71,72]). The mesozooplankton was dominated by copepods in the study area (~80 % [73]) and like SZP, it showed a patchy distribution among stations [73]. Copepods consume PP directly, but also feed on SZP organisms [74]. Finally, the macrozooplankton organisms krill and salps showed highly variable abundances in the sampled area. The abundances of krill and salps ranged between 0-14,598 ind. 1000 m^{-3} and 0-4750 ind. 1000 m^{-3} respectively (Ryan Driscoll, personal communication). Both, krill and salps are known to exert a significant grazing pressure on the plankton community (krill: 50.8 – 59 % of PP [75,76], salps: 0.3-108 % of the daily PP [77]). Furthermore, both species feed on all above-described trophic levels [78], selectively influencing the entire plankton community, based on the individual food preferences of both species [78]. Certainly, the specific pathways via which the discussed groups directly and indirectly led to the, in chapter 2 observed patchy distribution of biological parameter values, are far too complex to be deciphered based on the given dataset. However, it seems likely that if all grazers are capable to exert a significant grazing pressure and at the same time occur in patches, this could explain the observed patchy distribution of biological parameter values in chapter 2. This conclusion is corroborated by Plum et al. 2021, who provided evidence that predator-prey interactions were decisive for the features of some size classes. The source stresses the importance of top-down control and emphasizes that the consideration of predator–prey interactions, in addition to bottom-up effects is crucial for our understanding of the WAP ecosystem [73].

5.2.2 Empirical clues for the influence of grazers larger 200 µm on the dilution experiments

The impact of large grazers (mesozooplankton and larger) on the individual sampling sites can be sensed from observations made during the dilution experiments. Table 4 shows the changes between the initial samples and the undiluted bottles after three days of incubation at the three stations in percentage.

Table 1 Changes in measured parameters from the initial samples to the undiluted seawater bottles (1.0 dilution) after the incubation, given in percentage of initial values. Chlorophyll a (Chl a), community particulate organic carbon (POC$_{all}$), community particulate organic nitrogen (PON$_{all}$), autotrophic picoeukaryotes of all size fractions (PE$_{all}$), autotrophic nanoeukaryotes (NE), heterotrophic bacteria (Bacteria$_{all}$). All values in means ± standard deviation.

Parameter	26	61	106
Chl a	+41 ± 17	+59 ± 21	+43 ± 25
POC$_{all}$	-16 ± 6	+121 ± 26	+78 ± 26
PON$_{all}$	-28 ± 5	+89 ± 15	+73 ± 15
PE$_{all}$	+61 ± 14	+69 ± 25	+81 ± 28
NE	-36 ± 22	+202 ± 75	+36 ± 36
Bacteria$_{all}$	+11 ± 6	+110 ± 23	+50 ± 9

It is evident that at station 26, the changes among the different parameters between initial values and undiluted bottles are bidirectional and smaller, than at station 61, where all values increased significantly upon incubation. This strong difference exists, although the evaluation of an extensive set of physical and chemical parameters suggested (chapter 2), that both stations were under the influence of the ACC and could be clustered into the same oceanographic group, contrasting for example stations from the Bransfield Strait (chapter 2). It has been observed before that upon elimination of large grazers by filtration in an experiment, the trophic network in the plankton community can shift [79,80]. Since a dilution experiment is geared towards measuring the grazing impact of SZP, only grazers smaller 200 µm in size are included. Although not conclusively provable, drawing on the available data, it is probable that the exclusion of larger grazers released the grazing pressure off the shown parameters, resulting in a general increase of values (15 out of 18 values shown in Table 1). The fact, that this increase was by far stronger at station 61 than at station 26 furthermore suggests that the grazing pressure of larger grazers was stronger at the former station during the period of sampling. Copepods graze on items >5 µm [81] making it intuitive, why an exclusion of copepods could entail an increase in Chl a, POC, PON and nanoeukaryotes. In contrast, to explain increases in picoeukaryote and bacterial numbers (<2 µm) upon incubation, salps, krill and appendicularians are predestinated [36]. All three groups were encountered in the sampled region[73]. Also, they were all excluded from the incubation and capable of grazing items down to ~1 µm [82,83], 2-3 µm [84] and <0.2 µm [81] in size respectively. The grazing pressure by salps, krill and appendicularians is certainly not restricted to these small grazing items. Hence, an exclusion of these groups in the incubation could explain the increase in bacteria and picoeukaryotes, but it would also contribute to releasing grazing pressure on all plankton groups <200 µm in the dilution experiment. While on the one hand, grazing appears to be a promising factor to explain the patchiness of the sampled

region, it needs to be stated that this release of meso- and macrozooplankton grazing pressure constitutes a growth enhancing bottle effect, which likely led to an overestimation of the gross growth rate during the dilution experiments.

Based on all results in chapter 2 and 3, hypothesis 4 can be accepted in the sense that in the absence of conclusive empirical proof, sufficient indication has been compiled to tentatively accept that grazers significantly contributed to the patchy distribution of biological parameters in the sampled area.

5.3 Salps may benefit diatoms and carbon sequestration

The increase of water temperatures in the Fe limited [6,85], low chlorophyll [19–21] waters north of the WAP [86] incurs a withdrawal of krill from its northern habitats to the higher latitudes of the Antarctic shelf, while salps replace krill in the vacated regions [61,87]. In these waters, plankton communities on the one hand comprise stocks of small, rapidly regenerating cells inside the microbial loop [36], and on the other hand, large, heavily silicified and well protected diatoms [22,23,81] with slow growth rates that are less susceptible to SZP and copepod grazing [88]. Grazer mediated recycling is an important source of dFe [89] in the Fe-limited open ocean surface waters, in its magnitude comparable for example to dust deposition and upwelling [56]. While krill and salps both release Fe into the water [58,59,64,65,90], ranking 3rd and 4th in importance of Fe release respectively, behind microzooplankton and carnivorous zooplankton [91], salp fecal pellets have been shown to first, release more dFe per FP carbon and second, to make dFe more bioavailable than krill FP (chapter 4). This observation inspires the question: Will the predicted and observed increase in salps consequently increase SO productivity and carbon sequestration?
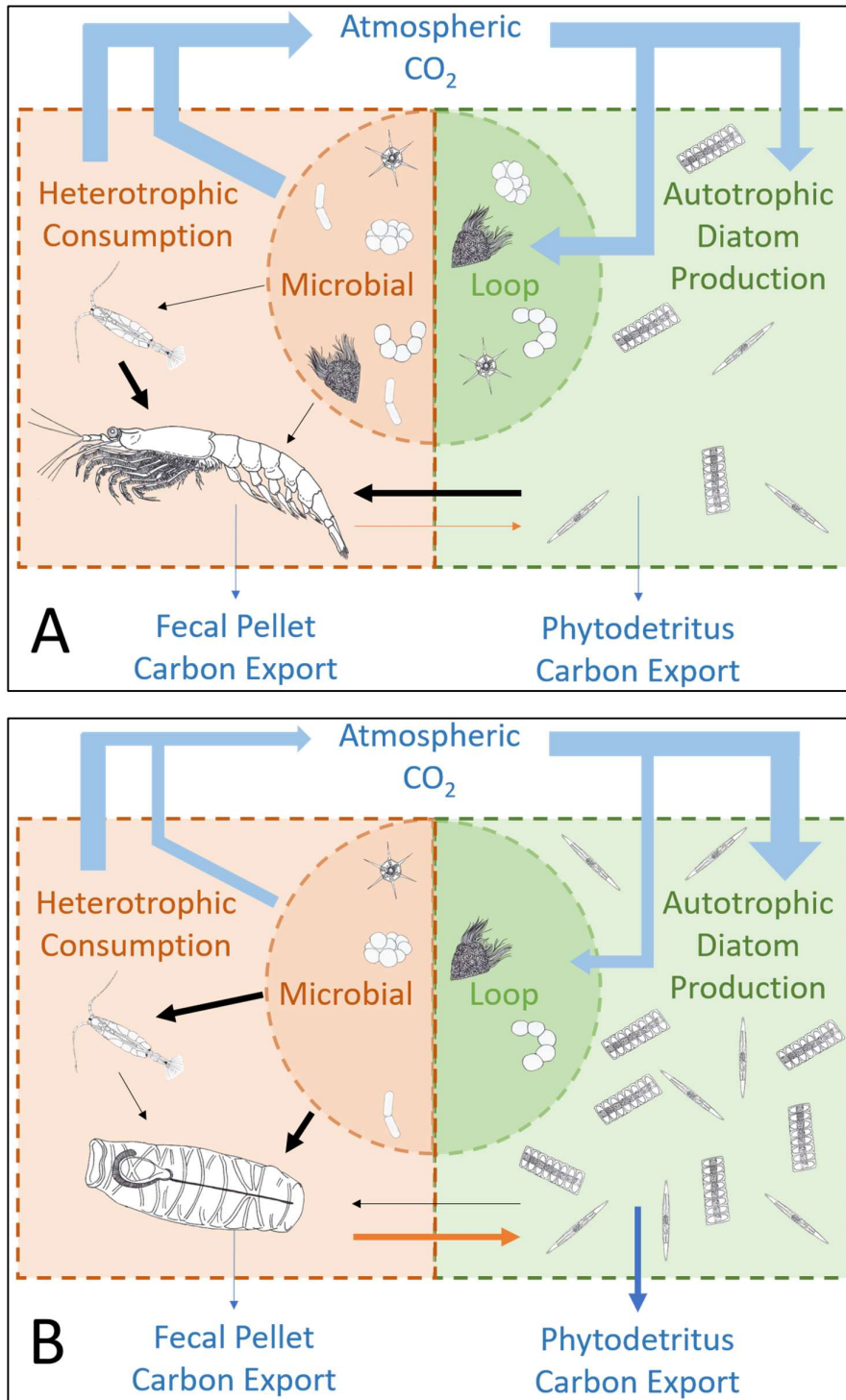
Figure 1 Expected ecosystem and carbon flux change, if krill (A) is replaced by salps (B). Black arrows represent predation/grazing pressure. Orange arrows represent Fe fertilization. Blue arrows represent carbon flux. Arrow width and organism densities represent relative expected changes between panels and are not quantitative.

5.3.1 Salp Fe-release may benefit diatoms bottom-up

In chapter 4, the carbon fixation potential based on the increase of dFe availability to phytoplankton, if krill was replaced by salps, was calculated to increase by 0.6 ± 0.5 g C m^{-2} d^{-1} in the sampled area of the Drake Passage. However, this increase in carbon fixation potential is likely not distributed evenly among all functional groups of the plankton community. During the studies presented in chapters 2 and 4, it was consistently measured that most of the dFe was absorbed by the large size fraction (>2 μm) of the plankton. It has been observed before, that large diatoms benefited most from dFe additions in Fe fertilization experiments [88], since they generally reach Fe limitation earlier than smaller cells, due to their high dFe demand and unfavorable surface to volume ratio [92,93]. In contrast, smaller species with a lower dFe demand react less to Fe limitation [94], but are prone to consumption by grazers [95]. If more dFe was bioavailable owing to more recycling via salp FP, the majority of additional dFe would likely fall to the large diatoms, particularly because silica is abundantly available in the high latitude areas, the presented studies were performed in (chapter 2). The addition of the growth-limiting nutrient could likely entail a growth benefit for these large diatom species (Figure 2).

5.3.2 Salp grazing spares diatoms benefitting them top-down

In addition to bottom-up dFe supply, a change of krill to salp dominance could influence the grazing environment, further benefiting large, well-protected diatoms. Krill was shown to target diatoms [96], while significant shares of undigested diatoms in salp FP (identified by sequencing of intact 18S rRNA), suggest that salps cannot digest them effectively [78,97]. It has been hypothesized that the share of diatoms which salps undoubtedly digest, originates from ingested krill FP that contain already broken diatoms [78]. Taking into consideration that a large share of salp FP falls apart during sinking, and is not efficiently exported to depth [98,99], undigested diatoms may be released back into the water within the euphotic zone where they possibly continue to grow. Overall, a shift of krill to salps would likely release grazing pressure from large diatoms, benefitting their growth (Figure 2). Since diatoms play an important role in the biological carbon pump [72,100], the deduction that improving conditions for the growth of diatoms may also benefit the efficiency of the carbon pump is probable.

5.3.3 Salp grazing may reduce respiration in the microbial loop

The SZP community of the microbial loop constitutes the largest phytoplankton biomass sink in the oceans [25,26]. During the dilution experiments it was shown that SZP induced grazing mortality of POC reached 3.567 ± 0.29 g POC m^{-2} d^{-1}, matching its gross growth rate of 2.994 ± 0.91 g POC m^{-2} d^{-1} (chapter 3) plus the hypothetical increase in carbon fixation potential by salp FP (0.6 ± 0.5 g C m^{-2} d^{-1}) (chapter 4) at DP station 26. Salps could significantly influence this SZP grazing pressure in three ways. First, salps are known to preferentially graze on flagellates since salp stomachs were shown to contain larger shares of dinoflagellates and other heterotrophic, as well as autotrophic flagellates than krill

stomachs [20,78]. This food preference in combination with their food selectiveness [78], high clearance rates [77] and fast procreation [77,101], makes salps dangerous predators for flagellates. Second, salps target copepods less than krill [78]. Consequently a decrease of krill and a simultaneous increase of salps would reduce grazing pressure on copepods, who in turn graze on SZP [74], thusly ultimately increasing grazing pressure on SZP. Third, as a virtue of their capability to graze on very small food items [82,83], salps are in principle food rivals to SZP. Consequently, salps may lead to a bottom-up pressure on SZP. Combining all three aspects, an increase of salps and a concurrent decrease of krill is likely to reduce SZP activity, hampering carbon respiration and release by this planktonic group (Figure 2).

5.3.4 Salps may increase particle aggregation

In principle, a more thorough particle clearance can be expected in areas, where salps replace krill. First, because ingestion rates of salps are among the highest recorded for grazers and the highest ever observed for herbivorous zooplankton in the SO [77]. Second, because salps can repackage smaller prey items than krill into their FP (down 1 μm [82,83] in comparison to down to 2-3 μm respectively [84]). Furthermore, judging by the results of chapter 3, we have to assume that an unknown, but significant share of the SZP grazed POC were TEP (chapter 3). TEP are very sticky [40] and play an important role in the formation of aggregates [49], which increases sedimentation. Although TEP were not directly measured in the course of the experiments, cues were presented, that suggested that TEP constituted a regular prey item in the dilution experiments (chapter 3). If this hypothesis could be validated, SZP grazers counteracted carbon sedimentation in two complimenting ways. First by direct consumption of POC and respiration of carbon and second, by consuming an important coagulation agent (TEP), thusly decreasing the sedimentation of carbon. Hence, a decrease of SZP activity, mediated by salp occurrence, should increase carbon export.

Based on all results in chapter 3, chapter 4 and the literature, hypothesis 5 can be accepted, suggesting that the occurrence of salps may be beneficial for carbon export. Not so much based on direct carbon export by salp FP, but the decrease of carbon recycling in the euphotic zone, in combination with a fertilization of heavily protected cells, either able to sediment on their own, or coagulated by TEP.

5.4 Future research directions

From the studies presented here, three main directions for future research can be derived.

1) Key conclusions of this dissertation are based on the novel approach to include POC as a directly measured parameter in dilution experiments. If POC shall be measured in future dilution experiments, its validity needs to be confirmed and possibly a frame of conditions, in which this parameter can be sensibly used, needs to be constrained.

2) While significant results were obtained that showed that salp FP make Fe more bioavailable to phytoplankton than krill FP, similar studies should be performed in order to confirm the described effect.

3) As discussed in chapter 3, TEP may have had a significant influence on the POC dynamics in our dilution experiments. Furthermore, from Supplementary Figure 1 of chapter 2, a mismatch of POC and PON values in the size fractionated measurements can be derived, due to lacking correlations of POC with PON (usually tied together according to the Redfield ratio) and of POC with other biomass parameters. For these irregularities, the occurrence of a carbon rich particle, such as TEP could be responsible. However, the presence of TEP and its influence on many of the performed measurements is a mere hypothesis, based on the interpretation of observations, and logical deductions, but lacking direct empirical confirmation. Given the impact that TEP may have on the carbon cycle, an investigation of the TEP dynamics at the austral WAP appears promising.

5.5. References cited in chapter 5

1. van Leeuwe, M. A. *et al.* Annual patterns in phytoplankton phenology in Antarctic coastal waters explained by environmental drivers. *Limnol Oceanogr* **65**, 1651–1668 (2020).

2. Boyd, P. W. Environmental factors controlling phytoplankton processes in the Southern Ocean. *J Phycol* **38**, 844–861 (2002).

3. Vernet, M. *et al.* Primary production within the sea-ice zone west of the Antarctic Peninsula: I-Sea ice, summer mixed layer, and irradiance. *Deep Sea Res 2 Top Stud Oceanogr* **55**, 2068–2085 (2008).

4. Trimborn, S., Hoppe, C. J. M., Taylor, B. B., Bracher, A. & Hassler, C. Physiological characteristics of open ocean and coastal phytoplankton communities of Western Antarctic Peninsula and Drake Passage waters. *Deep Sea Res 1 Oceanogr Res Pap* **98**, 115–124 (2015).

5. Martin, J. H. Glacial-interglacial CO2 change: The Iron Hypothesis. *Paleoceanography* **5**, 1–13 (1990).

6. Balaguer, J., Koch, F., Hassler, C. & Trimborn, S. Iron and manganese co-limit the growth of two phytoplankton groups dominant at two locations of the Drake Passage. *Commun Biol* **5**, 1–12 (2022).

7. Annett, A. L. *et al.* Comparative roles of upwelling and glacial iron sources in Ryder Bay, coastal western Antarctic Peninsula. *Mar Chem* **176**, 21–33 (2015).

8. Hopkinson, B. M. *et al.* Planktonic C: Fe ratios and carrying capacity in the southern Drake Passage. *Deep Sea Res 2 Top Stud Oceanogr* **90**, 102–111 (2013).

9. Fourquez, M., Obernosterer, I., Davies, D. M., Trull, T. W. & Blain, S. Microbial iron uptake in the naturally fertilized waters in the vicinity of the Kerguelen Islands: Phytoplankton-bacteria interactions. *Biogeosciences* **12**, 1893–1906 (2015).

10. Garibotti, I. A., Vernet, M., Smith, R. C. & Ferrario, M. E. Interannual variability in the distribution of the phytoplankton standing stock across the seasonal sea-ice zone west of the Antarctic Peninsula. *J Plankton Res* **27**, 825–843 (2005).

11. Greene, R. M., Geider, R. J. & Falkowski, P. G. Effect of iron limitation on photosynthesis in a marine diatom. *Limnol Oceanogr* **36**, 1772–1782 (1991).

12. Greene, R. M., Geider, R. J., Kolber, Z. & Falkowski, P. G. Iron-induced changes in light harvesting and photochemical energy conversion processes in eukaryotic marine algae. *Plant Physiol* **100**, 565–575 (1992).

13. Strzepek, R. F., Hunter, K. A., Frew, R. D., Harrison, P. J. & Boyd, P. W. Iron-light interactions differ in Southern Ocean phytoplankton. *Limnol Oceanogr* **57**, 1182–1200 (2012).

14. Balaguer, J. *et al.* Iron and manganese availability drives primary production and carbon export in the Weddell Sea. *Current Biology* **33**, 4405-4414.e4 (2023).

15. Hawco, N. J., Tagliabue, A. & Twining, B. S. Manganese Limitation of Phytoplankton Physiology and Productivity in the Southern Ocean. *Global Biogeochem Cycles* **36**, (2022).

16. Browning, T. J., Achterberg, E. P., Engel, A. & Mawji, E. Manganese co-limitation of phytoplankton growth and major nutrient drawdown in the Southern Ocean. *Nat Commun* **12**, 1–9 (2021).

17. Bazzani, E., Lauritano, C. & Saggiomo, M. Southern Ocean Iron Limitation of Primary Production between Past Knowledge and Future Projections. *J Mar Sci Eng* **11**, (2023).

18. Gutt, J. *The Expedition on the Research Vessel 'Polarstern' to the Antarctic in 2013 (ANT-XXIX/3). Reports on Polar and Marine Research* vol. 665 (2013).

19. de Jong, J. *et al.* Natural iron fertilization of the Atlantic sector of the Southern Ocean by continental shelf sources of the Antarctic Peninsula. *J Geophys Res Biogeosci* **117**, 1–25 (2012).

20. Schulz, I. *et al.* Remarkable structural resistance of a nanoflagellate-dominated plankton community to iron fertilization during the Southern Ocean experiment LOHAFEX. *Mar Ecol Prog Ser* **601**, 77–95 (2018).

21. Deppeler, S. L. & Davidson, A. T. Southern Ocean Phytoplankton in a Changing Climate. *Front Mar Sci* **4**, (2017).

22. Smetacek, V., Assmy, P. & Henjes, J. The role of grazing in structuring Southern Ocean pelagic ecosystems and biogeochemical cycles. *Antarct Sci* **16**, 541–558 (2004).

23. Assmy, P. *et al.* Thick-shelled, grazer-protected diatoms decouple ocean carbon and silicon cycles in the iron-limited Antarctic Circumpolar Current. *Proc Natl Acad Sci U S A* **110**, 20633–20638 (2013).

24. Turner, R. E. *et al.* Fluctuating silicate:nitrate ratios and coastal plankton food webs. *Proc Natl Acad Sci U S A* **95**, 13048–13051 (1998).

25. Calbet, A. & Landry, M. R. Phytoplankton growth, microzooplankton grazing, and carbon cycling in marine systems. *Limnol Oceanogr* **49**, 51–57 (2004).

26. Schmoker, C., Hernández-León, S. & Calbet, A. Microzooplankton grazing in the oceans: impacts, data variability, knowledge gaps and future directions. *J Plankton Res* **35**, 691–706 (2013).

27. Calbet, A. & Landry, M. R. Phytoplankton growth, microzooplankton grazing, and carbon cycling in marine systems. *Limnol Oceanogr* **49**, 51–57 (2004).

28. Burkill, P. H., Edwards, E. S. & Sleight, M. A. Microzooplankton and their role in controlling phytoplankton growth in the marginal ice zone of the Bellingshausen Sea. *Deep Sea Research Part II: Topical Studies in Oceanography* **42**, 1277–1290 (1995).

29. Tsuda, A. & Kawaguchi, S. Microzooplankton grazing in the surface water of the Southern Ocean during an austral summer. *Polar Biol* **18**, 240–245 (1997).

30. Garzio, L., Steinberg, D., Erickson, M. & Ducklow, H. Microzooplankton grazing along the Western Antarctic Peninsula. *Aquatic Microbial Ecology* **70**, 215–232 (2013).

31. Price, L. M. Microzooplankton Community Structure and Grazing Impact Along the Western Antarctic Peninsula. (College of William and Mary, 2012). doi:10.25773/v5-8b8j-1h33.

32. Li, C., Sun, S., Zhang, G. & Ji, P. Summer feeding activities of zooplankton in Prydz Bay, Antarctica. *Polar Biol* **24**, 892–900 (2001).

33. Pearce, I., Davidson, A. T., Thomson, P. G., Wright, S. & van den Enden, R. Marine microbial ecology off East Antarctica (30 - 80°E): Rates of bacterial and phytoplankton growth and grazing by heterotrophic protists. *Deep Sea Res 2 Top Stud Oceanogr* **57**, 849–862 (2010).

34. Pearce, I., Davidson, A. T., Wright, S. & Van Den Enden, R. Seasonal changes in phytoplankton growth and microzooplankton grazing at an Antarctic coastal site. *Aquatic Microbial Ecology* **50**, 157–167 (2008).

35. Azam, F. *et al.* The Ecological Role of Water-Column Microbes in the Sea. *Mar Ecol Prog Ser* **10**, 257–263 (1983).

36. Azam, F., Smith, D. C. & Hollibaugh, J. T. The role of the microbial loop in Antarctic pelagic ecosystems. *Polar Res* **10**, 239–244 (1991).

37. Ducklow, H. W. *et al.* Marine pelagic ecosystems: The West Antarctic Peninsula. *Philosophical Transactions of the Royal Society B: Biological Sciences* **362**, 67–94 (2007).

38. Fagerbakke, K., Heldal, M. & Norland, S. Content of carbon, nitrogen, oxygen, sulfur and phosphorus in native aquatic and cultured bacteria. *Aquatic Microbial Ecology* **10**, 15–27 (1996).

39. Fukuda, R., Ogawa, H., Nagata, T. & Koike, I. Direct Determination of Carbon and Nitrogen Contents of Natural Bacterial Assemblages in Marine Environments. *Appl Environ Microbiol* **64**, 3352–3358 (1998).

40. Engel, A. & Passow, U. Carbon and nitrogen content of transparent exopolymer particles (TEP) in relation to their Alcian Blue adsorption. *Mar Ecol Prog Ser* **219**, 1–10 (2001).

41. Martiny, A. C. *et al.* Strong latitudinal patterns in the elemental ratios of marine plankton and organic matter. *Nat Geosci* **6**, 279–283 (2013).

42. Mari, X. Carbon content and C:N ratio of transparent exopolymeric particles (TEP) produced by bubbling exudates of diatoms. *Mar Ecol Prog Ser* **183**, 59–71 (1999).

43. Sugimoto, K., Fukuda, H., Baki, M. A. & Koike, I. Bacterial contributions to formation of transparent exopolymer particles (TEP) and seasonal trends in coastal waters of Sagami Bay, Japan. *Aquatic Microbial Ecology* **46**, 31–41 (2007).

44. Zamanillo, M. *et al.* Distribution of transparent exopolymer particles (TEP) in distinct regions of the Southern Ocean. *Science of the Total Environment* **691**, 736–748 (2019).

45. Corzo, A. *et al.* Spatial distribution of transparent exopolymer particles in the Bransfield Strait, Antarctica. *J Plankton Res* **27**, 635–646 (2005).

46. Ortega-Retuerta, E., Reche, I., Pulido-Villena, E., Agustí, S. & Duarte, C. M. Uncoupled distributions of transparent exopolymer particles (TEP) and dissolved carbohydrates in the Southern Ocean. *Mar Chem* **115**, 59–65 (2009).

47. Van Oostende, N., Moerdijk-Poortvliet, T. C. W., Boschker, H. T. S., Vyverman, W. & Sabbe, K. Release of dissolved carbohydrates by Emiliania huxleyi and formation of transparent exopolymer particles depend on algal life cycle and bacterial activity. *Environ Microbiol* **15**, 1514–1531 (2013).

48. Passow, U. & Alldredge, A. L. A dye-binding assay for the spectrophotometric measurement of transparent exopolymer particles (TEP). *Limnol Oceanogr* **40**, 1326–1335 (1995).

49. Larsson, M. E. *et al.* Mucospheres produced by a mixotrophic protist impact ocean carbon cycling. *Nat Commun* **13**, 1–15 (2022).

50. Tranvik, L. J., Sherr, E. B. & Sherr, B. F. Uptake and utilization of 'colloidal DOM'' by heterotrophic flagellates in seawater'. *Mar Ecol Prog Ser* **92**, 301–309 (1993).

51. Passow, U. & Alldredge, A. L. Do transparent exopolymer particles (TEP) inhibit grazing by the euphausiid Euphausia pacifica? *J Plankton Res* **21**, 2203–2217 (1999).

52. Teixeira, I. G. & Figueiras, F. G. Feeding behaviour and non-linear responses in dilution experiments in a coastal upwelling system. *Aquatic Microbial Ecology* **55**, 53–63 (2009).

53. Calbet, A. & Saiz, E. Effects of trophic cascades in dilution grazing experiments: From artificial saturated feeding responses to positive slopes. *J Plankton Res* **35**, 1183–1191 (2013).

54. Landry, M. R. & Hassett, R. P. Estimating the grazing impact of marine micro-zooplankton. *Mar Biol* **67**, 283–288 (1982).

55. Lannuzel, D. *et al.* First report on biological iron uptake in the Antarctic sea-ice environment. *Polar Biol* **46**, 339–355 (2023).

56. Ratnarajah, L., Nicol, S. & Bowie, A. R. Pelagic Iron Recycling in the Southern Ocean: Exploring the Contribution of Marine Animals. *Front Mar Sci* **5**, 1–9 (2018).

57. Ratnarajah, L. Regenerated iron : How important are different zooplankton groups to oceanic productivity ? *Current Biology* **31**, R848–R850 (2021).

58. Schmidt, K. *et al.* Zooplankton Gut Passage Mobilizes Lithogenic Iron for Ocean Productivity. *Current Biology* **26**, 2667–2673 (2016).

59. Ratnarajah, L. & Bowie, A. R. Nutrient Cycling: Are Antarctic Krill a Previously Overlooked Source in the Marine Iron Cycle? *Current Biology* **26**, R884–R887 (2016).

60. Atkinson, A., Siegel, V., Pakhomov, E. & Rothery, P. Long-term decline in krill stock and increase in salps within the Southern Ocean. *Nature* **432**, 100–103 (2004).

61. Atkinson, A. *et al.* Krill (Euphausia superba) distribution contracts southward during rapid regional warming. *Nat Clim Chang* **9**, 142–147 (2019).

62. Ratnarajah, L. & Bowie, A. R. Nutrient Cycling: Are Antarctic Krill a Previously Overlooked Source in the Marine Iron Cycle? *Current Biology* **26**, R884–R887 (2016).

63. Schmidt, K. *et al.* Seabed foraging by Antarctic krill: Implications for stock assessment, bentho-pelagic coupling, and the vertical transfer of iron. *Limnol Oceanogr* **56**, 1411–1428 (2011).

64. Schlosser, C. *et al.* Mechanisms of dissolved and labile particulate iron supply to shelf waters and phytoplankton blooms off South Georgia, Southern Ocean. *Biogeosciences* **15**, 4973–4993 (2018).

65. Cabanes, D. J. E. *et al.* First Evaluation of the Role of Salp Fecal Pellets on Iron Biogeochemistry. *Front Mar Sci* **3**, 1–10 (2017).

66. Sangrà, P. *et al.* The Bransfield current system. *Deep Sea Res 1 Oceanogr Res Pap* **58**, 390–402 (2011).

67. Ferreira, A. *et al.* Climate change is associated with higher phytoplankton biomass and longer blooms in the West Antarctic Peninsula. *Nat Commun* **15**, (2024).

68. Löder, M. G. J., Meunier, C., Wiltshire, K. H., Boersma, M. & Aberle, N. The role of ciliates, heterotrophic dinoflagellates and copepods in structuring spring plankton communities at Helgoland Roads, North Sea. *Mar Biol* **158**, 1551–1580 (2011).

69.	Monti-Birkenmeier, M. *et al.* Spatial distribution of microzooplankton in different areas of the northern Antarctic Peninsula region, with an emphasis on tintinnids. *Polar Biol* **44**, 1749–1764 (2021).

70.	Lalli, C. M. & Parsons, T. R. *Biological Oceanography - An Introduction*. (Elsevier Butterworth-Heinemann, Burlington, 1993). doi:10.1016/0022-0981(96)02604-4.

71.	Hernández-León, S. & Ikeda, T. A global assessment of mesozooplankton respiration in the ocean. *J Plankton Res* **27**, 153–158 (2005).

72.	Turner, J. T. Zooplankton fecal pellets, marine snow, phytodetritus and the ocean's biological pump. *Prog Oceanogr* **130**, 205–248 (2015).

73.	Plum, C. *et al.* Mesozooplankton trait distribution in relation to environmental conditions and the presence of krill and salps along the northern Antarctic Peninsula. *J Plankton Res* **43**, 927–944 (2021).

74.	Calbet, A. & Saiz, E. The ciliate-copepod link in marine ecosystems. *Aquatic Microbial Ecology* **38**, 157–167 (2005).

75.	Perissinotto, R., Pakhomov, E. A., McQuaid, C. D. & Froneman, P. W. In situ grazing rates and daily ration of Antarctic krill Euphausia superba feeding on phytoplankton at the Antarctic Polar Front and the Marginal Ice Zone. *Mar Ecol Prog Ser* **160**, 77–91 (1997).

76.	Pakhomov, E. A., Perissinotto, R., Froneman, P. W. & Miller, D. G. M. Energetics and feeding dynamics of euphausia superba in the South Georgia region during the summer of 1994. *J Plankton Res* **19**, 399–423 (1997).

77.	Perissinotto, R. & A. Pakhomov, E. The trophic role of the tunicate Salpa thompsoni in the Antarctic marine ecosystem. *Journal of Marine Systems* **17**, 361–374 (1998).

78.	Pauli, N.-C. *et al.* Selective feeding in Southern Ocean key grazers—diet composition of krill and salps. *Commun Biol* **4**, 1061 (2021).

79.	Buma, A. G. J., de Baar, H. J. W., Nolting, R. F. & van Bennekom, A. J. Metal enrichment experiments in the Weddell-Scotia Seas: Effects of iron and manganese on various plankton communities. *Limnol Oceanogr* **36**, 1865–1878 (1991).

80.	de Baar, H. J. W. Synthesis of iron fertilization experiments: From the Iron Age in the Age of Enlightenment. *J Geophys Res* **110**, C09S16 (2005).

81.	Atkinson, A., Ward, P., Hunt, B. P. V., Pakhomov, E. A. & Hosie, G. W. An overview of Southern Ocean zooplankton data: Abundance, biomass, feeding and functional relationships. *CCAMLR Science* **19**, 171–218 (2012).

82.	Harbison, G. R. & McAlister, V. L. The filter-feeding rates and particle retention efficiencies of three species of Cyclosalpa (Tunicata, Thaliacea). *Limnol Oceanogr* **24**, 875–892 (1979).

83.	Madin, L. P. Field observations on the feeding behavior of salps (Tunicata: Thaliacea). *Mar Biol* **25**, 143–147 (1974).

84.	Siegel, V. *Biology and Ecology of Antarctic Krill*. (Springer International Publishing, 2016). doi:10.1007/978-3-319-29279-3.

85.	Martin, J. H., Fitzwater, S. E. & Gordon, R. M. Iron deficiency limits phytoplankton growth in Antarctic waters. *Global Biogeochem Cycles* **4**, 5–12 (1990).

86.	Vaughan, D. G. *et al.* Recent rapid regional warming on the Antarctic Peninsula. *Climate Change* **60**, 243–274 (2003).

87.   Pakhomov, E. A., Froneman, P. W. & Perissinotto, R. Salp/krill interactions in the Southern Ocean: spatial segregation and implications for the carbon flux. *Deep Sea Research Part II: Topical Studies in Oceanography* **49**, 1881–1907 (2002).

88.   Smetacek, V. *et al.* Deep carbon export from a Southern Ocean iron-fertilized diatom bloom. *Nature* **487**, 313–319 (2012).

89.   Boyd, P. W. & Ellwood, M. J. The biogeochemical cycle of iron in the ocean. *Nat Geosci* **3**, 675–682 (2010).

90.   Tovar-Sanchez, A., Duarte, C. M., Hernández-León, S. & Sañudo-Wilhelmy, S. A. Krill as a central node for iron cycling in the Southern Ocean. *Geophys Res Lett* **32**, 1–4 (2007).

91.   Maldonado, M. T., Surma, S. & Pakhomov, E. A. Southern Ocean biological iron cycling in the pre-whaling and present ecosystems. *Philosophical Transactions of the Royal Society A: Mathematical, Physical and Engineering Sciences* **374**, 20150292 (2016).

92.   Lancelot, C., Hannon, E., Becquevort, S., Veth, C. & De Baar, H. J. W. Modeling phytoplankton blooms and carbon export production in the Southern Ocean: Dominant controls by light and iron in the Atlantic sector in Austral spring 1992. *Deep Sea Res 1 Oceanogr Res Pap* **47**, 1621–1662 (2000).

93.   Morel, F. M. M., Rueter, J. G. & Price, N. M. Iron nutrition of phytoplankton and its possible importance in the ecology of ocean regions with high nutrient and low biomass. *Oceanography* **4**, 56–61 (1991).

94.   Timmermans, K. R. *et al.* Growth rates of large and small Southern Ocean diatoms in relation to availability of iron in natural seawater. *Limnol Oceanogr* **46**, 260–266 (2001).

95.   Price, N. M., Ahner, B. A. & Morel, F. M. M. The equatorial Pacific Ocean: Grazer-controlled phytoplankton populations in an iron-limited ecosystem. *Limnol Oceanogr* **39**, 520–534 (1994).

96.   Haberman, K. L., Ross, R. M. & Quetin, L. B. Diet of the Antarctic krill (Euphausia superba Dana): II. Selective grazing in mixed phytoplankton assemblages. *J Exp Mar Biol Ecol* **283**, 97–113 (2002).

97.   von Harbou, L. *et al.* Salps in the Lazarev Sea, Southern Ocean: I. Feeding dynamics. *Mar Biol* **158**, 2009–2026 (2011).

98.   Pauli, N.-C. *et al.* Krill and salp faecal pellets contribute equally to the carbon flux at the Antarctic Peninsula. *Nat Commun* **12**, 7168 (2021).

99.   Iversen, M. H. *et al.* Sinkers or floaters? Contribution from salp pellets to the export flux during a large bloom event in the Southern Ocean. *Deep Sea Research Part II: Topical Studies in Oceanography* **138**, 116–125 (2017).

100. Buesseler, K. O. *et al.* Revisiting Carbon Flux Through the Ocean's Twilight Zone. *Science (1979)* **316**, 567–570 (2007).

101. Heron, A. C. Population ecology of a colonizing species: The pelagic tunicate Thalia democratica - I. Individual growth rate and generation time. *Oecologia* **10**, 269–293 (1972).

Universität Bremen | Fachbereich 02 | Postfach 33 04 40, 28334 Bremen

Universität Bremen
Fachbereich 2
Prüfungsamt Chemie
z. Hd. Frau Frauke Ernst
Leobener Straße

28359 Bremen
Deutschland

Prüfungsamt
Chemie

Frauke Ernst
Geschäftsstelle
Fachbereich 02
Leobener Str. / NW2
D-28359 Bremen

Verwaltungspavillon 06
Tel. 0421 218-62802
Fax 0421 218-9862802
frauke.ernst@uni-bremen.de
www.fb2.uni-bremen.de

Versicherung an Eides Statt

Name, Vorname	
Matrikel-Nr.	
Straße	
Ort, PLZ	

Ich, _____ (Vorname, Name)

versichere an Eides Statt durch meine Unterschrift, dass ich die vorstehende Arbeit selbständig und ohne fremde Hilfe angefertigt und alle Stellen, die ich wörtlich dem Sinne nach aus Veröffentlichungen entnommen habe, als solche kenntlich gemacht habe, mich auch keiner anderen als der angegebenen Literatur oder sonstiger Hilfsmittel bedient habe.

Ich versichere an Eides Statt, dass ich die vorgenannten Angaben nach bestem Wissen und Gewissen gemacht habe und dass die Angaben der Wahrheit entsprechen und ich nichts verschwiegen habe.

Die Strafbarkeit einer falschen eidesstattlichen Versicherung ist mir bekannt, namentlich die Strafandrohung gemäß § 156 StGB bis zu drei Jahren Freiheitsstrafe oder Geldstrafe bei vorsätzlicher Begehung der Tat bzw. gemäß § 161 Abs. 1 StGB bis zu einem Jahr Freiheitsstrafe oder Geldstrafe bei fahrlässiger Begehung.

_____
Ort, Datum / Unterschrift

CONTRIBUTION

Declaration on the contribution of the candidate to a multi-author article/manuscript.

Contribution of the candidate in % of the total workload (up to 100% for each of the following categories).

Chapter 2, Publication I
Experimental concept and design: ca. 10%
Experimental work and/or acquisition of (experimental) data: ca. 40%
Data analysis and interpretation: ca. 80%
Preparation of Figures and Tables: ca. 100%
Drafting of the manuscript: ca. 80%

Chapter 3, Publication II
Experimental concept and design: ca. 0%
Experimental work and/or acquisition of (experimental) data: ca. 20%
Data analysis and interpretation: ca. 80%
Preparation of Figures and Tables: ca. 100%
Drafting of the manuscript: ca. 80%

Chapter 4, Publication III
Experimental concept and design: ca. 0%
Experimental work and/or acquisition of (experimental) data: ca. 20%
Data analysis and interpretation: ca. 80%
Preparation of Figures and Tables: ca. 100%
Drafting of the manuscript: ca. 80%

_____   _____

Ort, Datum   Unterschrift